

**Preparation and Characterization of Alumina
Powders and Suspensions**

By

Aylin M.ŞAKAR

**A Dissertation Submitted to the
Graduate School in Partial Fulfillment of the
Requirements for the Degree of**

MASTER OF SCIENCE

**Department: Materials Science and Engineering
Major: Materials Science and Engineering**

**Izmir Institute of Technology
Izmir, Turkey**

September, 2000

We approve the thesis of Aylin M.ŞAKAR

Date of Signature



28.09.2000

Asst. Prof. Dr. Hürriyet POLAT

Supervisor

Department of Chemistry



28.09.2000

Prof. Dr. Muhsin ÇİFTÇİOĞLU

Co-Supervisor

Department of Chemical Engineering



28.09.2000

Assoc.Prof. Dr. Şebnem HARSA

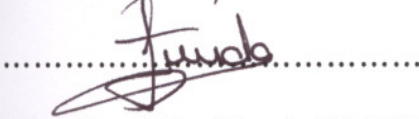
Department of Food Engineering



28.09.2000

Asst. Prof. Dr. Sedat AKKURT


Department of Mechanical Engineering



28.09.2000

Asst. Prof. Dr. Funda TIHMİNLİOĞLU

Department of Chemical Engineering



28.09.2000

Prof. Dr. Muhsin ÇİFTÇİOĞLU

Head of Interdisciplinary Materials Science and
Engineering Program

ACKNOWLEDGEMENTS

I would like to express my gratitude to Asst. Prof. Dr. Hürriyet Polat and Prof. Dr. Muhsin Çiftçiođlu for their understanding, help, guidance and contributions during this study and the preparation of this thesis.

I also would like to thank to Prof. Dr. Devrim Balköse for her valuable comments in FTIR analysis.

Special thanks are to all research assistants for their friendships, to Uđur Ünal for his help on rheological measurements and to the laboratory technicians for their help in the laboratory.

I am also grateful to Hatice Yılmaz for her help and kindly performing XRD analysis in Dokuz Eylül University, Mining Engineering Department.

Finally, I would like to thank to my family for their support and to my husband Ahmet, for his continued patience, understanding, encouragement and help. He contributed much to this study in all stages and I owe a special dept to him.

İZMİR YÜKSEK TEKNOLOJİ ENSTİTÜSÜ
REKTÖRLÜĐÜ
Kütüphane ve Dokümantasyon Daire B-1

ABSTRACT

This study involves the preparation of fine alumina powders derived from Bayer gibbsite and also aqueous alumina suspensions by using tri block copolymers. Preparation of alumina powders was performed by decomposition of gibbsite into transition alumina phase followed by controlled transformation to alpha phase. To increase transformation rate to α -alumina in transition phase hence influence the nucleation and growth rate of the solid-solid phase transformation ball milling and ultrasonication was applied. Gibbsite was thermally treated at 900 °C to reach a transition form of alumina. In some cases a heat treatment at 350 °C was applied to create a network of submicroscopic cracks in the heated gibbsite that may help grinding. Ball milling and ultrasonic treatment before calcination at 1100, 1200 °C and 1450 °C followed these heat treatments. Characterizations of the powders were performed with XRD, FTIR, thermal analysis, density measurements and particle size determinations.

According to the XRD patterns, complete transformation to alpha form occurred in powders previously heat treated at 900 °C, mechanically treated and then calcined at 1200 °C in 8 hours and 1450 °C in 2 hours. Powders that were calcined at 1100 °C and 1200 °C in 1-2 hours contained considerable amount of kappa form together with alpha.

The effect of the polyethylene oxide-polypropylene oxide-polyethylene oxide (PEO/PPO/PEO) block copolymers on the dispersion behaviour of alumina powder suspensions in water were investigated at $\Phi=0.125, 1.0, 14$ and 50 vol% solid loadings by rheological and turbidity measurements. To compare the effects of block copolymers with other type of dispersants, measurements of some other well known dispersants were also conducted at 10^{-7} to 10^{-3} M. The results indicated that type block copolymers with high EO percentage have a positive effect when they are used with ultrasonic treatment on the agglomerated alumina suspensions. But it was not able to create stable dispersions in the absence of ultrasonic bath application. Turbidity measurements at $\Phi=0.5$ wt% showed that some dispersants gave higher dispersion but the stability was reached after a time period. Ultrasonic treatment created stability but lowered the turbidity values.

ÖZ

Bu çalışma alüminyum hidroksitten başlayarak ince taneli alümina tozlarının ve blok kopolimerler kullanılarak sulu alümina süspansiyonlarının hazırlanmasını içermektedir. Alümina tozu hazırlanması aşamasında alüminyum hidroksit, kalsine edilerek alümina ara formuna geçiş sağlandı ve bunu alfa fazına dönüşüm izledi. Bu aşamada alfa alümina formunun, diğer geçiş ara formlar içindeki dönüşüm hızını arttırmak için toz üretim prosesinin çeşitli kısımlarında öğütme ve ultrasonik işlemler uygulandı. Alüminyum hidroksiti bir alümina ara formuna dönüştürmek için 900 °C'de ısıtılma işlemi uygulandı. Bazı durumlarda ise alüminyum hidroksit, öğütülmesini kolaylaştıracağı düşüncesiyle kristal yapısında küçük çatlaklar oluşturmak için 350 °C'de ısıtılma işlemi tabi tutuldu. Bu ısıtılma işlemleri 1100, 1200 °C ve 1450 °C'deki kalsinasyondan önce öğütme ve ultrasonik uygulama izledi. Tozların karakterizasyonu XRD, FTIR, termal analiz, yoğunluk ölçümleri ve tane büyüklüğü hesaplamaları ile yapıldı.

XRD sonuçlarına göre alfa formuna tam dönüşüm önceden 900°C 'de ısıtılma işlemi görmüş ve mekanik işleme tabi tutulmuş tozların 1200 °C'de 8 saat ayrıca 1450 °C'de 2 saat kalsinasyonu ile sağlandı. 1100 ve 1200 °C'de 1-2 saat kalsine edilen tüm tozların alfa ile birlikte kappa formunu da içerdiği saptandı.

Blok kopolimer grubunda olan polietilen oksit - polipropilen oksit-polietilen oksit (PEO/PPO/PEO), $\Phi = 0.125, 1.0, 14$ ve 50 (hacimsel) alümina konsantrasyonlarında alümina-su süspansiyonlarının dispersiyon özelliklerine olan etkisi reometre ve türbidimetre ölçümleri ile incelendi. Blok kopolimerler ile diğer dispersantların etkilerinin karşılaştırılması için farklı tipte 10^{-7} ile 10^{-3} M arası konsantrasyonlarda çeşitli dispersantlar denendi. Sonuçlara göre yüksek PE yüzdelerine sahip blok kopolimerlerin ultrasonik uygulama ile birlikte kullanıldığında agrege olmuş alümina süspansiyonları üzerinde olumlu etkiye sahip olduğu gözlemlendi. Fakat ultrasonik uygulama yapılmadığı durumlarda stabil dispersiyonlar oluşturulamadı. Türbidimetre sonuçlarına göre (ağırlıkça) %0.5 katı konsantrasyonunda dispersantların çoğu stabilite üzerinde etkili oldu ancak stabiliteye zamanla ulaşılabilir. Ultrasonik uygulama, düşük türbidite değerleri vermesine rağmen stabilite sağlanmasında etkili oldu.

TABLE OF CONTENTS -

LIST OF FIGURES	vii
LIST OF TABLES	xiii
CHAPTER I: INTRODUCTION	1
CHAPTER II: ALUMINA.....	4
× 2.1 Structure and Transition Forms	4
× 2.2 Types and Applications.....	6
× 2.3 Alumina Production Methods.....	7
2.3.1 Bayer Process	8
2.4 Aluminum Hydroxides.....	10
2.5 Phase Relations of Aluminum Hydroxides and Oxides.....	11
2.5.1 Thermal Decomposition of Aluminum Hydroxides	11
2.5.1.1 Thermal Decomposition of Gibbsite	14
2.6 Nucleation and Growth	16
2.6.1 Effects of Seeding.....	17
× 2.6.2 Effects of Mechanical Treatment.....	20
× 2.7 AQUEOUS ALUMINA SUSPENSIONS	22
× 2.7.1 Interaction Forces in Dispersed Systems.....	24
✓ 2.7.1.1 Electrostatic Stabilization	27
× 2.7.1.2 Polymeric Stabilization	30
× 2.7.1.2.1 Steric Stabilization.....	30
× 2.7.1.2.2 Depletion Stabilization.....	32
2.7.1.2.3 Surfactants.....	33

2.7.1.2.3.1 PEO/PPO/PEO Block copolymers.....	35
2.7.2 Rheology	40
2.7.3 Dispersion and Rheology Studies on Alumina	43
CHAPTER III: EXPERIMENTAL	46
3.1 Materials	46
3.2 Powder Preparation Methods.....	48
3.3 Powder Characterization	53
X 3.4 Suspension Preparation Methods	54
X 3.5 Suspension Characterization	56
CHAPTER IV: RESULTS AND DISCUSSION.....	57
4.1 Powder Preparation and Characterization	57
4.1.1 Thermal Analysis.....	57
4.1.2 Particle Size Characterizations	59
X 4.1.3 Density Measurements	62
4.1.4 Fourier Transform Infra-Red Analysis.....	64
4.1.5 X-ray Powder Diffraction Analysis.....	68
X 4.2 Suspension Preparation and Characterization.....	74
4.2.1 Rheological Measurements.....	74
4.2.2 Turbidity Measurements.....	103
4.2.3 Discussion for Stabilization Mechanisms of Block Copolymers in the Absence of Adsorption on Alumina.....	125
CONCLUSIONS	127
RECOMMENDATIONS	130
REFERENCES	131

LIST OF FIGURES

Figure 2.1. Crystal structure of alpha alumina	5
Figure 2.2. Relations between some properties of calcined gibbsite [57]	15
Figure 2.3. Formation of α -alumina in untreated and die-pressed γ -alumina powders at 1150 °C [9]	21
Figure 2.4. Formation of α -alumina in ball milled γ -alumina powders annealed at 1150 °C [9].....	21
Figure 2.5. Schematic presentation of slip casting [46]	24
Figure 2.6. Potential energy diagram of interaction between the two particles [58].....	26
Figure 2.7. Electrical double layer models for particle charging in a polar liquid [58].....	28
Figure 2.8. Schematic of two particles having adsorbed polymer molecules [35].....	31
Figure 2.9. Polymeric stabilization by free polymer molecules in solution [8]	32
Figure 2.10. Basic molecular structure of a surface-active agent [48]	34
Figure 2.11. Orientation of surfactants in liquid medium [48]	34
Figure 2.12. Equations representing the synthesis of the PEO-PPO-PEO copolymers.....	36
Figure 2.13. Structural formulas of surfactants used in this study.....	37
Figure 2.14. Variation of shear stress with shear rate for different models of flow behaviour [47]	42
Figure 3.1. Powder processing diagram of M-1, M-2, M-3 and M-4	50
Figure 3.2. Powder processing diagram of M-5, M-6 and M-7.....	51

Figure 3.3. Powder processing diagram of M-8.....	52
Figure 3.4. A schematic representation of suspension preparation methods	55
Figure 4.1. TGA thermogram of gibbsite	58
Figure 4.2. DTA curve of gibbsite.....	58
Figure 4.3. Particle size distribution of the AKP-53.....	61
Figure 4.4. Particle size distribution of Aldrich alumina	61
Figure 4.5. FTIR spectra of (a) AKP-53, (b) Aldrich, (c) M-7A	64
Figure 4.6. FTIR spectra of (a) Gibbsite, (b) M-4, (c) M-1A	65
Figure 4.7. FTIR spectra of (a) M-1P (b) M-8, (c) M-6A.....	66
Figure 4.8. XRD diagrams of AKP-53, M-1A, M-2 and M-5	71
Figure 4.9. XRD diagrams of M-6A, M-7A and M-8.....	72
Figure 4.10. XRD diagrams of M-7C, M-7B, M-6B, M-1B	73
Figure 4.11. Structure of PAA polymer segments [6].....	75
Figure 4.12. Shear rate vs. shear stress graphs of AKP-53 suspensions prepared with Method I, II and IV at 50 vol%-(80wt%) solid loading.....	81
Figure 4.13. Shear rate vs. viscosity graphs of AKP-53 suspensions prepared with Method I, II and IV at 50 vol%-(80wt%) solid loading.....	82
Figure 4.14. Shear rate vs. shear stress graphs of AKP-53 suspensions prepared with Method I, II and IV at 14 vol%-(40wt%) solid loading.....	83
Figure 4.15. Shear rate vs. viscosity graphs of AKP-53 suspensions prepared with Method I, II and IV at 14 vol%-(40wt%) solid loading.....	84
Figure 4.16. Shear rate vs. shear stress graphs of AKP-53 suspensions prepared with Method I, II and IV at 1 vol% -(4 wt%)solid loading.....	85
Figure 4.17. Shear rate vs. viscosity graphs of AKP-53 suspensions prepared with Method I, II and IV at 1 vol% -(4 wt%)solid loading.....	86
Figure 4.18. Shear rate vs. shear stress graphs of AKP-53 suspensions prepared with Method I, II and IV at 0,125 vol %-(0.5wt%) solid loading	87

Figure 4.19. Shear rate vs. viscosity graphs of AKP-53 suspensions prepared with Method I, II and IV at 0,125 vol %-(0.5wt%) solid loading	88
Figure 4.20. Shear rate vs. shear stress graphs of Aldrich alumina suspensions prepared with Method I, II and IV at 50 vol%-(80wt%) solid loading.....	89
Figure 4.21. Shear rate vs. viscosity graphs of Aldrich alumina suspensions prepared with Method I, II and IV at 50 vol%-(80wt%) solid loading.....	90
Figure 4.22. Shear rate vs. shear stress graphs of Aldrich alumina suspensions prepared with Method I, II and IV at 14 vol%-(40wt%) solid loading.....	91
Figure 4.23. Shear rate vs. viscosity graphs of Aldrich alumina suspensions prepared with Method I, II and IV at 14 vol%-(40wt%) solid loading.....	92
Figure 4.24. Shear rate vs. shear stress graphs of Aldrich alumina suspensions prepared with Method I, II and IV at 1 vol% -(4 wt%) solid loading	93
Figure 4.25. Shear rate vs. viscosity graphs of Aldrich alumina suspensions prepared with Method I, II and IV at 1 vol% -(4 wt%) solid loading	94
Figure 4.26. Shear rate vs. shear stress graphs of Aldrich alumina suspensions prepared with Method I, II and IV at 0,125 vol %-(0.5wt%) solid loading	95
Figure 4.27. Shear rate vs. viscosity graphs of Aldrich alumina suspensions prepared with Method I, II and IV at 0,125 vol %-(0.5wt%) solid loading	96
Figure 4.28. Shear rate vs. viscosity graphs of Aldrich alumina suspensions prepared with Method I, II and III at 50 vol%-(80wt%) solid loading.....	97
Figure 4.29. Shear rate vs. viscosity graphs of Aldrich alumina suspensions prepared with Method I, II and III at 14 vol%-(40wt%) solid loading.....	98
Figure 4.30. Shear rate vs. viscosity graphs of Aldrich alumina suspensions prepared with Method I, II and III at 0,125 vol %-(0.5wt%) solid loading	99.
Figure 4.31. Shear rate vs. viscosity graphs of M-7A alumina suspensions prepared with Method I, II, III and IV at 14 vol%-(40wt%)solid loading.....	100
Figure 4.32. Shear rate vs. viscosity graphs of M-7A alumina suspensions prepared with Method I, II, III and IV at 0.125 vol% -(0.5 wt%).....	101

Figure 4.33. Shear rate vs. viscosity graphs of AKP-53 suspensions prepared with Method I and III at 0.125, 14, 50 vol % solid loading.....	102
Figure 4.34. Effect of method type on turbidity of the alumina suspensions as a function of time <i>Solid wt %: 0.5-; Alumina type: AKP-53; Temp: 29.1°C; pH: 5.8</i>	104
Figure 4.35. Effect of stirring time on turbidity of alumina suspensions prepared by Method I as a function of time. <i>Solid wt %: 0.5; Alumina type: AKP-53; Temp: 29.1°C; pH: 5.0</i>	105
Figure 4.36. Effect of conditioning time on turbidity of the alumina suspensions prepared by Method I and II as a function of time. <i>Solid wt%: 0.5; Alumina type: AKP-53; Temp: 29°C; pH: 5.2</i>	106
Figure 4.37. Effect of conditioning and ultrasonic treating time on turbidity of the alumina suspensions prepared by Method I and II as a function of time. <i>Solid wt%: 0.5; Alumina type: AKP-53; Temp: 30°C; pH: 5.3</i>	106
Figure 4.38. Effect of indifferent electrolyte, NaCl, on turbidity of the alumina suspensions prepared by Method I as a function of time. <i>Solid wt%: 0.5; Alumina type: AKP-53; Temp: 30.2°C; pH: 6.4</i>	107
Figure 4.39. Effect of polymeric surfactant, P-104, concentration on turbidity of AKP-53 alumina suspensions prepared by Method I, II and III as a function of time. <i>Solid wt%: 0.5; Alumina type: AKP-53; Temp: 27.1°C; pH: 5,3-6,3</i>	108
Figure 4.40. The reproducibility of turbidity versus time measurements at different P-104 concentrations. (Method II) <i>Solid wt%: 0.5; Alumina type: AKP-53; Temp: 27.0°C; pH: 6,3</i>	109
Figure 4.41. Effect of polymer, PAA, concentration on turbidity of AKP-53 alumina suspensions prepared by Method I, II and III as a function of time. <i>Solid wt%: 0.5; AKP-53; Temp: 25.1°C; pH: 4,5</i>	110
Figure 4.42. The reproducibility of turbidity versus time measurements at different PAA concentrations. <i>Solid wt%: 0.5; Alumina type: AKP-53; Temp: 25.3°C; pH: 4,5</i>	111

Figure 4.43. Effect of polymer, F-127, concentration on turbidity of AKP-53 alumina suspensions prepared by Method I, II and III as a function of time. <i>Solid wt%: 0.5; Alumina type: AKP-53; Temp: 29.1°C; pH: 5,3</i>	112
Figure 4.44. The reproducibility of turbidity versus time measurements at different F-127 concentrations. <i>Solid wt%: 0.5; Alumina type: AKP-53; Temp: 29.1°C; pH: 5.3</i>	113
Figure 4.45. Effect of surfactant, SDS, concentration on turbidity of AKP-53 alumina suspensions prepared by Method I, II and III as a function of time. <i>Solid wt%: 0.5; Alumina type: AKP-53; Temp: 24.6°C; pH: 5.2-7,6</i>	114
Figure 4.46. Effect of Citric acid concentration, on turbidity of AKP-53 alumina suspensions prepared by Method I, II and III as a function of time. <i>Solid wt%: 0.5; Alumina type: AKP-53; Temp: 20.5°C; pH: 6,1-2,77</i>	115
Figure 4.47. Effect of polymer, 10R-8, concentration on turbidity of AKP-53 alumina suspensions prepared by Method I, II and III as a function of time. <i>Solid wt%: 0.5; Alumina type: AKP-53; Temp: 29.1°C; pH: 5.0</i>	116
Figure 4.48. Effect of polymer, 6400, concentration on turbidity of AKP-53 alumina suspensions prepared by Method I, II and III as a function of time. <i>Solid wt%: 0.5; Alumina type: AKP-53; Temp: 24.1°C; pH: 5.2</i>	117
Figure 4.49. Effect of polymer, F-127, concentration on turbidity of Aldrich alumina suspensions prepared by Method I, and III as a function of time. <i>Solid wt%: 0.5; Alumina type: Aldrich; Temp: 30.1°C; pH: 5.0</i>	118
Figure 4.50. The reproducibility of turbidity versus time measurements at different PAA concentrations for Aldrich alumina suspension. <i>Solid wt%: 0.5; Alumina type: Aldrich; Temp: 30.1°C; pH: 5.0</i>	119
Figure 4.51. Effect of method type on turbidity of the Aldrich alumina suspensions in the presence of Pluronic F-127 (10^{-3} M). <i>Solid wt%: 0.5; Alumina type: Aldrich; Temp: 29°C; pH: 5.0</i>	120
Figure 4.52. Effect of method type on turbidity of the alumina suspensions in the presence of PAA (10^{-3} M). <i>Solid wt%: 0.5; Alumina type: Aldrich; Temp: 29.1°C; pH: 5.0-7.0</i>	121

Figure 4.53. Effect of polymer, F-68, concentration on turbidity of Aldrich alumina suspensions prepared by Method I and IV as a function of time. *Solid wt%: 0.5; Alumina type: Aldrich; Temp: 27°C; pH: 4.6*..... 122

Figure 4.54. A schematic representation of the possible stabilization mechanisms of surfactant in alumina suspensions 126

LIST OF TABLES

Table 2.1. Transition sequences of aluminium hydroxides [57]	12
Table 2.2. Ceramic consolidation techniques [50].....	23
Table 3.1. Important properties of surfactants used in this study [2].....	47
Table 3.2. Compositions of surfactants used in this study [56].....	47
Table 3.3. Processing methods of prepared powders	53
Table 4.1. Below 1 μm and 5 μm fractions of some selected powders in different processing steps	60
Table 4.2. Density and dimensions of the pellets before and after sintering	63
Table 4.3. Interplanar spacings and relative line intensities of α and κ [57].....	70

CHAPTER I

INTRODUCTION

Ceramics can be defined as inorganic and non-metallic materials or compounds. They have been produced for centuries. The earliest ceramic articles were made from naturally occurring raw materials. However during the past 50 years it was found that naturally occurring minerals could be refined or new compositions synthesized to achieve required properties.

Alumina (Al_2O_3) is the most widely used oxide ceramic because it is plentiful, relatively low in cost and equal to or better than most oxides in mechanical properties [57]. The advanced ceramics generally require chemical conversion of raw materials into intermediate compounds, which lend themselves to purification and subsequent chemical conversion into the final desired form.

In general ceramic materials undergo reconstructive transformation. They transform by nucleation and growth with high activation energies. For ceramic fabrication it is necessary to transform the ceramic powder to the stable form before consolidation as low densities are usually obtained on sintering if the ceramic powder undergoes transformation during heating. However because of the elevated temperatures imposed by the high activation energy the ceramic powder becomes coarsened, aggregated and generally unsuitable for ceramic processing and fabrication without subsequent processing [50, 30]. Nucleation and growth of these powders that undergo transformation during calcination may be affected by parameters and techniques such as seeding, mechanical treatment, and thermal treatment environment.

Many researchers had studied the transformation to metastable alumina forms starting from different aluminium hydroxides. Also a number of researchers have attempted to influence the transformation to alpha alumina by using additives such as $\alpha\text{-Al}_2\text{O}_3$, CuO, MgO, $\alpha\text{-Fe}_2\text{O}_3$, $\alpha\text{-Cr}_2\text{O}_3$. Seeding of a

transition alumina with these additives accelerates the kinetics of transformation and prevents formation of a vermicular microstructure [51,37,30,10,32,49,39].

A mechanical pre-treatment (compaction or dry ball milling) of transition alumina powders significantly affects the kinetics of the transformation and very high compaction pressures ($>2.5\text{Gpa}$) can prevent the formation of a vermicular microstructure characterized by the coexistence of contiguous solid and pore phases [32].

The recent studies generally involve importance of seeding of the transition form aluminas before transformation to alpha alumina. Especially mechanism of gamma to alpha transformation has been subject of several published studies. On the other hand a few studies [9] have been observed about mechanical treatment to improve nucleation and growth of α -alumina. Also there was no attention on the effect of ultrasonic treatment on nucleation and growth rate of alumina. Previous studies related with the effects of both seeding and mechanical treatment on phase transformations will be discussed with more detail in Chapter II.

In ceramic processing after the powder preparation with suitable properties it is important to treat these powders before the consolidation step. Generally ceramic powders need a pre-consolidation step before the forming process. That is, in all kinds of forming techniques homogenisation of the powders by the help of all different chemical aids are necessary. Especially in some forming techniques like slip casting and tape casting usage of these chemical aids such as dispersing agents has a major importance for successful consolidation process. On this manner, in ceramic applications, for the preparation of alumina powder suspensions to create an effective dispersion and stabilization, usage of some different dispersing agents maybe required.

There are many studies that investigate the effect of different type of dispersants such as polyacrylic acid, polymethacrylic acid, citric acid, sodium dodecyl sulfate, benzoic acid derivatives, anionic and cationic surfactants on the dispersion and stabilization behaviour of alumina [6,11,12,19,24,53].

An alternative dispersant for alumina suspensions might be the polyethylene oxide-polypropylene oxide- polyethylene oxide (PEO/PPO/PEO) type block copolymers. Because they are effective over a wide pH range, wide structural variations make them effective for a variety of particle types and their high molecular weight provides effective steric stabilization [4]. There are many studies related with dispersion and adsorption behaviours of these polymers on many materials [1,13,16,38]. However there is very little information on the use of these polymers with alumina.

In this study, the objective was to prepare the fine alumina powders starting from Bayer gibbsite and obtain stable alumina suspensions in water by using PEO/PPO/PEO tri block copolymers.

During the powder preparation, thermal decomposition of gibbsite was achieved. It was attempted to increase the transformation rate to alpha alumina by mechanical treatment process like ball milling and use of ultrasonic bath. For the alumina suspension preparation, a tri block copolymer was preferred because they are important class of surfactants and find widespread industrial applications that include dispersion stability. Hence it was intended to investigate their effect on alumina particles in water.

CHAPTER II

ALUMINA

Many of the raw materials used in the ancient times are still used today and form the basis of the ceramic industry. These ceramic products are often referred to as traditional ceramics. The clay minerals are the main source for the production of these ceramics.

On the other hand, new ceramics, which are produced by refined or synthesized, are referred to as advanced ceramics. They include the oxide ceramics such as Al_2O_3 , ZrO_2 , MgO , etc. Among other oxides, alumina (Al_2O_3) is the most widely utilized one. It has a major importance as a raw material for the production of both traditional and advanced ceramics.

2.1 Structure and Transition Forms

There are many poly-types of alumina. Alpha alumina with hexagonal type of corundum structure is the most thermally and chemically stable one. Alumina has a mixed ionic and covalent bond structure. It has a low formation energy and high melting point as $2050\text{ }^\circ\text{C}$. Its single crystals are transparent [37].

Alumina has some intermediate, metastable forms. Haber in 1925 divided the alumina into two series, which is alpha and gamma that depends upon their calcination temperatures. The symbol alpha was applied to the more abundant form in nature and calcined at higher temperature [57].

The name gamma was given to an undescribed alumina by Ulrich in 1925. This term has been used in many cases for all the alumina transition forms occurred in the low temperature calcination of alumina. Then it was restricted

the name gamma to the product obtained in the dehydration sequence of gibbsite and boehmite at 500 °C [57].

As new forms have been identified, they have been assigned Greek letters. These transition phases are denoted as χ (chi), η (eta), ϵ (epsilon), δ (delta), θ (theta), γ (gamma), β (beta) and κ (kappa). Some additional monoclinic Al_2O_3 forms have been identified recently as θ' , θ'' , κ' and λ [32]. All of these metastable forms have partially disordered crystal structures based on a close packed oxygen sub-lattice with varying interstitial aluminum configurations. As equilibrium is approached the structures become more ordered until stable alpha alumina is formed.

The crystal structure of alpha alumina is often described as having O^{2-} anions in a hexagonal closed packed arrangement with Al^{+3} cations occupying two thirds of the octahedral interstices [28, 57, 32, 34].

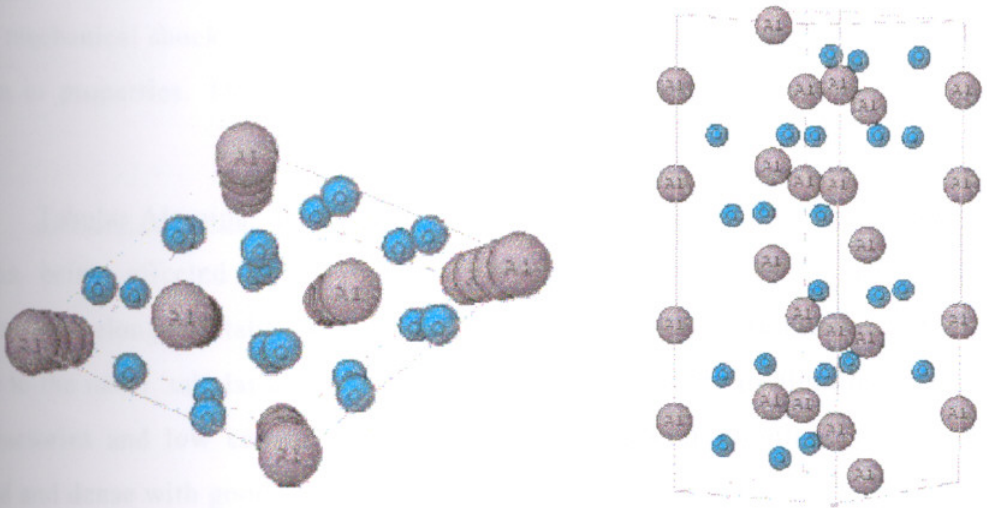


Figure 2.1. Crystal structure of alpha alumina.

All the metastable aluminas can be divided into two broad categories; a face centered cubic (fcc) and hexagonal closed packed (hcp) arrangement of oxygen anions [32].

The alumina structures based on (fcc) packing of oxygen include γ , η (cubic), θ (monoclinic) and δ (either tetragonal or orthorhombic) [32, 35].

While usually treated as cubic, gamma alumina has a slightly tetragonally distorted defect spinel structure (c/a about 0.99, the distortion varying with heat treatment). Also delta alumina has a tetragonal super structure [34]. On the other hand alumina structures based on the (hcp) packing are presented by α (trigonal), κ (orthorhombic) and χ (hexagonal) forms.

2.2 Types and Applications

Five types of alumina are generally considered for use in ceramic products: [14, 35, 57]

Activated Alumina: It is highly porous (about 200-400 m^2/g surface area) with granular form of alumina. This type of alumina generally used as a catalyst, catalyst carriers and adsorbent. It exhibits high resistance to thermal and mechanical shock and abrasion. Also it can hold moisture without change in form or properties. The crystalline structure is normally chi, eta, gamma and rho.

Tabular Alumina: They are nearly 100% alpha phase. The conversion to alpha being affected by heating the material above 1870°C. The large, hexagonal, elongated tablet shaped alpha alumina crystals characterize and give rise to the name 'tabular alumina'. They are used especially in alumina graphite refractories and low cement refractories mixes. Tabular alumina crystals are hard and dense with good thermal conductivity and high crushing strength [34].

Fused Alumina: Melting calcined alumina at above 2040 °C in an electric arc furnace produces them. It is produced in 2 forms: white and brown. White fused alumina is made from calcined Bayer alumina. Brown fused alumina is made from bauxite ore under conditions that allow only partial removal of impurities such as ferrosilicon [34].

Calcined Alumina: They are available in many grades based on the degree of calcination and Na_2O content (< 0.01 to nominally 0.5%). Fully calcined aluminas are primarily alpha phase. Calcined aluminas have the

hardness and durability character. There are 4 main uses of calcined aluminas. In the production of fused alumina, in the production of ceramics with high alumina content, as an additive material such as in refractory, as a polishing material [25].

Colloidal Alumina: It is an aqueous dispersion of nanometer sized alumina particles. The alumina particles are treated with an acid to produce a positive surface charge, which causes the particles to repel each other.

The important characteristics of alumina are the thermal resistivity, high hardness and electrical insulation and also the chemical stability. In addition to these its production process and the economic cost are the other factors within its advantages. However it has some limitations such as low toughness, poor thermal shock resistance and low temperature strength.

Alumina is also very important raw material in the production of traditional ceramics such as grinding media, wear resistant tiles, insulators, dinnerware, seals, and valves. In the high temperature engineering applications there are pipes, plates and jigs for high temperature uses, transparent tubes for sodium lamps, wear resistant parts like wire guides and nozzles, mechanical seals and cutting tools. In electrical applications it is used as spark plug insulators, electronic substrates, electrical insulation. In addition to these, because of their fine particle size, high surface area and catalytic activity of their surfaces, the transition alumina finds applications in industry as adsorbents, coating, soft abrasives, catalyst or catalyst carriers [32].

2.3 Alumina Production Methods

The powders which are used in advanced ceramics manufacturing such as alumina are generally in sub micrometer size range and tend to have a quite narrow size distribution to ensure rapid and uniform sintering leading to uniform grain size in the final product [46].

On the other hand abrasives must be available in many sizes. Refractories generally require a bimodal or multimodal particle size distribution. Many different powder synthesis, sizing, purification techniques have been developed to achieve the various required distribution. Today a great number of these techniques are available, differing widely in the characteristics of the produced powders, as well as in parameters such as yield and cost of production [47].

Important amount of the alumina production in the world is made from bauxite with the exception of few operations. Production methods are completely chemical and consist of only extraction of alumina from its impurities. Main types of alumina production methods can be grouped as:

Electrothermal Method: In this method mixture of the ore and the reducing material is melted in an electrical furnace so that impurities are reduced and melted alumina is obtained. Examples are Pedersen Process, Hall Process.

Sinter Method: This method can be applied both for the bauxites with high silica content and some type of clays. In this process the feed should contain necessary amount of sodium and potassium oxide for the conversion to alumina, limestone and nepheline.

Acidic Method: It is based on the principle of treatment of the ore with mineral acid solutions such as hydrochloric acid.

Basic Method: This method depends on the reaction of bauxite with NaOH and Na_2CO_3 . At the end of the reaction, aluminium oxide dissolves and the soluble sodium aluminate is obtained. Bayer Process is an example of this method [25].

2.3.1 Bayer process

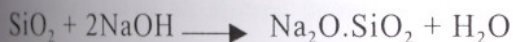
Bayer process is applied to the ores with low silica content. In other words this process is applied to high quality bauxites which contains more than 50% alumina and less than 15% silica. It consists five primary operations: Raw material preparation, digestion, clarification, precipitation, and calcination.

The first step involves crushing, blending and grinding of bauxite. In the process the ore is ground in ball mills with sodium hydroxide. Sometimes some lime is added to the mixture for caustification. Aim of this is to recover NaOH from harmful Na_2CO_3 .

Digestion step requires the dissolving of alumina from bauxite in a caustic soda solution under heat and pressure. During that operation most of the alumina goes into solution as sodium aluminate. In this step following reactions occur in the system:



Digestion is performed in steel autoclaves or in tubular reactors at temperatures up to 250 °C, 30 atm. with caustic concentrations up to 190 g/l. The digest slurry is held at temperature for an additional 15-30 minutes to decrease the silica concentration of the liquor by formation of a sodium aluminium silicate, which is insoluble in any aqueous solution.



Clarification step involves the separating of undissolved mud from sodium aluminate liquor. Pulp coming from autoclaves includes sodium aluminate solution and the insoluble residues known as red mud. Iron, silica and titanium from the bauxite remain insoluble and are removed by settling and filtration. But impurities like V_2O_5 , Cr_2O_3 and P_2O_5 get into solution. This mud

may have a very fine particle size. The fine solids behave as relatively stable colloidal suspensions so some flocculants such as starch are added.

Precipitation requires hydrolysis of the sodium aluminate. To carry out precipitation, aluminate liquor is seeded with the fines and the mixture is agitated. The seed grows to crystal agglomerates that are easy to separate and wash [25].

The filters feed large rotary kilns or fluid bed calciners where the obtained aluminium hydroxides are heated to 1100–1200 °C. By calcination hydrated alumina, is turned to unaqueous alumina. The types of hydrated aluminas obtained from bauxite in some cases by Bayer process and also their decomposition sequences will be discussed in the following headlines.

2.4 Aluminum Hydroxides

Alumina occurs in nature as impure hydroxides. These are the essential constituents of bauxite ores. Bauxite, is an impure mixture of boehmite, diaspore which are the α and β forms of $\text{AlO}(\text{OH})$, respectively and also other hydroxides.

Gibbsite (hydrargillite) is $\alpha\text{-Al}(\text{OH})_3$. It is a naturally occurring mineral but the Bayer process can be used to produce it. The oxygen ions in the gibbsite structure form close-packed layers with aluminium cations sandwiched in octahedrally coordinated interstices between the layers [32]. Grains of gibbsite precipitated in Bayer process are aggregates of tabular and prismatic crystals. Gibbsite usually contains some alkali metal ions. The highest alkali concentrations are found in technical trihydroxide produced by the Bayer process. It was showed that sodium is atomically dispersed in the crystal lattice of gibbsite.

Most of the technical trihydroxide is used as an intermediate in the manufacture of aluminium. Other industrial uses are white pigment, filler for

paper, fireproofing and reinforcing agent for plastics and rubber and as a raw material for the preparation of aluminium compounds [57, 32].

Bayerite, that is $\beta\text{-Al(OH)}_3$, is rarely found in nature but it can be prepared in the laboratory. The oxygen coordination in the bayerite structure is similar to that in gibbsite, but the distribution of hydrogen atoms is different [32]. It is produced commercially, principally for catalysts and applications requiring high purity aluminum hydroxides.

Boehmite, that is $\alpha\text{-AlO(OH)}$, is the major constituent of bauxite minerals and also it can be produced in the laboratory. For example by neutralizing aluminium salts at temperatures close to the boiling point of water. Heating pseudoboehmite results in the formation of transition alumina in a sequence similar to that associated with bayerite.

Samples of boehmite usually contain water in excess of the theoretical 15%. This water is probably bound as Al(OH)_3 , as judged by the temperature, kinetics and heat requirements of its decomposition. But some authors do not accept this hypothesis and consider the excess water as intercrystalline.

Diaspore, $\beta\text{-AlO(OH)}$ occurs in nature. The structure consists of hexagonal layers of oxygen [34]. The oxygen ions are nearly equivalent, each being joined to one other oxygen by way of a hydrogen ion and being arranged in hexagonal close packing. Since diaspore is usually associated with older bauxite, high pressure and elevated temperatures is necessary for the formation [57]. But also it can form at ambient temperatures and pressures.

2.5 Phase Relations of Aluminum Hydroxides and Oxides

Technical aluminum oxide is prepared by calcining gibbsite up to 1300°C . During heating the hydroxide undergoes a series of structural changes that yield technically valuable properties of the partially calcined product, such as high surface activity and large specific surface area [57]. The variables of the calcination process and the structures of the transition forms between the stable

hydroxides and the alpha alumina have been studied extensively during the past 50 years.

2.5.1 Thermal Decomposition of Aluminum Hydroxides

In many investigations the transformation of hydrous and transitional oxides of aluminum have been conducted with systems in which the nucleation step has not been controlled. These transformations have been widely characterised in terms of pore development.

Decomposition sequence of alumina is strongly dependent on the starting material and how it is processed. For example, if the starting material is boehmite then the most probable sequence is gamma (γ), delta (δ), theta (θ) and alpha (α). On the other hand, if the starting material is gibbsite, the sequence may include chi (χ), kappa (κ) and alpha (α). Another polymorph that is diaspore transforms directly to alpha alumina. During the transformation of all these aluminas, highly porous microstructure is developed [34].

Moreover, the sequence of transformation is not reversible when the temperature is decreased. In other words, neither alpha alumina nor the other high temperature forms can be converted to alumina that occur at lower temperatures. Hence they may be classified thermodynamically stable. At partial pressures of water vapour far below saturation and in the absence of mineralisers, a series of transformation occur that is demonstrated in Table 2.1.

Wilson and Stacey [59] studied these aluminium oxide phases derived from boehmite. According to them, the dehydration of crystalline boehmite is topotactic and produces γ -alumina. The subsequent transformation to δ and θ alumina is also topotactic (that is, changes in crystal structure are accomplished without changes in crystal morphology).

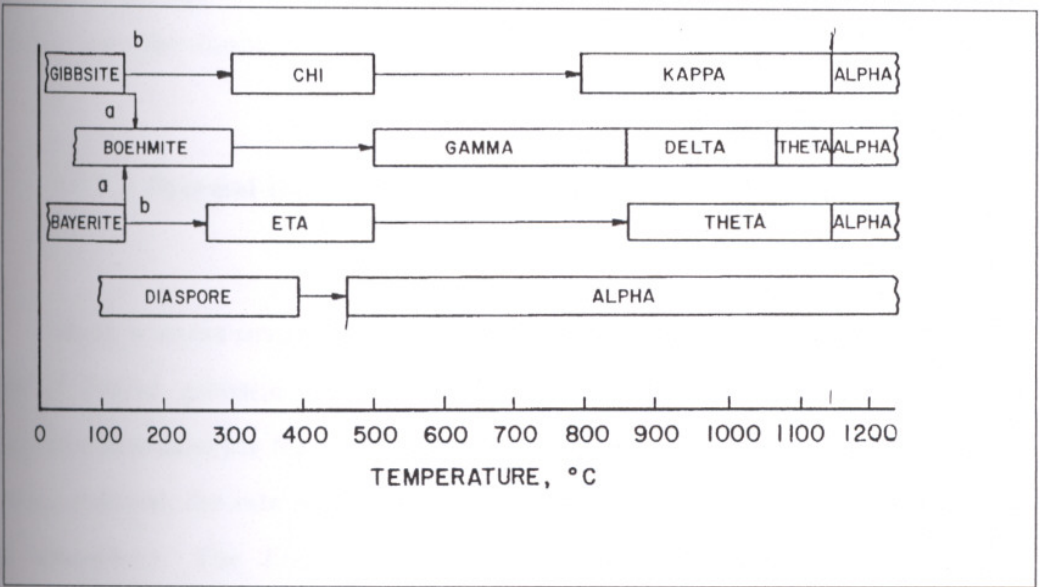
According to Levin et al. [32] the sequences of the phase transformations reported in the literature on passing from the metastable alumina structures to the final stable α alumina are approximate. This means, no direct experimental

evidence has confirmed the existence of a direct δ to θ transformation or disproved a direct γ to α transformation. Published experimental results suggest that the γ to α transformation is not direct.

Table 2.1. Transition sequences of aluminum hydroxides [57].

Path a: > 1 atm.- moist air, > 1°C/min., particle size >100 μ m

Path b: 1 atm.- dry air, < 1 °C/min., particle size < 10 μ m



Also according to the same authors it is possible to reach alpha alumina starting from tohdite. This conversion is followed by the following mechanism,

$5 \text{ Al}_2\text{O}_3 \cdot \text{H}_2\text{O}$ (Tohdite) convert to κ' at (700-800 °C) will followed by κ at (850 °C) and it will convert to α at 900 °C.

Iler [23] studied the conversion of boehmite to transition aluminas and α alumina. For this purpose starting materials were fibrillar colloidal boehmite, finely divided boehmite in the form of thin elongated platelets and macroscopic boehmite crystals. In the range 500 to 700 °C boehmite was converted to fibrillar γ (gamma) without unchanged in size. At about 1000 °C it yielded θ (theta)- alumina. Finally in the range 1000 to 1100 °C all the aluminas were converted to alpha.

Levin and Brandon [32] noticed that the transformation from fcc-based transition aluminas to alpha alumina often proceeds by nucleation and growth of individual single crystals of alpha alumina, with an internal porous vermicular-like microstructure, characterized by the coexistence of contiguous solid and pore phases. The development of a vermicular microstructure has been found to be a major obstacle inhibiting the pressureless sintering of nanosized transition alumina powders at low temperatures ($< 1300\text{ }^{\circ}\text{C}$). They also mentioned that the characterization of vermicular microstructure has received little attention, and no detailed attempt to analyse the morphology and the crystallography of this structure has been found in the literature.

2.5.1.1 Thermal Decomposition of Gibbsite

Many workers investigated the relationships between the specific surface area of heated gibbsite and variables of calcination. There is a general agreement that absolute figures depend on the purity and the particle size of the starting material, the rate of the heating and the vapour pressure of the water in the atmosphere. The Figure 2.2 illustrates the relationships between the temperature, specific surface area, density and loss on ignition of calcined gibbsite. Since the process is accompanied by an increase in density from 2.42 to 3.98 g/cm^3 a large internal surface area is created. Neither weight loss nor surface area is linear functions of temperature and time of calcination.

Dehydroxylation and change in density create a network of sub microscopic cracks in the heated gibbsite crystal. The internal surface area reaches a maximum at calcination temperatures between $300\text{-}400\text{ }^{\circ}\text{C}$. The initial step in the thermal decomposition of hydroxides is the diffusion of protons that react with OH^- ions to form H_2O . This process removes the binding forces in the gibbsite structure and changes the chemical composition. The layers break up into many areas of short- range order [57].

Most investigators agree that boehmite and a disordered transition alumina are formed upon heating of coarse gibbsite at about $400\text{ }^{\circ}\text{C}$. Calcination

of fine crystalline gibbsite, especially at low water vapour pressures, leads to the transition form only. Some researchers believed that this transition alumina is the χ -chi form. The stacking sequence of the layers of χ -alumina is strongly disordered. When fine-grained gibbsite is rapidly heated to about 300 °C under high vacuum an amorphous product, that is rho- alumina is obtained.

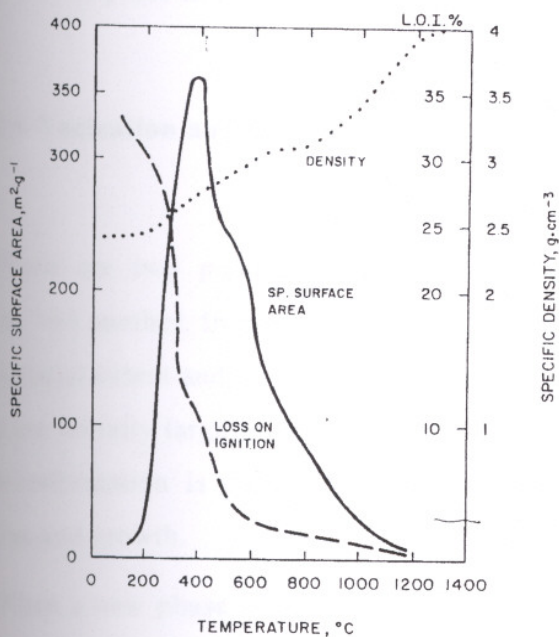


Figure 2.2. Relations between some properties of calcined gibbsite [57].

In 1958 it was distinguished two types of pores in the transition to χ -alumina. Between 225 and 250°C pores of about 30 Å were formed by the initial release of water resulting in surface area of 60 m²/g. As the dehydration proceeded, a second system of slit shaped pores developed having diameters of 10 Å and additional surface area of 200 to 250 m²/g. This texture was retained throughout the transition to alpha alumina. Surface area rises to a peak as 350 m²/g for one-hour calcination at 400 °C in dry air. It was pointed out that the highest surface area occurred at a composition of $\text{Al}_2\text{O}_3 \cdot 0.5\text{H}_2\text{O}$ for many atmospheres, temperatures and times of heating [57].

X-ray diffraction patterns of samples heated above 800 °C indicate a better-ordered transition form, κ -alumina. It has a loss on ignition of 1 to 2 %.

Only after prolonged heating above 1100 °C this value reduced 0.1 to 0.2 %. According to the Table 2.1, κ -alumina transforms to α -alumina at about 1150 °C in dry air, 1 atm. with $< 1^\circ\text{C}/\text{min}$. heating rate.

With the loss of practically all OH ions, the anion lattice of kappa is better ordered than that of the low temperature χ -form. In addition, a reordering of cations takes place in the transition χ to κ -alumina [57, 32].

2.6 Nucleation and Growth

There are two general types of processes by which one phase can transform into another. In the first type changes are initially small in degree but large in spatial extent and in the early stages of transformation. In the other type changes are initially large in degree but small in spatial extent. The first type of phase transformation is called spinodal decomposition and the latter termed nucleation and growth.

When a new phase is formed by nucleation and growth process, it must start in a very small region and then increase in size. Nucleation from a homogeneous phase is called homogeneous nucleation. However when the surfaces, grain boundaries, second phase particles and other discontinuities in the structure serve as favourable sites, the process is called heterogenous nucleation.

After a stable nucleus has been formed it grows at a fixed rate by conditions of temperature and the degree of supersaturation. The rate of growth is determined by the rate at which material reaches the surface and the rate at which it can build into the crystal structure [29].

The transformation from faced centred cubic (fcc) based transition aluminas to alpha alumina derived by calcination of various salts and hydroxides often proceeds by nucleation and growth of the individual single crystals of alpha alumina with an internal porous vermicular like microstructure, associated with the large volume change accompanying the transformation [32].

2.6.1 Effects of Seeding

The concept of seeding in order to enhance the kinetics and to control the development of the desired phase has been widely used in the synthesis of ceramics [51]. Seeding of a transition alumina with α alumina particles accelerates the kinetics of transformation and prevents formation of a vermicular microstructure. They are shown to act as nuclei for transformation and to result in an increase in the transformation kinetics and lowering transformation temperature. Seed concentration, seed matrix dispersion and size are critical parameters for successful control of the transformation. Many authors have added a variety of potential nucleation aids such as α - Al_2O_3 , CuO , MgO , α - Fe_2O_3 , α - Cr_2O_3 to alumina gels. The effect of these "seeds" is primarily dependent on the similarity of the crystal structure to α - Al_2O_3 .

Messing and co-workers [37] have demonstrated the controlled transformation and sintering of boehmite prepared by sol-gel in the presence of α -alumina seeding. According to their studies addition of α -alumina particles per 1 cm^3 of γ -alumina could effectively seed the alpha alumina phase transformation. The transformation temperature decreased as $170 \text{ }^\circ\text{C}$ with seeding and the incubation time was reduced from hours to a few minutes. In addition to these effects the refinement and reduction of alpha alumina sintering temperature to below $1200 \text{ }^\circ\text{C}$ was more important. They attributed the temperature reduction for the sintering to the avoidance of the development of the characteristic vermicular microstructure, microstructural refinement and reduction of diffusion distances.

Wakao and Hibino [29] added a number of different oxides up to 10 wt% to an aluminium sulphate derived γ -alumina and they reported that the temperature of the θ to α -alumina transformation was reduced in all cases, with CuO and Fe_2O_3 lowering the transformation temperature to as low as $1050 \text{ }^\circ\text{C}$. Bye and Simpkin added chromium and iron via a solution technique to γ -alumina powder. They showed that the transformation temperature was lowered to 995°C with 5% Fe but Cr additions had no effect.

Kumagai and Messing [30] added 1.5 wt% α -alumina to pseudoboehmite gels and found the α -alumina crystallization peak temperature was reduced from 1215°C to 1075°C. Similarly, hematite (α -Fe₂O₃) seeds lower the crystallization peak because hematite has the corundum crystal structure. Additives with a crystal structure very different from α -alumina tend to have less significant or no effects on the transformation to α alumina.

Dynys and Halloran [10,51] added the equivalent of 0.4 wt% MgO, α -Fe₂O₃ and α -Cr₂O₃ via water-soluble salts to aluminium secbutoxide derived boehmite. They showed α -Fe₂O₃ enhanced the transformation kinetics while α -Cr₂O₃ and MgO additions had no effect in transition. Also they have reported a nucleation density of 10⁸ cm⁻³ for an alum derived γ -alumina. The reason for the strong influence of seed concentration is due to the degree of grain refinement (volume per seed) by controlled transformation. The effects of seed concentration and seed/matrix dispersion probably explain why they did not observe an effect on the α alumina transformation when they added α -alumina particles to an γ -alumina powder.

Shaklee and Messing [3] used HF as a mineraliser for the transformation of γ to α -alumina. They proposed that vapour transport by AlF₂O increased the transformation rates. The transformation to alpha alumina was complete after 30 minutes at 900 °C when optimum reactant concentrations were used.

In another work, the influence of different additives on the kinetics of the phase transformation has been studied. According to this study, less than 1 wt% of additive did not change the sequence of the polymorphic transformation during dehydroxylation of aluminium trihydroxide, but it has been observed that the promotion of α -alumina formation is accompanied by destabilization of θ -alumina. The influence of the additives on the transformation has been related to the respective radii and then charge of the specific cations. The additives promote α -alumina formation for differences in ionic radii between the host and foreign cations of < 33%, whereas a difference in the radii of >33% stabilize the less dense δ or θ -alumina forms [32].

Saito et al. [49] studied the effects of various SiO_2 phases on the γ alumina to α -alumina phase transition. According to their results by adding amorphous SiO_2 such as fumed silica was considered to retard the transition by preventing particles from coming into contact and suppressing heterogeneous nucleation on the γ -alumina surface. On the other hand addition of a crystalline SiO_2 , such as quartz and cristobalite, showed a different effect. They attributed the reason of acceleration of the γ to α phase transition to the heterogeneous nucleation mechanism.

Bagwell and Messing [3] studied transformation kinetics and coarsening rates in unseeded and α -alumina seeded γ -alumina powders heated in dry air and water vapour. According to their results altering both nucleation and growth process accelerated the transformation. Seeding the transformation with α alumina effectively eliminated the barrier to nucleation. Also the presence of the water vapour accelerated diffusion in the system. Seeding with α -alumina increased the transformation rates and reduced incubation times by providing low-energy sites for nucleation and growth of the α -alumina transformation.

In another study influence of zirconium and magnesium dopants on the transformation from the transition aluminas to α -alumina have been studied. The addition of magnesium cations enhanced the rate of the transformation from γ or δ alumina into the α -alumina form, whereas the addition of zirconium cations inhibited the transformation. Also it was demonstrated that the presence of water vapour enhances the rate of the transformation [32].

The published results showed that additives can influence both the temperature and the rate of the gamma to alpha form transformation, and they can change the sequence of intermediate phases during transformation.

2.6.2 Effects of Mechanical Treatment

A mechanical pre-treatment like compaction or dry ball milling of transition alumina powders significantly affects the kinetics of the transformation. Dynys and Halloran studied the formation of α -alumina in γ alumina, which is obtained from ammonium alum at 1150 °C.

According to their results, mechanical treatments of the gamma alumina markedly increased the density of the nuclei and the transformation rate. The nucleation density affects the final grain size by dictating the volume of transition alumina matrix. To determine the effect of mechanical pre-treatment, they compared the transformation kinetics of untreated powders with the kinetics of powders, which had been either compacted in a biaxial, die or dry ball-milled or both [9]. They reported that the nucleation frequency increased from 10^8 to 10^{12} cm^{-3} after ball milling the γ -alumina powder in an alumina ball mill with alumina media. They also demonstrated that the compaction of the γ -alumina powder prior to transformation increased the transformation kinetics. They carried out experiments to determine whether α -alumina 'debris' or particles generated during milling may have increased the transformation kinetics, but it was concluded that the mill 'debris' was not responsible for the increased nucleation frequency.

According to the results the reason for the improvement of the nucleation rate may be enhancement by the creation of the new surfaces during milling. But the observation that the BET surface area was nearly unaffected by milling suggested that little new surface has been created. It was possible that this small new surface could provide potent sites for nucleation. A possible explanation for the increase in the nucleation frequency could be framed in terms of a break down of the foamy macrostructure of the calcined powder.

As a result they concluded that the mechanical pre-treatment apparently increases the rate of nucleation frequency of α -alumina, but the mechanism remains uncertain. Nucleation of α -alumina in γ -alumina precursor at a high compaction pressure may occur by shear of the atomic planes in the γ -alumina.

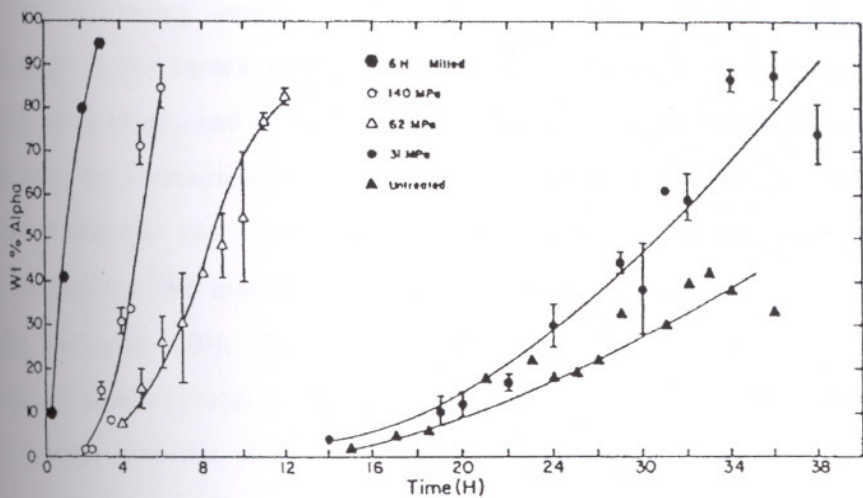


Figure 2.3. Formation of α -alumina in untreated and die-pressed γ -alumina powders at 1150 °C [9].

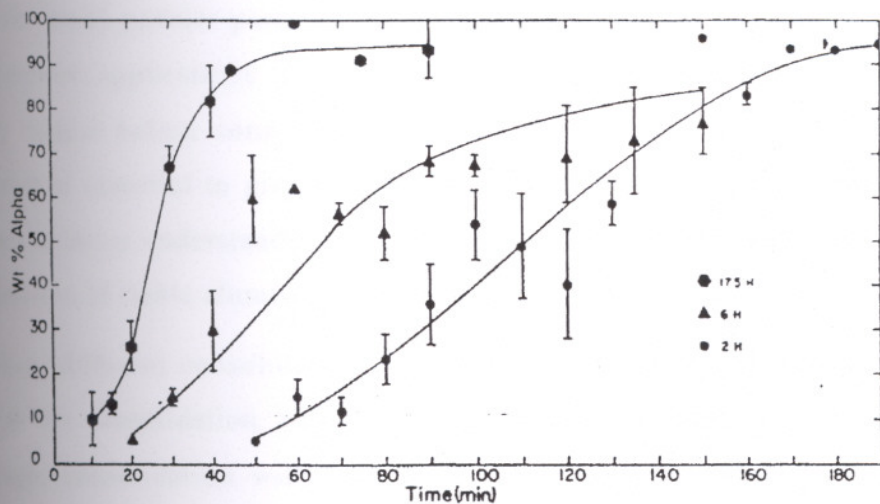


Figure 2.4. Formation of α -alumina in ball milled γ -alumina powders annealed at 1150 °C [9].

2.7 AQUEOUS ALUMINA SUSPENSIONS

Colloidal processing of advanced ceramic powders such as alumina has received an increasing amount of attention in recent years [17]. A clear understanding of the interactions between the particles dispersed in aqueous media with each other, and with the surrounding phase has a great importance for those who are interested in the outcome of such processes as flocculation, dispersion, flotation, etc. An understanding of these interactions therefore essential to improve the quality of the alumina ceramics produced by colloidal processing methods [20]. In other words, key factors for the successful production of these ceramics are the homogenisation and dispersion of the powder particles and the stability of the suspension. In general, the goal in colloidal processing of ceramic powders is to achieve homogeneous suspensions with high solid loading and defined rheological properties [21].

Alumina powder dispersions in liquids are normally very unstable because the small powder particles have tendency to create agglomerates [35]. So in ceramic applications of this powder, a pre-consolidation step may generally require before consolidation of this powders to specified shape. At this point it is essential to give some information about ceramic consolidation techniques to better understanding of importance of the colloidal processing and the preparation of stable alumina dispersions.

Many different consolidation techniques are used in industry. They are divided as dry consolidation, that is pressing; plastic forming or consolidation with dough; consolidation with slip, that is casting [35]. Major compaction techniques are listed in Table 2.2.

Slip casting and pressing are the major consolidation techniques in the production of alumina ceramics. Feed having a slurry consistency may be formed by the casting technique. In slip casting, the slurry is poured into a porous mold. Capillary section of the mold absorbs liquid from the slurry and particles that consolidate on the surface of the mold form a cast. Pressure or vacuum may be applied to increase the casting rate [50,47,43,34]. Since slip

casting is the most widespread of all the consolidation techniques and it is commonly used for production alumina ceramics it will be mentioned in detail in the following paragraphs.

Table 2.2. Ceramic consolidation techniques [50].

Pressing	Fugitive- mold casting
Uniaxial	Gel casting
Isostatic	Tape casting
Hot pressing	Waterfall
Hot isostatic pressing	Plastic forming
Slip Casting	Extrusion
Drain casting	Injection molding
Solid casting	Roll forming
Vacuum casting	Compression Molding
Pressure casting	
Centrifugal casting	

During slip preparation step the powder, binder, wetting agents, dispersing agents and sintering aids are added to the mill with the proper casting liquid and milled to achieve mixing, wetting and particle size reduction. The type of the additives, which will be used for the slip preparation, differs according to the type of the casting process.

In slip casting and other consolidation techniques usage of the processing additives has a major importance. For example in tape casting, cast films must be strong but also flexible after drying. This requires high concentration of binder and plasticizer. On the other hand, in slip casting process usage of dispersing agents become important since a successful casting operation depends on homogenisation and dispersion of the slurry [50]. Figure 2.5 shows the schematic representation of slip casting process.

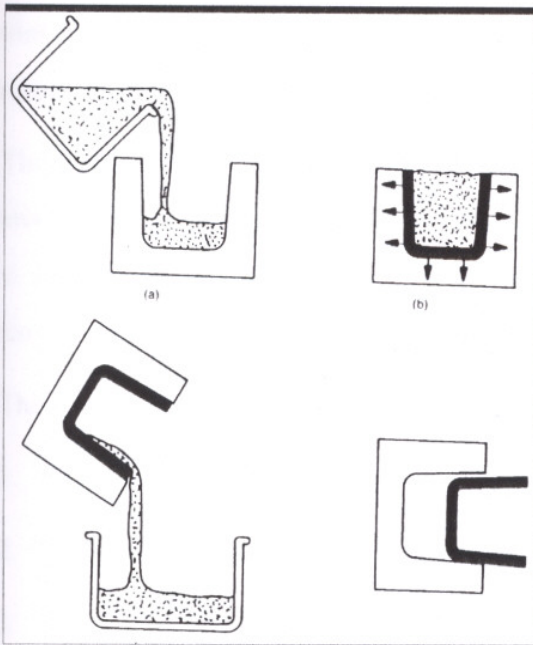


Figure 2.5. Schematic representation of slip casting [46].

In all casting slips it is essential to have a significant part of the particles in the colloidal range of size. This is important because it controls the rheology and sedimentation behaviour of the particles. The particle size distribution has a strong influence on the packing character during cast formation and thus it will influence the properties of the green body. The other main factor is the character of the particle interactions. These control flocculation or dispersion behaviour of the particles, which make the slip [35].

2.7.1 Interaction Forces In Dispersed Systems

The key element in colloidal processing of alumina powders is control over the interparticle forces within the suspension during all stages of processing. Certain steps in wet powder processing depend on repulsive forces between the particles, whereas other steps may require attractive ones.

Most substances gain surface electrical charge when brought into contact with a polar medium. Alumina particles have a positive charge in water below

their point of zero charge. This electrical charge may result from one or more mechanisms which involve ionisation, ion adsorption or ion dissolution [58].

The nature of the forces acting between particles creates the properties of the mixture. Here it is also important to note that the length time scales. For instance, some of the forces depend on the particles separation distance and may only become important at close distances of separation.

The most important types of interparticle interactions are as follows:

1. Electrical double layer interactions
2. Van der Waals attractions
3. Steric interactions

Repulsive electrostatic forces produced by the interaction of particles, which carry charges. They have an important effect especially in polar solvents with high dielectric constant, especially in water.

Attractive Van der Waals forces are always present. Because they are produced by the interactions of atoms with electron nucleus dipoles on the surface of the particles.

On the other hand, repulsive steric forces are important especially in nonpolar organic solvents. But they are also affected in polar solvents. They are due to interaction long chain molecules, like polymers [35].

The tendency of colloidal particles to undergo aggregation may be analysed by the help of the DLVO theory of Derjaguin and Landau and Verwey and Overbeek [52]. In this theory the stability of a dispersion of hydrophobic charged colloidal particles in an aqueous medium is described by the pair wise interactions between the particles.

The total potential energy of interaction V , between two particles as a function of their surface to surface separation H , can be represented by the summation of two interaction energy terms:

$$V = V_A + V_R \tag{2-1}$$

Here V_R represents the electrical double layer repulsive energy between two charged particles and V_A is the Van der Waals attractive energy. For any particle system, diagrams of V against H can be drawn, from which it can be explained that attraction tends to control at both very small particle separations and large separations. The energy minimum corresponding to these situations are shown by the primary minimum and the secondary minimum respectively. The Figure 2.6 represents the potential energy diagram of interactions between the two particles.

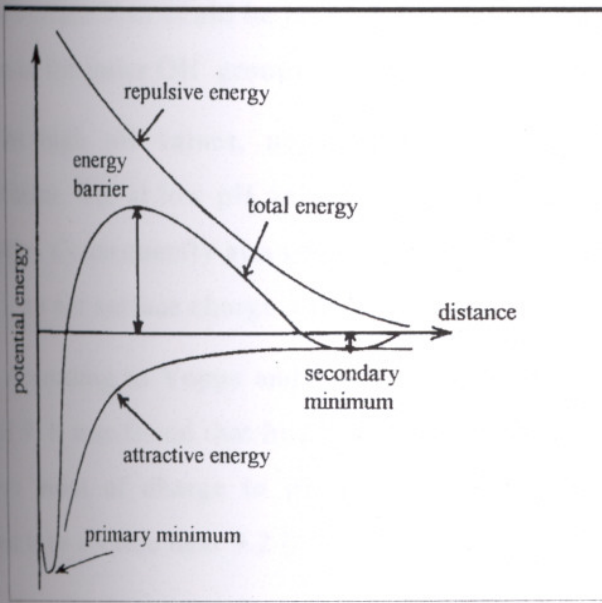


Figure 2.6. Potential energy diagram of interaction between the two particles [58].

Stabilization can only be achieved when the electrical repulsion is sufficient to overcome the aggregation influence of the Van der Waals attraction. When this condition is achieved the net repulsion can be seen in the potential energy diagram as primary maximum (V_{max}). This point is created by the changes in V_R and V_A but also by the existence of another term V_S . This term arises from the short-range steric interactions and also it exists between the adsorbed layers when the particles undergo a close approach [22, 26, 52, 27]. As a result, the total interaction energy equation becomes:

$$V = V_A + V_R + V_S \quad (2-2)$$

In addition to these in some cases another interaction term that arise from bound water related with the adsorbed surfactant head group may included to above equations. But since it is a more specific interaction term, general equation was given with the summation of three terms.

2.7.1.1 Electrostatic Stabilization

Depending on the pH of the ionic environment or medium negatively charged surface ions could be created. On the contrary binding H^+ ions from the medium to the polar OH^- groups can create positively charged ions.

At high pH values, negatively charged surface sites are greater and predominant. But at low pH values, the positive charge will be effective on the net charge. Consequently at a certain value, which is called zero point of charge (pH_{ZPC}), no net surface charge will be present.

According to Yopps and Fuerstenau the point of zero charge of alumina is at pH 9. It was found that heat treatment of synthetic alpha alumina decreased the zero point of charge to pH 6.7 but that aging for seven days in water returned it to a value near 9.2 [57].

Here the important fact is that, the charged particle surface portions will attract with counter ions from the solution. They will surround the particle and some portion of them will bond to the surface.

According to the theory, which is called 'double layer theory' these particles will create, a thin layer. It contains strongly bound, immobile, charged molecules. This is called Stern layer. On the other hand, the larger portion of the counter ions will form an adjacent layer, which contains loosely bound molecules. This is called diffuse layer and its molecules extend much deeper into the medium. Schematic representation of the electrical double layer was demonstrated in Figure 2.7.

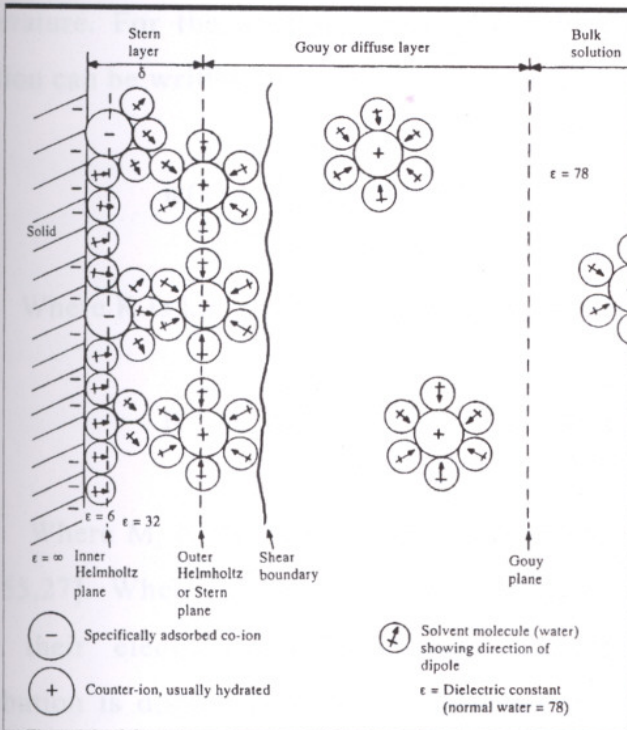


Figure 2.7. Electrical double layer models for particle charging in a polar liquid [58].

The classical aspects of this theory have been developed by Gouy (in 1910), Chapman (in 1917), Debye and Henkel (in 1923). Later modifications have been made by Stern (in 1924) and Grahame (in 1948). Among these models, the simplest is the capacitor model. In this model the interface is considered to a charge storage device like a parallel plate capacitor. In most situations such a model is inappropriate. In that case, a model, which divides the double layer into two regions like Stern layer and diffuse layer, is more realistic [58,35,22].

For the diffuse layer the Poisson-Boltzman equation can be written in one dimension:

$$d^2\psi / dx^2 = - (e/\epsilon)\Sigma z_i n_{i_0} \exp (z_i e\psi / kT) \quad (2-3)$$

Where ψ is the potential at a distance x from the surface, ϵ is the permittivity of the medium, n_{i_0} is the bulk concentration of ions of charge z_i , e is the electronic unit charge, k is the Boltzman constant and T is the absolute

temperature. For the assumption of, low charge $(z_i e \psi / kT) < 1$ cases this equation can be written as,

$$\psi(x) = \psi_\delta \exp(-Kx) \quad (2-4)$$

Where K is known as the inverse Debye length,

$$K = \left\{ (1000 e^2 N_A / \epsilon K T) \sum z_i^2 M_i \right\}^{0.5} \quad (2-5)$$

Where M_i is the molar concentration and N_A is the Avogadro's constant [58, 55, 27]. When two particles, which carry similar, charge approach each other their electrical double layers overlap so the equilibrium charge distribution is disturbed. The repulsion potential increases as the free energy increase after this event. This repulsive potential energy can be written as [22],

$$V_R = (KT/ze)^2 a \gamma^2 \exp- KH \quad (2-6)$$

$$\text{Where, } \gamma = (e^{x/2} - 1 / e^{x/2} + 1) \text{ and } x = ze\psi_d / kT \quad (2-7)$$

In the presence of the adsorbed layers;

$$V_R = 32 \pi \epsilon_r \epsilon_o (KT/ze)^2 (a+\delta) \gamma^2 \exp- KH \quad (2-8)$$

Where H refers to the separation between the adsorbed layers of the particles. If these were the only forces acting then particle would not be aggregate. But the presence of Van der Waals attraction forces may cause agglomeration. If it is taken the basic expression for identical particles, the net attraction energy can be written as,

$$V_A = -A_{12}A/12 h \quad (2-9)$$

Where A_{12} , is the Hamaker constant for the system of two identical solids separated by a second liquid medium [58].

2.7.1.2 Polymeric Stabilization

Polymeric stabilization is a general term to describe all aspects of the stabilization of colloidal particles by polymer molecules. It may be achieved by two different mechanisms [8]:

- (1) Steric stabilization
- (2) Depletion stabilization

2.7.1.2.1 Steric Stabilization

Steric stabilization is a term generally applied to colloid stabilization by polymers [22]. According to William R. [35], the most industrially significant type of interaction is the steric interactions. It arises if adsorbed molecules, commonly polymers, are present on the surface of the particles. Especially in non-polar organic systems electrostatic repulsion will not be so important. On the contrary, stabilization by adsorption of polymer molecules plays the main role. Molecules, which consist hydrocarbons, attached themselves to the particle surface by anchoring head groups. Also the rest of the molecule extends into the liquid medium. These hydrocarbon chains are responsible for the steric hindrance effect.

Particle anchoring may be achieved by hydrogen bonding of hydroxyl groups in the polymer to the oxide particle surface. If shorter surfactant molecules are exist anchoring can be occurred by acid-base reactions. Also multiple anchoring of one polymer molecule to a suitable group is very efficient, because the molecule forms loops and tails, which cover the large part of the surface. But these parts of the molecules should be suitable to the medium. If not, attraction may occur between the polymer chains. The steric layer may consist of loops, tails and trains of the polymer segment [35].

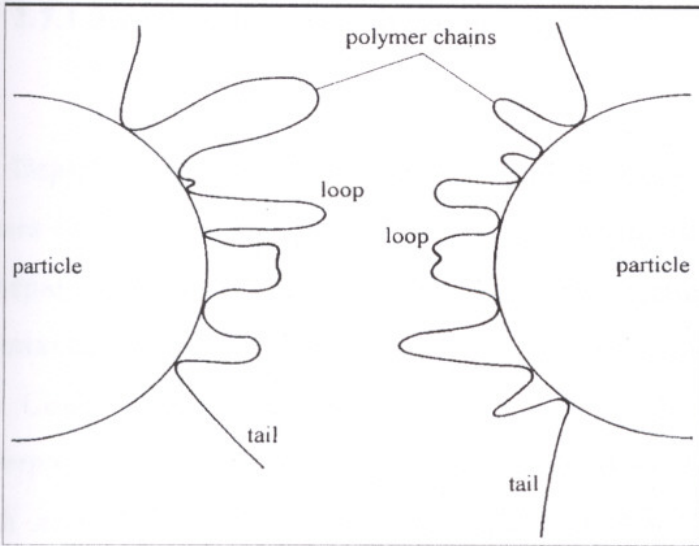


Figure 2.8. Schematic of particles having adsorbed polymer molecules [35].

Polymers, surfactants and polyelectrolytes have been shown to decrease the rate of flocculation of dispersed particles. The adsorbed layer acts as barrier that prevents the particles to get closer. The adsorbed layer must therefore be thick enough to control the interparticle interactions and prevent close approach. Stabilization against flocculation becomes more difficult as the particle size increases [12].

The steric mechanism has two elements that contribute to overall stability of the system. The first is the interpenetration effect of the solvated polymers related to approach of the particles. It leads to an overall increase in the segment density of the solvated polymer. Also it gives rise to the interparticle osmotic pressure. Connected with it, this effect gives rise to the repulsive potential.

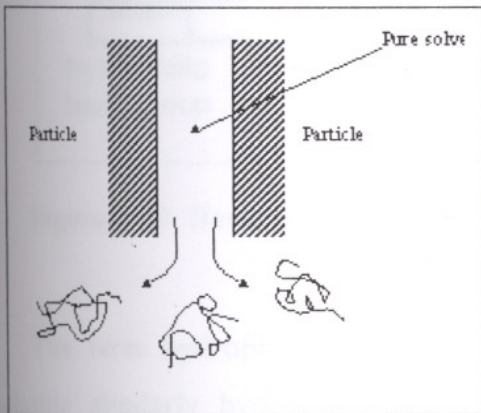
If approach of the particles continues, the constraint of the polymer leads to decrease in the configurational entropy of the polymer and increase in the overall free energy of interaction. Also it will lead to repulsive component to the interaction potential. Both osmotic and entropies contributions to the interaction potential will lead to repulsion and colloidal stability [58,46,35,29]. The success of steric stabilization depends on the surface coverage, the configuration of the adsorbed polymers and the thickness of the adsorbed layer.

2.7.1.2.2 Depletion Stabilization

Depletion stabilization refers to stabilization of colloidal suspensions by polymers in free solution. In the case of the approach of two particles from a large separation distance, closer approach of the particles must be accompanied by demixing of the polymer molecules and the solvent in the interparticle region. Consequently, work must be done to make the polymer molecules leave the interparticle region. This corresponds to repulsion between the particles that, if high enough, can lead to stabilization of the suspension. This type of stabilization is referred to as depletion stabilization [8].



(a) Depletion stabilization at separation greater than the diameter of the polymer coil.



(b) Depletion flocculation at small separations.

Figure 2.9. Polymeric stabilisation by free polymer molecules in solution [8].

2.7.1.2.3 Surfactants

A surfactant (contraction of the term surface-active agent) is a substance that, when present at low concentration in a system, has the property of adsorbing onto the surface or interfaces of the system and altering a marked degree the surface or interfacial free energies of those surfaces. The term interface indicates to a boundary between any two immiscible phases, the term surface indicates an interface where one phase is a gas, usually air.

The applications of surfactants in science and industry are so common. It ranges from primary process such as the recovery and purification of raw materials in the mining and petroleum industries, to enhancing the quality of the finished products such as paints, cosmetics, ceramics, pharmaceuticals and foods [48].

Surface active agents have some structural groups that have either little attraction for the solvent or the strong attraction for the solvent that is called lyophobic and lyophilic groups respectively [48, 47].

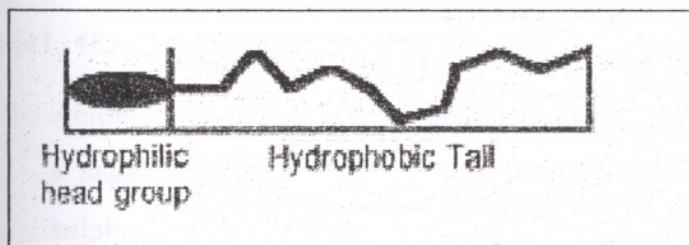


Figure 2.10. Basic molecular structure of a surface active agent [45].

The term hydrophobic can be often used instead of the more general 'lyophobic' similarly, hydrophilic can be employed instead of 'lyophilic'. But that generality is implied when water based systems are used.

Materials that gain chemical groups leading to surface activity are generally called as amphiphilic (liking both). This definition explains that they have some affinity for two immiscible phases [41, 22]. The amphiphilic structure of surfactant molecule not only results in adsorption of the surfactant molecules

but also creates the orientation of the adsorbed molecules. This molecular orientation produces some important effects for the surface-active materials.

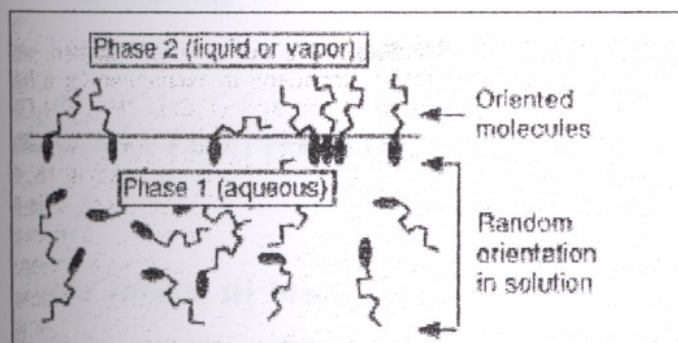


Figure 2.11. Orientation of surfactants in liquid medium [45].

Surfactants may be classified in many ways, depending on the intentions. For example, they may be classified according to its applications. Hence they may be classified as emulsifiers, foaming agents, wetting agents, dispersants, etc. The simplest structural classification may be done according to the nature of the solubilizing functionality. The most useful classification of the surfactants may be based on the nature of the hydrophil, with subgroups that is defined by the nature of the hydrophobe. The four general groups of surfactants are defined as follows [41, 48]:

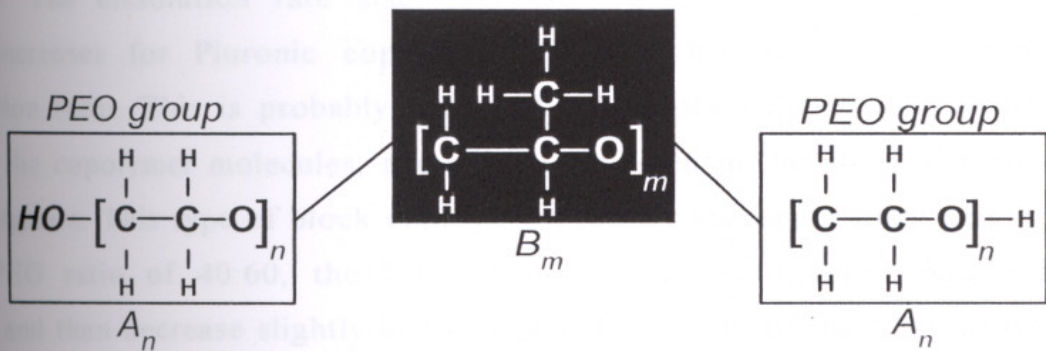
1. Anionic: In that type, the surface active portion of the molecule carry a negative charge such as soap, alkyl benzene sulphonate, carboxyl, sulphonate or sulphate.
2. Cationic: Surface active portion of the molecule bears a positive charge, for example salt of a long chain amine, quaternary ammonium chloride.
3. Non-ionic: Where the hydrophil has no charge but derives its water solubility from highly polar groups such as poly oxyethylene, mono glyceride of long chain fatty acids.
4. Zwitterionic: Both positive and negative charges may be present in the surface active portion, like long chain amino acids and sulfobetaine.

4. Zwitterionic: Both positive and negative charges may be present in the surface active portion, like long chain amino acids and sulfobetaine.

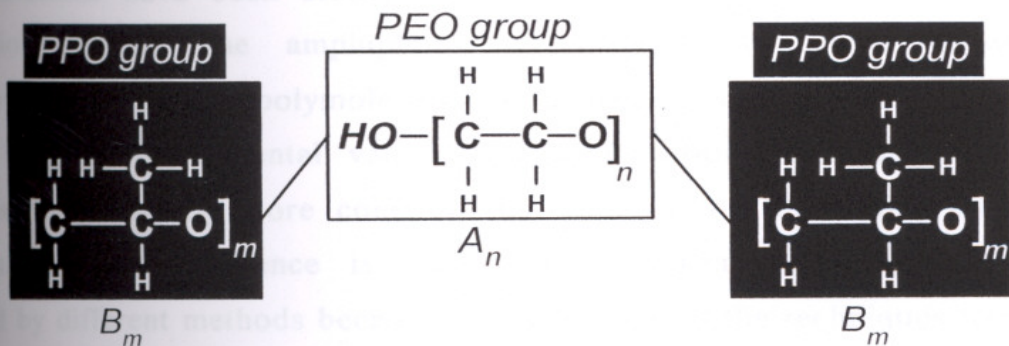
2.7.1.2.3.1 PEO/PPO/PEO Block copolymers

Water soluble tri block copolymers of polyethylene oxide (PEO) and polypropylene oxide (PPO) are often denoted PEO/PPO/PEO or $(EO)_{n_1}(PO)_m(EO)_{n_2}$ are commercial available non-ionic macromolecular surface active agents. They are an important class of surfactants and find widespread industrial applications in detergency, dispersion stabilization, foaming, emulsification, lubrication, pharmaceuticals, bioprocessing. Commercial names for these surfactants are Poloxamers (manufactured by ICI) and Pluronics (manufactured by BASF) [2].

These surfactants are synthesized by the sequential addition of propylene oxide (PO) and ethylene oxide (EO) to a low molecular weight water-soluble propylene glycol. The PEO/PPO/PEO type block co-polymers were water soluble and consisted of a polypropylene oxide chain linked to polyethylene oxide chains at both ends (Figure 2.13). Generally, copolymers with a medium to high ethylene oxide content provide optimum dispersion. Within this range the nature of the particle to be dispersed determines the surfactant selection. For example, products high in ethylene oxide (80%) are more effective for inorganic pigments, while products with medium EO content (40-50%) are more effective for organic pigments [4,7]. Industrially used tri block copolymers of EO-PO range in molecular weight from 1000 to 30,000 [48]. Figure 2.12 and 2.13 show the synthesis and structural formulas of PEO/PPO/PEO block copolymers respectively.



a) PEO/PPO/PEO type tri block copolymers (F-68, F-127, 6400, P-104) (Table 3.1): n = Number of EO groups, m = Number of PO groups.



b) PPO/PEP/PPO type tri block copolymers (Pluronic 10R-8) (Table 3.1): m = Number of PO groups, n = Number of EO groups.

Figure 2.13. Structural formulas of PPO/PEO tri block copolymers.

The PEO content in PEO/PPO/PEO copolymers influences the rate of dissolution: this rate decreases as the relative proportion of the PEO block increases. The dissolution rate also decreases as the copolymer molecular weight increases for Pluronic copolymer groups with the same PPO/PEO composition ratio. This is probably result of the degree of hydrogen bonding between the copolymer molecules, and is also reflected in the physical form of the copolymers. This type of block copolymers exhibit maximum foam height at a PPO/PEO ratio of 40:60, the foam properties of each copolymer series increase and then decrease slightly as the molecular weight of the PPO segment increases. Copolymers with high PPO content are effective defoamers. Also copolymers with PPO blocks of high molecular weight are generally better emulsifiers than the lower molecular weight homologs. The thickening power of each series of copolymers increases as the PPO block molecular weight increases and as the PPO/PEO ratio decreases [56].

Micelle formation properties of PEO/PPO/PEO block copolymer in aqueous solutions have been studied extensively. The critical micellization concentration (CMC), the amphiphile concentration at which micelles (thermodynamically stable polymolecular aggregates) start forming, is a parameter of great fundamental value. The micellization amphiphilic block copolymers are inherently more complex that that of low molecular weight surfactants. A large difference is often noted between the CMC vales determined by different methods because the sensitivity of the techniques to the quantity of dispersed copolymers present in solution may vary. For common surfactants, a considerable amount of CMC data has been collected by Mukerjee and Mysels whereas for block copolymers only little CMC data have been available in the literature [1, 2, 56].

Light scattering and fluorescence spectroscopy experiments have shown that PPO/PEO/PPO block copolymers of suitable PPO/PEO composition and molecular weight do indeed form polymolecular aggregates in solution. The CMC of this type of block copolymers decreases with increasing temperature. Wanka et al. [2] reported that aggregation numbers increase with temperature, while the micelle radius remains approximately constant [56].

It is apparent from the experimental studies that PPO/PEO/PPO copolymers which are relatively less hydrophobic, either due to a high PEO content or low molecular weight, do not form micelles at room temperatures, but do start to aggregate at higher temperatures. This can be explained by the fact that water becomes a poorer solvent for both ethylene oxide and propylene oxide segments at higher temperatures [56].

2.7.2 Rheology

Rheology is the science of deformation and flow. The rheological characterization of formulated dispersions is an essential parameter in formulation development [58]. Also the well defined rheological properties is essential during the processes like pumping, transporting, milling, mixing and forming ceramic systems. Ceramic slurries are commonly multi-component systems and relatively complex [46].

Flowing liquid or objects moved relative to a liquid phase generate shearing effects. To produce a certain shear rate dv/dx , an adequate shear stress τ has to be provided for the molecules to be moved relative to each other [35].

When a shear stress τ is linearly dependent on the velocity gradient, ($-dv/dy$), the liquid is called Newtonian.

$$\tau = \eta_L (-dv / dy) \quad (2-10)$$

The constant of proportionality is the coefficient of the viscosity η . The velocity gradient ($-dv / dy$) is the shear rate γ .

The viscosity of a suspension η_s is greater than the viscosity of the liquid medium η_L in the suspension. Also the ratio is referred to as the relative viscosity η_r . For a very dilute suspension of non-interacting spheres in a Newtonian liquid, the viscosity of the laminar flow is described as,

$$\eta_r = \eta_s / \eta_L \quad (2-11)$$

In liquids containing large molecules, laminar flow may orient the molecules or particles. When orientation reduces the resistance to shear, the stress required to increase the shear rate. This behaviour can be described as,

$$\tau = K \gamma^n \quad (2-12)$$

Where K is the consistency index and $n < 1$ is the shear thinning constant. It indicates the departure from Newtonian behaviour. The apparent viscosity decreases with increasing shear rate and this behaviour is called the shear

thinning or pseudoplastic. The apparent viscosity of this material described by the power law equation is,

$$\eta_a = K \dot{\gamma}^{n-1} \quad (2-13)$$

Also the pseudoplasticity is the characteristic behaviour of weakly flocculated suspensions [43,34,40]. The mechanism for this effect can be described in terms of the release of the liquid medium entrapped within agglomerated flocks. Pseudoplastic or shear thinning systems show a decrease in viscosity with increasing shear rate. Power law materials have no yield point.

In densely packed suspensions the viscosity may increase with increasing shear rate. Such behaviour is referred to as shear thickening or dilatant and may arise at shear rates above a critical value when shear planes are disrupted. Dilatancy can provoke insufficient flow during slurry processing. It indicates that the existence of an extremely concentrated, stabilized dispersion with insufficient compatibility between the medium and the stabilizing molecules [43, 34].

Slurries containing bonded molecules require a stress called the yield stress. Also the material is called a Bingham plastic when the flow behaviour is described by the equation,

$$\tau = \tau_y + \eta_p \dot{\gamma} \quad (2-14)$$

The apparent viscosity η_a of a Bingham material is higher when the yield stress is higher and decreases with increasing shear rate. A Bingham system behaves similarly to a Newtonian system in that once the shear stress exceeds a certain value, the yield stress, the shear stress is proportional to the rate of shear.

Another equation often used to describe the shear stress–shear rate behaviour of a system containing weakly bonded particles is the Casson equation:

$$\tau^{0.5} = k_1 + k_2 \dot{\gamma}^{0.5} \quad (2-15)$$

Where k_1 and k_2 are structure dependent constants. This equation provides shear thinning behaviour with non-linear dependence of the shear stress on shear rate.

For some materials the apparent shear resistance and viscosity may decrease with shearing time. This is called thixotropy. In other words, time dependent shear thinning and time dependent shear thickening behaviour is referred to thixotropy and rheopexy respectively. For sterically stabilized slurry is left undisturbed for a certain period, weak interlinked bonds may be generated. If the effect of thixotropy is not pronounced, for example if the times of destruction and recovery are short, this behaviour is considered to be an advantage in some steps of the ceramic processing [40, 46, 35, 47].

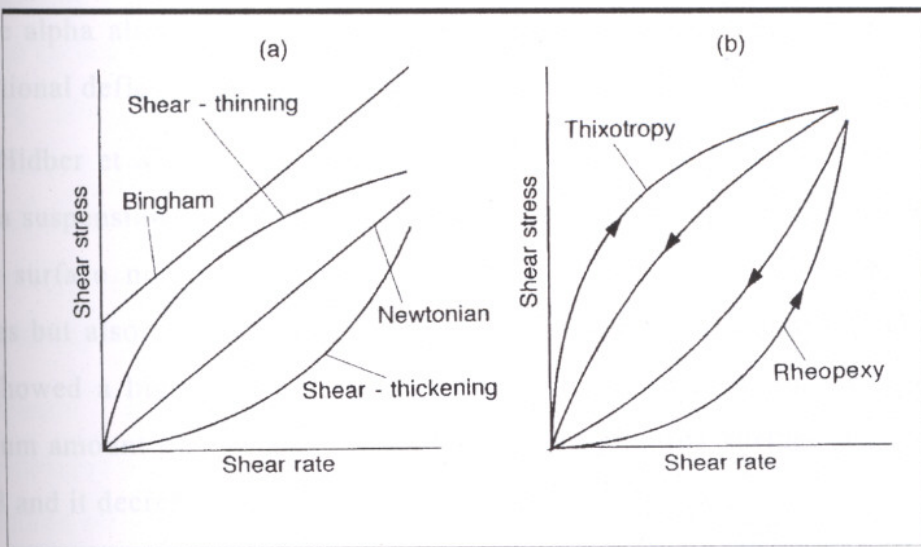


Figure 2.14. Variation of shear stress with shear rate for different models of flow behaviour [47].

2.7.3 Dispersion and Rheology Studies on Alumina

Many researches was investigated the effects of different type of dispersing agents on the dispersion, stability and rheology of the alumina suspensions.

For example, Cesarano J. and Aksay [6] used polyacrylic acid (PAA) and polymethlyacrylic acid (PMAA) for processing of highly concentrated (60 vol%) alpha alumina suspensions in water. PAA and PMAA are stabilizing alumina suspensions by electrostatic stabilization mechanism. Cesarano showed that, for alumina suspensions that contain PAA the transition from a flocculated state to a dispersed state corresponded to the adsorption saturation limit at various pH values.

Many other researchers used both of PAA and PMAA dispersants to disperse alpha alumina suspensions. They postulated that these were the most conventional deflocculants for alpha alumina water system [15, 24].

Hidber et al. [19, 21] was used citric acid, as a dispersant for aqueous alumina suspensions. According to their results, citric acid molecules adsorbed on the surface not only influence the surface charge of the alpha alumina particles but also create a steric barrier. This naturally occurring tricarboxylic acid, showed a high affinity to the alpha alumina surface. In their study the maximum amount of citric acid adsorbed on the alumina surface was measured at pH 3 and it decreased at pH 8.

Evanko et al. [12] investigated the dispersion behaviour of 15 wt% alumina suspensions by using anionic surfactants. In this study stabilizing effects of several anionic surfactants were investigated for concentrated dispersions of two different pseudoboehmite aluminas at pH 4 and 7. The anionic surfactants of ethoxylated fatty alcohol carboxylate free acid form and decyl(sulfophenoxy) benzenesulfonic acid, disodium salts were identified as effective in enhancing the stability of concentrated alumina dispersions. The stabilizing effect of all the surfactants enhanced at pH 4. According to the

results of the study these surface-active agents can stabilize alumina dispersions to a greater extent than electrostatic stabilization alone.

Sumita and Rhine [53] studied the effects of organic dispersants on processing of alumina. They investigated the effect of water-soluble polymers, such as benzoic acid and derivatives on the dispersion, packing and sintering of alumina, with 1% to 14.3 wt% dispersant concentration. Aromatic acids, such as 4-hydroxyl and 4-aminobenzoic acid were also found effective dispersants in this study. Each polymeric dispersant had an optimum effective concentration and excess dispersant had a negative effect on the alumina sediment volume.

Adsorption effects of polyelectrolytes on the rheological properties of alumina suspensions investigated by Guo et al [15]. A type of ammonium polyacrylate with a mean molecular weight of 15,000 was used in the study as a polyelectrolyte. According to their results optimum coverage for stabilization was observed at 95% for different solid loadings. They concluded that the full coverage is not necessarily required to achieve stabilization for a suspension that has non-high affinity adsorption. As the solid loading increases, stabilization of the suspensions becomes more difficult. A suspension that has a low solid loading can be stabilized with relatively low coverage, however for suspensions that have a higher solid loading, greater coverage is necessary to attain stability.

Esumi and Yamanaka [11] examined the effects of Sodium dodecylpoly(oxyethylene) sulphate on alumina suspensions at pH 3.5. Also they studied effect of polymer chain lengths. They found that the adsorption of SDE_nS on alumina decreases with increasing oxyethylene chain length and this adsorption behaviour significantly affects the stability of alumina dispersion. The dispersion of alumina exhibits a dispersion-flocculation-redispersion process by the adsorption of this surfactant.

Orth et al. [43] studied with block copolymers for stabilization of alpha alumina suspensions. For this purpose they used water-soluble P (MAA- block-PEO)(polymethacrylic acid block polyethyleneoxide) block copolymers. According to their results these block copolymers were highly efficient

dispersants for alpha alumina powders in aqueous solutions. Their dispersive effect is based on a combination of specific adsorption of the PMAA anchor block on the particle surface and shielding effects provided by the PEO stabilizing blocks. In addition the adsorption of the negatively charged PMAA block on the oppositely charged alumina surface reverses the electrophoretic potential of the oxide particles, process that is strongly pH dependent.

CHAPTER III

EXPERIMENTAL

3.1 Materials

Bayer gibbsite and transition alumina used in this work were obtained from Seydişehir Aluminum Company. Gibbsite was reported to have a chemical composition of 64% Al_2O_3 , 0.3% Na_2O , 0.015 % Fe_2O_3 , 0.015% SiO_2 and 80% of the powder with above 40 μm particles. The transition alumina was reported to have a composition of 98,5% Al_2O_3 , 0.5% Na_2O , 0.025 % Fe_2O_3 , 0.020% SiO_2 with minimum 25% α phase.

Two commercial high purity α - Al_2O_3 powders were used in this study. The first powder (AKP-53) has an average particle size of 0.29 μm , a BET surface area of 12.3 m^2/g , bulk density (tapped) of 1.5 g/cm^3 and loose bulk density of 1.1 g/cm^3 . The powder purity exceeded 99.99%, containing 140 ppm Si, 7 ppm Na, 20 ppm Mg, < 1 ppm Cu and 9 ppm Fe. This powder and above information was kindly supplied by Sumitomo Chemicals Co., Japan. The second powder with an average particle size of below 10 μm was purchased from Aldrich Chemicals Co.

The pH of the 20 vol% AKP-53 and Aldrich alumina suspensions was measured as 5.96 and 9.33 at 33°C respectively in distilled water without additives. The pH of the gibbsite suspension was measured as 9.36 at 26°C. In the case of transition alumina suspension the pH was measured as 9.8 at 23°C.

PEO/PPO tri block co-polymers (commercially known as Pluronics) were obtained from BASF Corporation, Washington, NJ. Structural formulas of block copolymers used in this study were indicated in Chapter II Figure 2.13. Their important properties and compositions are further listed in Table 3.1 and 3.2 respectively.

Table 3.1. Important properties of surfactants used in this study [2].

Code	Mol. weight	%PEO	Melt pour point ©	viscosity (cps)77°C
F-127.....	12600.....	70.....	56.....	3100
F-68.....	8400.....	80.....	52.....	1000
P-104.....	5900.....	40.....	32.....	390
PE-6400.....	2900.....	40.....	16.....	850
10R-8.....	4550.....	80.....

Table 3.2. Compositions of surfactants used in this study [56].

F-127.....	EO ₉₇ PO ₆₉ EO ₉₇
F-68.....	EO ₇₈ PO ₃₀ EO ₇₈
P-104.....	EO ₁₃ PO ₃₀ EO ₁₃

Polyacrylic acid (with an average molecular weight M_w of 2000) from Aldrich, citric acid with M_w : 192 (Merck) and sodium dodecyl sulphate M_w : 288 (Sigma) were also used as dispersing agents at concentrations ranging from 10^{-7} to 10^{-2} M.

Distilled water used during the experiments had a conductivity of 113.5 $\mu\text{s/cm}$ (24.6 °C) obtained from equipment Jencons Autostills DDI/C.

3.2 Powder Preparation Methods

Alumina powders were prepared from gibbsite by using eight different methods in this work. The processing steps for the first four methods are shown in Figure 3.1. The purpose of these variations in the processing steps was to influence the nucleation and growth rate of the solid-solid phase transformations. The powders were coded all at the end of the processing diagrams.

Gibbsite was wet ball milled for 16 hours in the first four methods. Multifix Ball mill was used with a plastic container with 4.9 cm radius and cylindrical zirconia media of 9.48 mm height. During milling, bulk volume was calculated by the summation of the ball volume and the void volume between the grinding media. The powders were ground at 115 rpm (85% of the critical speed).

The ball-milled gibbsite was further heat treated at 350 °C for 4 hours in methods 1 and 2. The particle size determination of the powders after milling was performed by using Stoke's law,

$$[V = (g_s - g_f) \rho x^2 / 18\mu]$$

Where;

g_s : Density of the solid

g_f : Density of the fluid

ρ : 9.81 m/s², x : particle size, μ : viscosity of the fluid

Settling time of the particles in the suspension was calculated by using terminal velocity that was obtained from the above equation at a specified height. The pH of the suspensions were adjusted to 3.5 with nitric acid to avoid agglomeration during sedimentation. Fractionation of the powders was accomplished by letting the suspensions for a preset time and separating the sediment and the suspension. Fractions below 1 μm and 5 μm from the powders were recovered and used for further processing.

Powders smaller than $1\ \mu\text{m}$ particle size were calcined at $1200\ ^\circ\text{C}$, for 2 to 8 hours in a high temperature furnace (Carbolite 1600 RHF, with $5^\circ\text{C}/\text{min}$ heating rate). The final powders were designated as M-1A and M-1B respectively. The powder labelled as M-1P in method 1 was ball milled for 9 more hours. The $< 5\ \mu\text{m}$ powder fraction was calcined at $1100\ ^\circ\text{C}$, for 2 hours under similar conditions.

The powder M-3 was prepared without heat treatment at $350\ ^\circ\text{C}$. Gibbsite was milled for 16 hours and the $< 5\ \mu\text{m}$ fraction of the powders was calcined at $1200\ ^\circ\text{C}$ for 2 hours.

In the preparation of powder M-4, the transition alumina was used as the starting material. It was ball milled and fractionated. The $< 5\ \mu\text{m}$ fraction was calcined at $1200\ ^\circ\text{C}$ for 2 hours. Powder processing steps of powders M-1, M-2, M-3 and M-4 were presented in Figure 3.1.

M-3

M-4

Figure 3.1

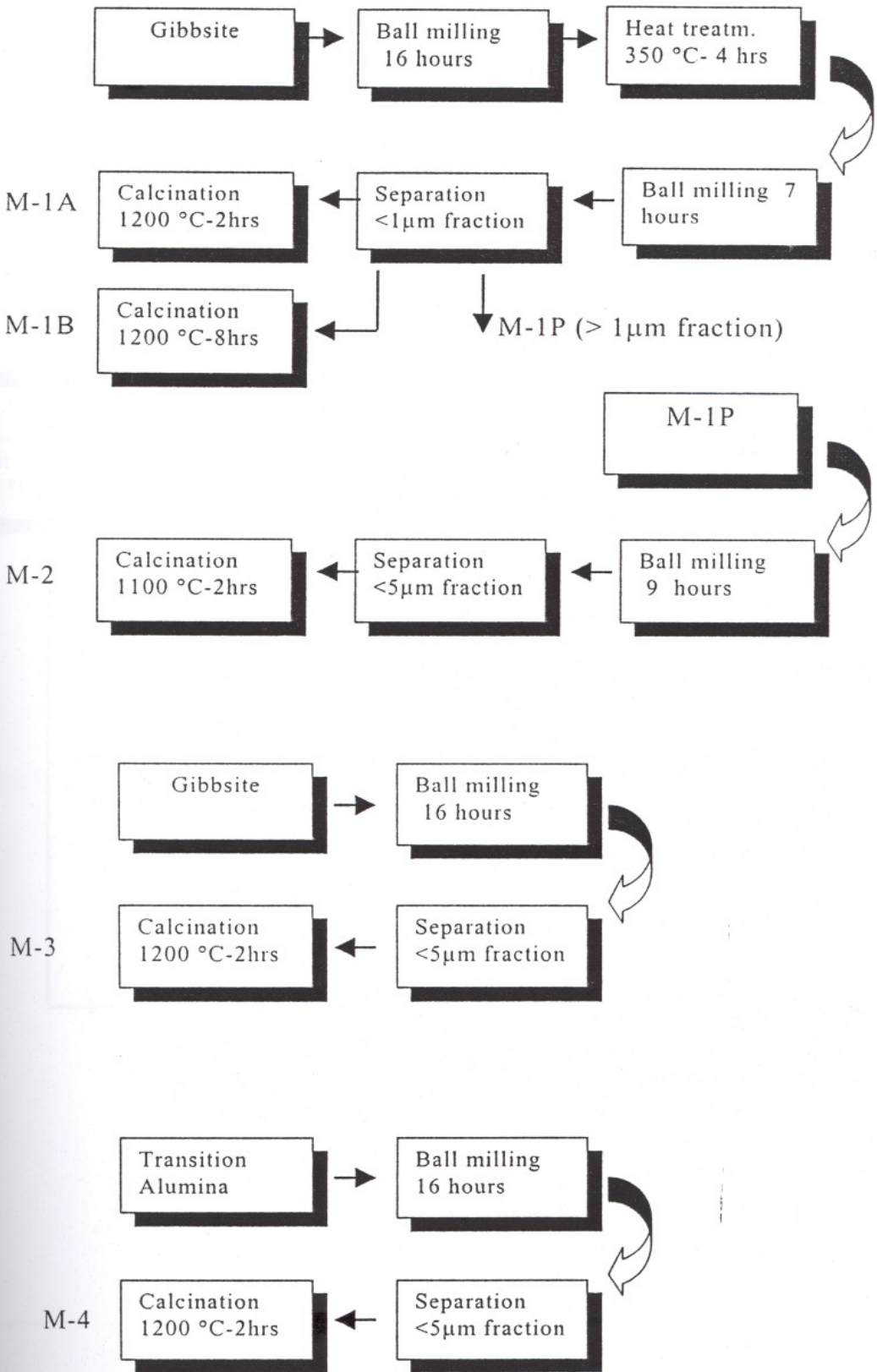


Figure 3.1. Powder processing diagram of M-1, M-2, M-3 and M-4.

Gibbsite was directly heat treated at 900 °C for 3.5 hours in methods 5 to 7 (M-5 to M-7) as indicated in Figure 3.2. The effect of ball milling and ultrasonic treatment was investigated on the transition to alpha alumina transformation.

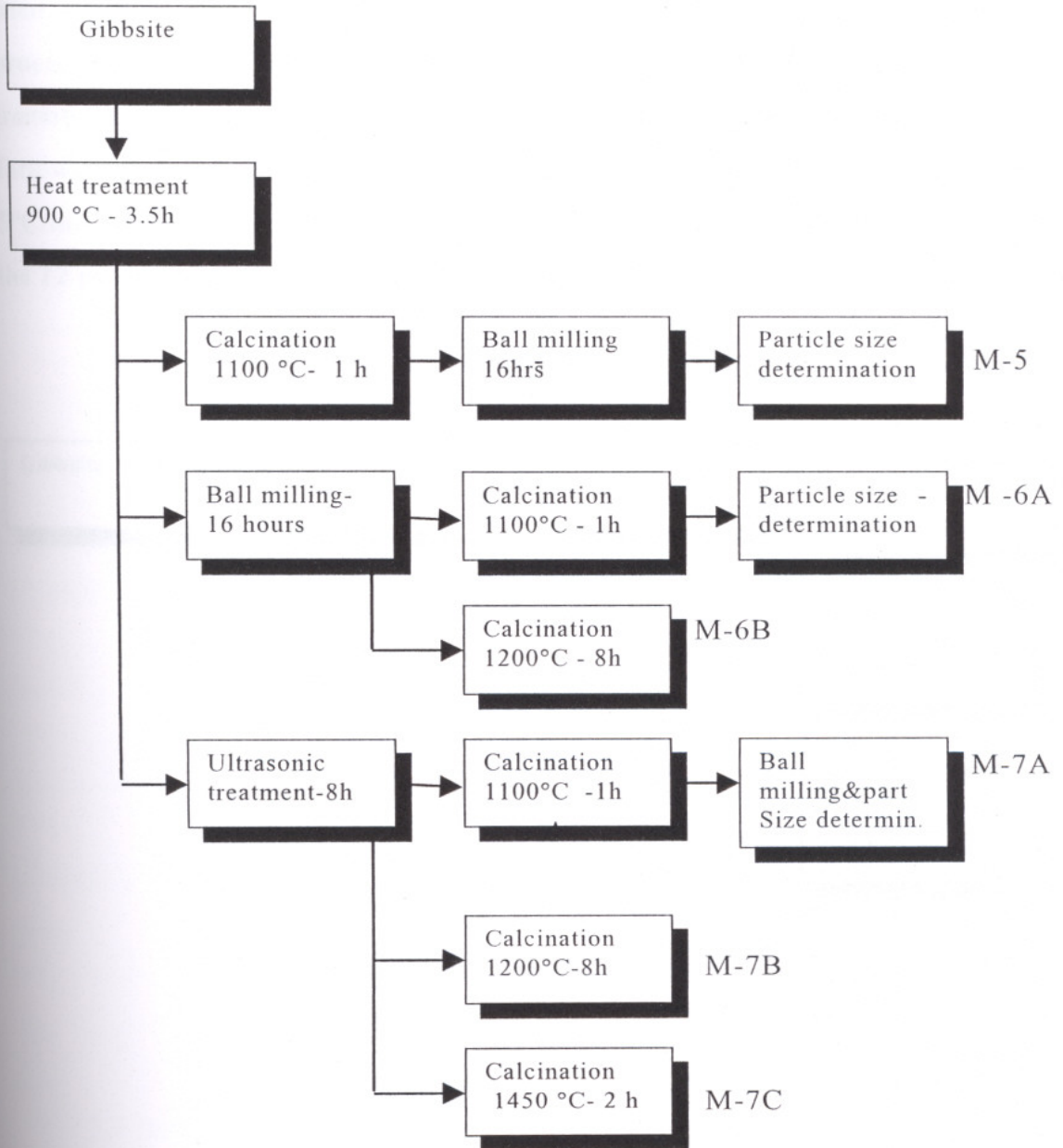


Figure 3.2. Powder processing diagram of M-5, M-6 and M-7.

In the preparation method of powder M-8, gibbsite was primarily ball milled for 5 hours that was followed by heat treatment at 350°C for 4 hours. The secondary ball milling was also performed for 5 hours with 1 hour ultrasonic treatment. For this purpose Elma Transsonic 660/H (35 kHz) ultrasonic bath was used. During ultrasonic treatment, samples were also stirred to enhance the process. Then powders were thermally treated at 900 °C to transform to a transition alumina. The third ball milling and ultrasonic treatment process followed this. Finally powders were calcined at 1100 °C for 1 hour with 5°C/min and ball milled after calcination. The powder preparation steps of all the 12 powders are further tabulated in Table 3.3.

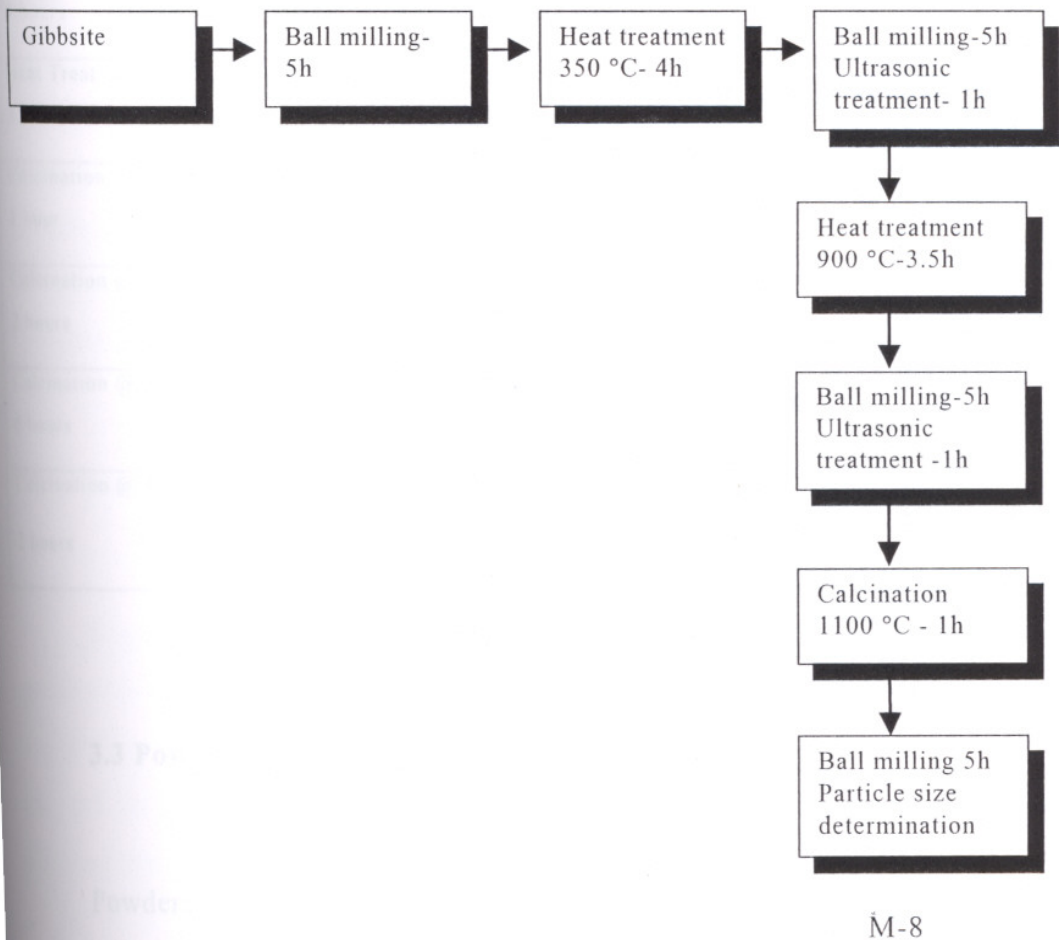


Figure 3.3. Powder processing diagram of M-8.

Table 3.3. Processing methods of prepared powders.

Powder Preparation Methods	M-1	M-1	M-2	M-3	M-4	M-5	M-6	M-6	M-7	M-7	M-7	M-8
	A	B					A	B	A	B	C	
1 st Grinding (Before heat treatment)	●	●	●	●	●							●
2 nd Grinding (After heat treatment)	●	●	●				●	●				●
Final Grinding (After calcination)						●			●			●
Ultrasonic Treatment									●	●	●	●
Heat Treat. @ 350 °C 4 hours	●	●	●									●
Heat Treat. @ 900 °C 3.5 hours						●	●	●	●	●	●	●
Calcination @1100 °C 1 hour			●			●	●		●			●
Calcination @1200 °C 2 hours	●			●	●							
Calcination @1200 °C 8 hours		●						●		●		
Calcination @ 1450°C 2 hours											●	

3.3 Powder Characterization

Powders with 3% PVA and 5% moisture were die pressed at 75 MPa by hydraulic hand press. Pellets were sintered at 1450°C for 2 hours in a high temperature furnace (Carbolite 1600 RHF). The sintered densities of the pellets

were determined by Archimedes method using a Sartorius BP 2108 with suitable density measurement apparatus.

Particle size distributions of the two commercial powders were determined by Mastersizer S.Ver.2.14, Malvern Instruments. Particle size information of the prepared powders were estimated and reported as a fraction of the total powder by use of Stoke's Law.

Thermal properties were examined by the Thermogravimetric Analyser (TGA- 51/51 H, Shimadzu Co.) at 1000°C with 10°C/min heating rate by using nitrogen as a carrier gas and Differential Thermal Analyser (DTA-50, Shimadzu Co.) at 1450°C.

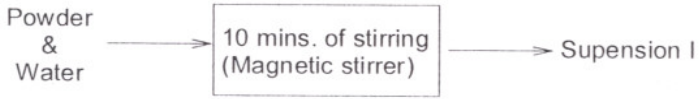
The Infrared Spectra of the powders were taken by Fourier Transform Infrared Spectroscopy (FTIR-8201, Shimadzu Co.). The pellets for the FTIR analysis were prepared by pressing a mixture of the 0.004 gr samples and the 0.2 gr KBr.

The phase identification in selected samples was determined by powder X-ray diffractometer (Jeol JSDX 100S4) by using monochromatic $\text{CuK}\alpha$ radiation with Ni filter. The 2θ was taken 6-80° with 2°/min scanning rate and 20 mm/min chart rate (In Dokuz Eylül University, Mining Engineering Department).

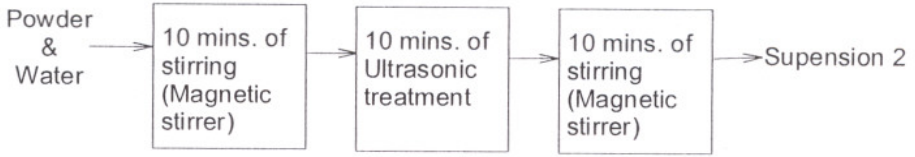
3.4 Suspension Preparation Methods

Suspensions were prepared by using AKP-53, Aldrich alumina and the powder M-7A. Solid loadings in suspensions were adjusted as 0.125, 1.0, 14, 50 vol % respectively (0.5, 4, 40, 80 wt %) for the viscosity measurements and only 0.5 wt % for turbidity measurements. Suspensions were prepared by using different methods. These are as follows (Figure 3.4.):

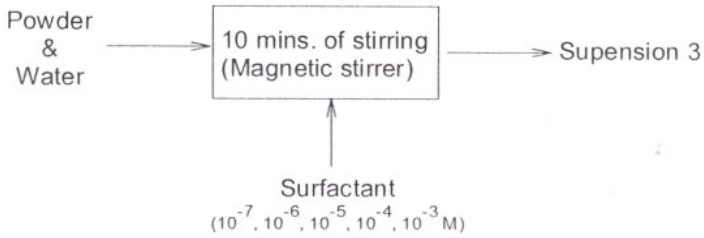
METHOD I:



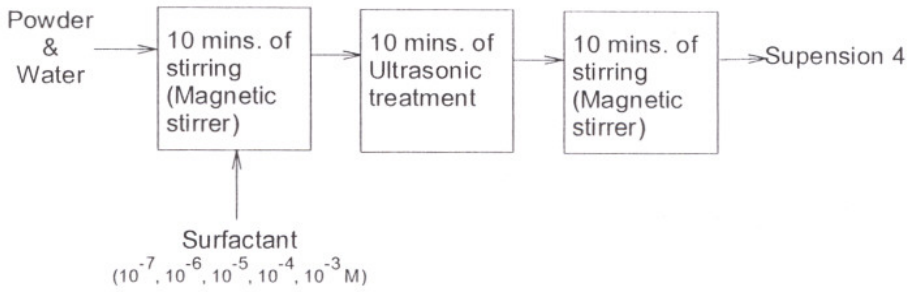
METHOD II:



METHOD III:



METHOD IV:



	Method I	Method II	Method III	Method IV
Stirring	●	●	●	●
Ultrasonic treatment		●		●
Use of surfactants			●	●

Figure 3.4. A schematic representation of suspension preparation methods.

3.5 Suspension Characterization

Rheological behaviour of the suspensions was determined by using Brookfield DV-III RV rheometer with ULA adaptor.

Viscosities of the suspensions were measured at different shear rates by using the following set conditions:

- Shear rate was set at maximum shear 250 s^{-1} .
- It was decreased to 100 s^{-1} by 10 s^{-1} in every 30 sec.
- Shear rate was then again increased by 10 increments up to 250 s^{-1} .

The shear rate range was varied between 0 s^{-1} to 200 s^{-1} for high solid loadings. The most effective parameter in defining the shear rate range was the applied torque.

Large differences between the initial increasing rate sweep and the later decreasing rate sweep were assumed due to flocculation.

Turbidity measurements were made by using an Omega Model (TRB-800) turbidimeter. The methods described in Figure 3.4 were used to prepare the suspensions. Measurements were done at preset time intervals as 30 sec, 1.0, 2.0, 4.0, 8.0, 16, 32 and 64 minutes.

CHAPTER IV

RESULTS AND DISCUSSION

4.1 Powder Preparation and Characterization

Powders that were prepared with the methods mentioned in previous chapter were characterized with XRD, FTIR, density measurements and particle size characterizations. The thermal behaviour of the gibbsite was also determined. Results will be discussed in the following paragraphs.

4.1.1 Thermal Analysis

Differential thermal and thermogravimetric analysis of gibbsite in Figures 4.1 and 4.2 showed that most of the hydroxyl ions are driven off below 400 °C. In this study some of the powders were thermally treated at 350 °C to obtain high surface area powder with a network of sub microscopic cracks. According to Wefers [1972] there are two endothermic peaks below this temperature in the DTA curve of a coarse grained gibbsite. The first one appears near 230 °C. It is followed by an exothermic effect at approximately 280 °C, attributed to the formation of boehmite by hydrothermal conditions due to the retarded diffusion of the water vapour out of larger grains. The exothermic reaction does not occur in DTA curves of the fine-grained trihydroxide [57]. Most investigators agree that boehmite and a disordered transition alumina (χ) are formed upon heating of coarse gibbsite to about 400 °C.

In this study there are three regions in the TGA curve of the gibbsite (Figure 4.1). The first stage between 250-330 °C is due to the decomposition of the hydroxide and the removal of water vapor. The total weight loss is about 25% in this stage.

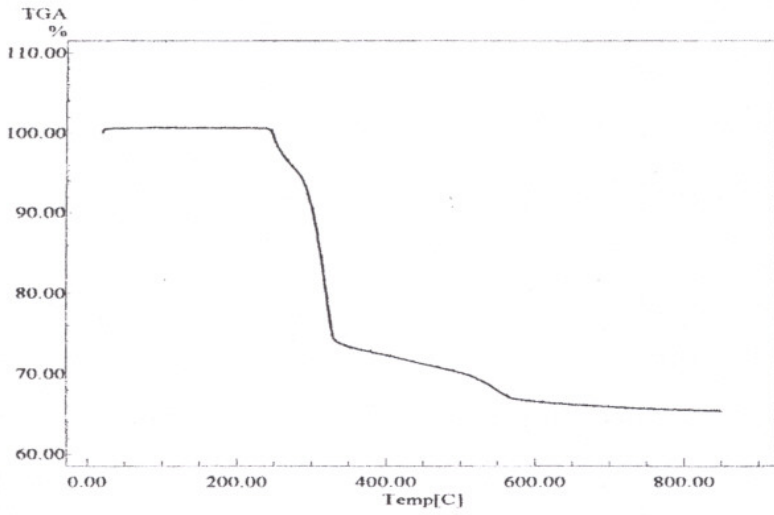


Figure 4.1. TGA thermogram of gibbsite.

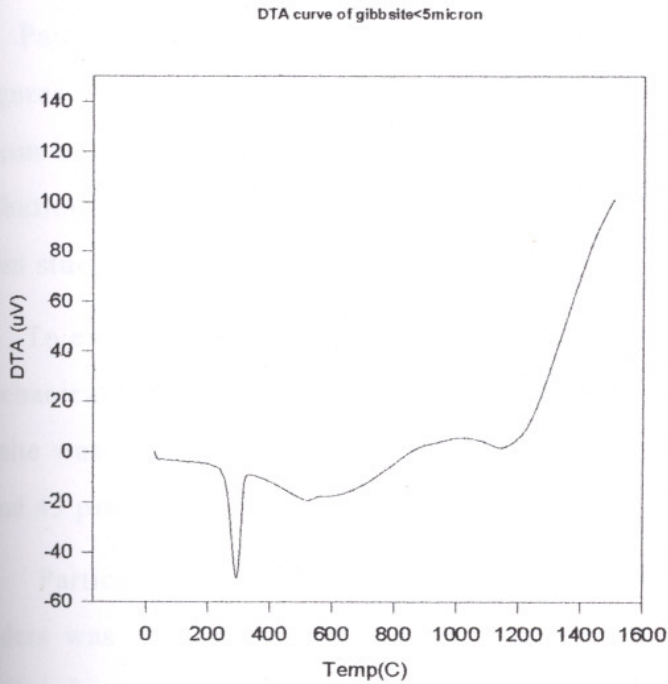


Figure 4.2. DTA curve of gibbsite.

In the DTA curve of the gibbsite there is an endothermic peak at 300 °C (Figure 4.2). This endothermic peak is located in the same temperature range as stage I in the TGA curve and can be attributed to the gibbsite decomposition.

The second stage, which is between 330-510 °C in the TGA curve, may be due to diffusion of the trapped water in the structure. The last stage, which is between 510- 550 °C, may be due to the decomposition of the boehmite formed in the first stage. There is also an endothermic depression in DTA curve in that temperature range similarly attributed to the decomposition of boehmite. In the last stage of the TGA curve weight loss is more rapid than the second stage but in quantity as 2 %. The total weight loss in the gibbsite was observed as

4.1.2 Particle Size Characterizations

Particle size distributions of the AKP-53 and Aldrich alumina were given in Figures 4.3 and 4.4 respectively. The reported particle size of the AKP-53 is 0.5 μm but the Figure 4.3 demonstrated rather coarse particle size. Since size distribution measurements were taken without the use of ultrasonic bath in the present study this difference was attributed to the existence of agglomerates.

To examine the particle size of the gibbsite dry sieving was applied with mechanical vibrator during 60 minutes. According to the results 49.7 % of the gibbsite was above 75 μm , 16.8% was below 45 μm and 33% was between the 45 μm .

Particle size of the gibbsite used in the preparation of M-1 to M-3 samples was calculated after 16 hours grinding. Fractionation of the ground gibbsite showed that 15.7% was below 1 μm and 42% was below 5 μm . After ultrasonic treatment that was followed by second grinding 14.3% of the gibbsite was determined to be below 1 μm and 70% was below 5 μm . The purpose of the ultrasonic treatment process at 350 °C was to obtain a disordered structure, which

may help the size reduction during grinding process. But relatively low percent of submicron fraction was obtained. The particle size of the transition alumina used in the preparation of M-4 was measured by dry sieving. Below 45 μm fraction of the powder was 34.2%. In the case of M-4 powder after grinding for 16 hours below 5 μm fraction was determined as 41.5 %.

In the case of M-5, 30.8% of the powder was smaller than 1 μm after final calcination and 16 hours grinding step. For the powder M-6A this value was obtained as 21% and 68% of the powder was < 5 μm . But the grinding step was before the calcination in the case of M-6A. The difference between the < 1 μm fractions of the M-5 and M-6A was attributed to the processing step of grinding. The grinding process that was applied after calcination step was more efficient in size reduction.

The below 1 μm fraction of the powder M-7A was determined as 45 % after calcination but it was 30.8% in the case of M-5. The only difference between the M-5 and M-7A was the usage of ultrasonic bath in the case M-7A. So it may be thought that usage of ultrasonic treatment before calcination may affect the particle size and the nucleation rate of the transition alumina.

In the case of M-8 below 1 μm fraction was obtained as 10%, which was the lowest value. Some agglomeration problem during fractionation might cause to obtain such a low value. Additional grinding process after calcination was eliminated this effect and below 1 μm fraction was obtained as 69%. These results were also tabulated in Table 4.1.

Table 4.1. Below 1 μm and 5 μm fractions of some selected powders in different processing steps.

Powders	After 1 st Grinding (%)	After 2 nd Grinding (%)	Before Calcination (%)	After Calcination (%)
M-1A < 1 μm	15,7	14,3	-	-
M-1A < 5 μm	42	70	-	-
M-4 < 5 μm	-	41,5	-	-
M-5 < 1 μm	-	-	-	30,8
M-6A < 1 μm	-	-	21	-
M-6A < 5 μm	-	-	68	-
M-7A < 1 μm	-	-	-	45
M-8 < 1 μm	-	-	10	69

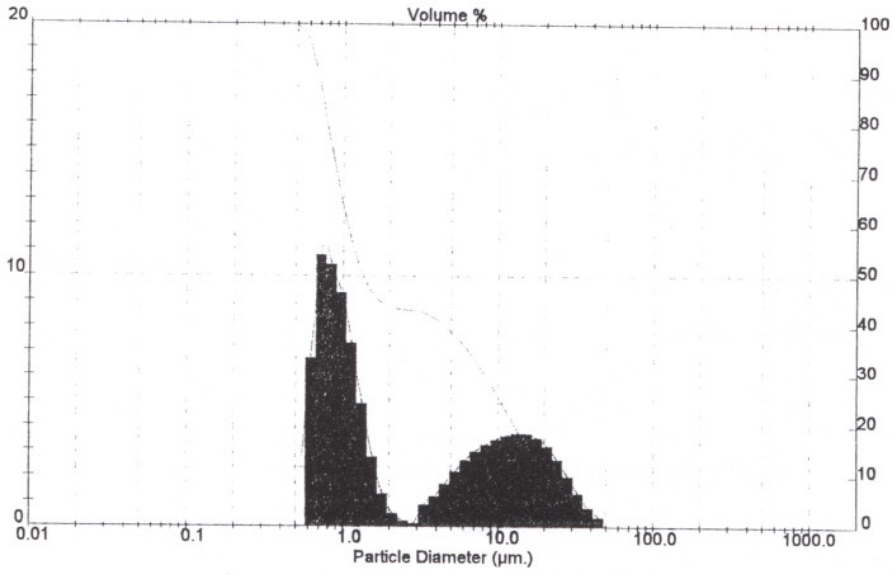


Figure 4.3. Particle size distribution of the AKP-53.

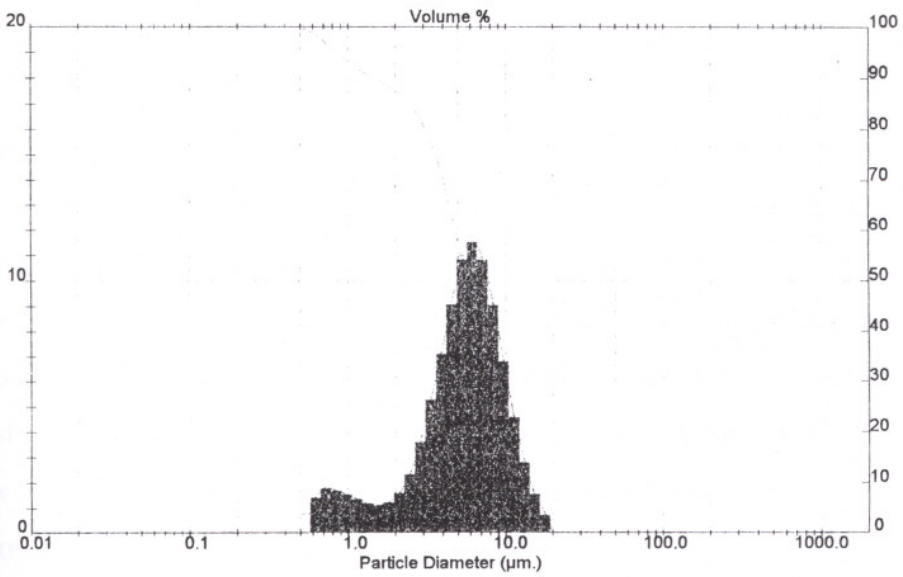


Figure 4.4. Particle size distribution of Aldrich alumina.

4.1.3 Density Measurements

In this study, densities of the powder pellets in green and sintered form were measured. Results were tabulated in Table 4.2 and show the average of three different measurements.

The sintered density of the AKP-53 powder pellet was measured as 3.87 g/cm³ with 97% theoretical density (TD). This value was taken as a reference to compare the densities with other powders.

The sintered densities of the pellets prepared by powders M-1A and M-2 were measured as 3.46 and 3.15 g/cm³, respectively. On the other hand, density of the powder M-3 was lower than M-1A and M-2. The only difference between these powders was the absence of the thermal treatment at 350 °C in the preparation step of M-3.

The powders M-5, M-6A and M-7A were all prepared through heat treatment at 900 °C. The highest sintered density was obtained in powder M-7A as 3.603 g/cm³ with 91% of theoretical density. The powder pellet of M-5 has rather low density as 3.116 g/cm³. The ultrasonic treatment that was applied to M-7A was absent in the powder M-5. So the rather high density of the M-7A might be attributed to the ultrasonic treatment effect. The sintered density of the powder pellet M-6A was determined as 2.935 g/cm³. This powder was ball milled before calcination to improve the transformation. But grinding before calcination to enhance the nucleation and growth rate did not influence the sintered density M-6A powder pellets. For the powder pellet of M-8 although ultrasonic treatment was applied sintered density was not high as M-7A. Theoretical density was calculated as only 77%.

Table 4.2. Density and dimensions of the pellets before and after sintering.

Powders	Green density (g/cm ³)	Sintered density (g/cm ³)	TD %	Dimensions before sintering		Dimensions after sintering	
				D Diameter (mm)	t thick. (mm)	D Diameter (mm)	t thick. (mm)
M-1A	1,618	3,466	87	14,32	3,60	11,57	2,90
M-2	1,5605	3,150	79	14,48	3,30	11,68	2,87
M-3	1,758	2,536	63	14,23	3,20	13,07	2,67
M-4	1,920	3,117	78	14,24	3,12	12,21	2,70
M-5	1,701	3,116	78	14,34	3,39	11,57	2,60
M-6A	1,589	2,935	73	14,34	3,36	11,98	2,82
M-7A	1,73	3,633	91	14,37	3,51	11,43	2,85
M-8	1,685	3,080	77	14,33	3,53	12,06	2,91
AKP-53	2,24	3,870	97	14,07	2,63	11,98	2,26
Aldrich	2,36	2,630	66	14,15	2,66	13,83	2,63
Gibs. @900°C	1,751	2,206	55	14,36	3,42	13,36	2,61

4.1.4 Fourier Transform Infra-Red (FTIR) Analysis

The bands that were observed between 400 to 850 cm^{-1} were due to Al-O stretching. Especially Al-O peak at 740 cm^{-1} exists in all powders. In the case of gibbsite this peak was observed at 741 cm^{-1} [57].

In all cases there was an unassigned peak at 813 cm^{-1} . For the powder M-1P there were some additional unassigned peaks at 960, 1080 cm^{-1} . This powder also contained OH bending peak at 1650 cm^{-1} . The powder M-8 showed OH bending peak at the same point.

According to D.H. Lee et al. [31] the infra-red bands at 3624-3620, 3527 and 3460 cm^{-1} along with a doublet at 3396 and 3328-3383 cm^{-1} are related with gibbsite type species.

In Figure 4.5(a) the FTIR spectrum indicates that the material is a hydrate. The strong and broad absorption bands are located in the region approximately at 3100, 3378, 3430, 3620, 3518 cm^{-1} . This absorption is associated with the OH stretching vibrations in molecular water [57]. FTIR spectrum for alumina AKP-53, Aldrich alumina does not show any distinct bands in these regions.

In powders M-1P, M-6, M-7, M-8 there was a carbonate peak at nearly 1400 cm^{-1} . This may be caused by CO_2 adsorption from the atmosphere.

Same authors [31] reported bands at 1520 -1570 cm^{-1} and/or 1350-1410 cm^{-1} on adsorption of CO_2 on gamma-alumina surface. These bands were associated with bicarbonate, unidentate or bidentate carbonate species but their exact assignment was unclear. The presence of surface impurities plays an important role adsorbing such species. For example, presence of Na^+ ion on the alumina surface enhances the ability of adsorbing CO_2 . According to them, the infra-red bands at 3305, 1520-1580 and 1390 cm^{-1} can be associated with the surface species which has a dawsonite-like structure in Bayer processed alpha alumina. CO_2 and Na^+ ions on the alumina surface, resulting in the formation of a dawsonite ($\text{NaAl}(\text{OH})_2\text{CO}_3$) on their surface.

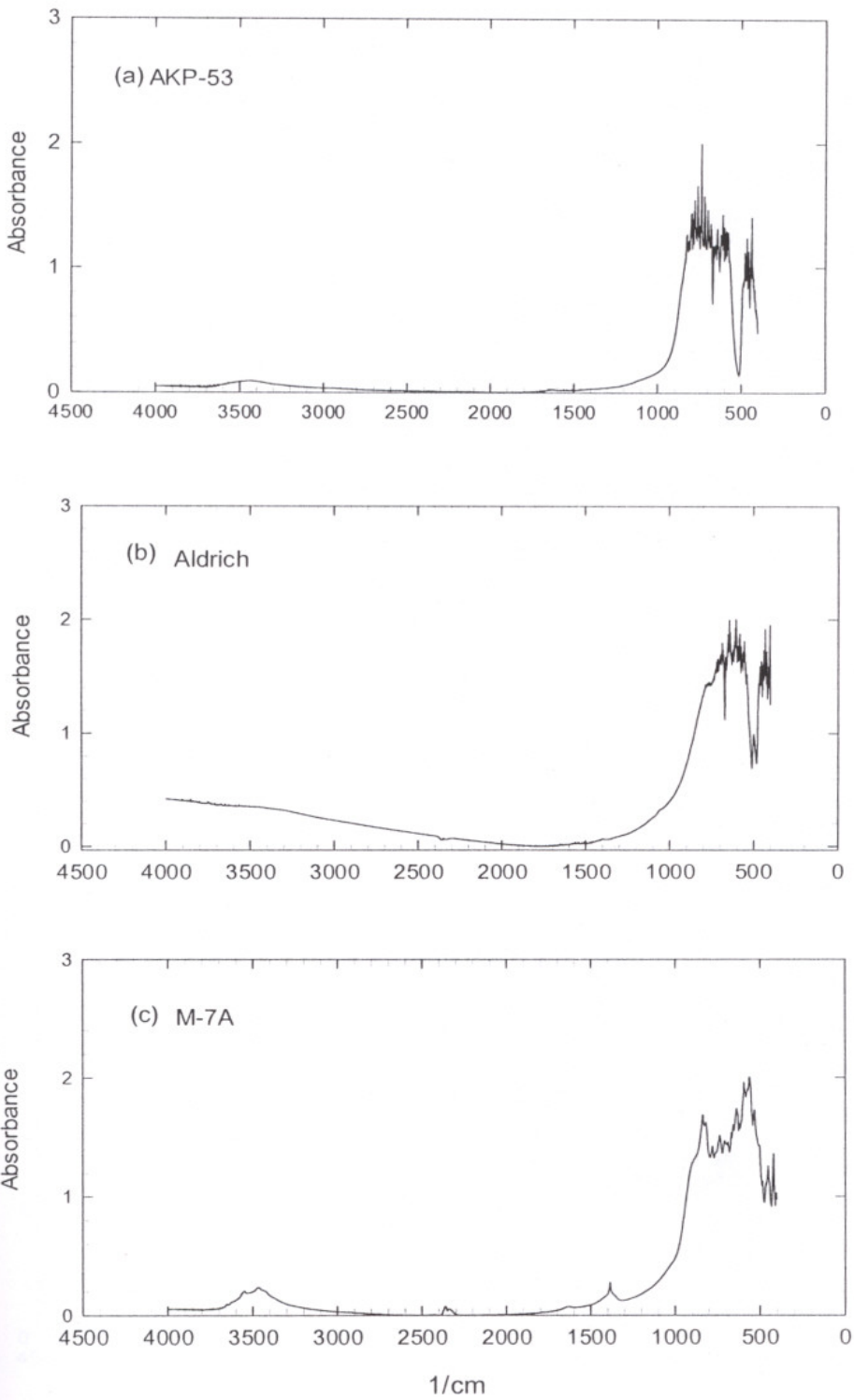


Figure 4.5. FTIR spectra of (a) AKP-53, (b) Aldrich, (c) M-7A

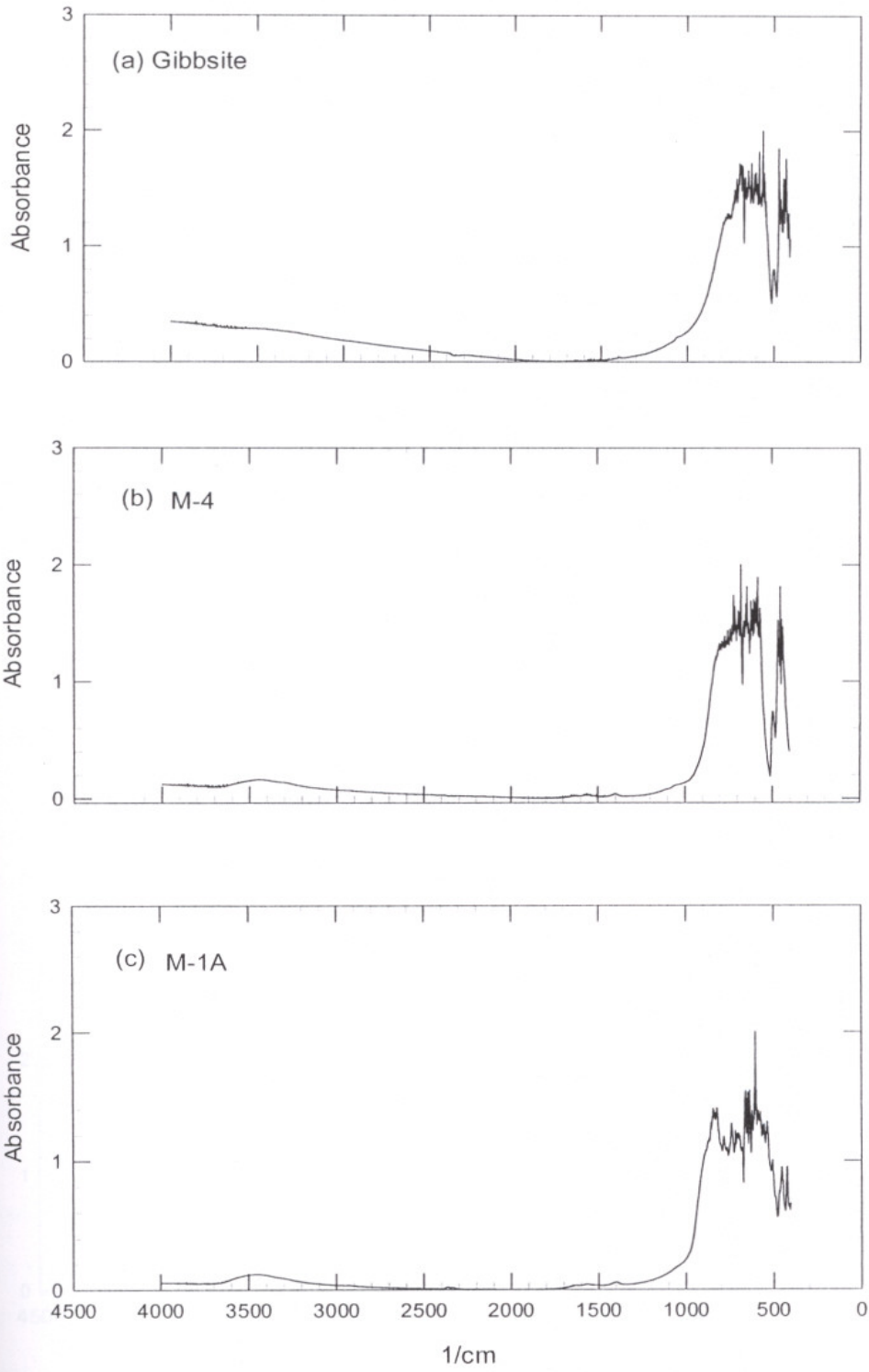


Figure 4.6. FTIR spectra of (a) Gibbsite, (b) M-4, (c) M-1A

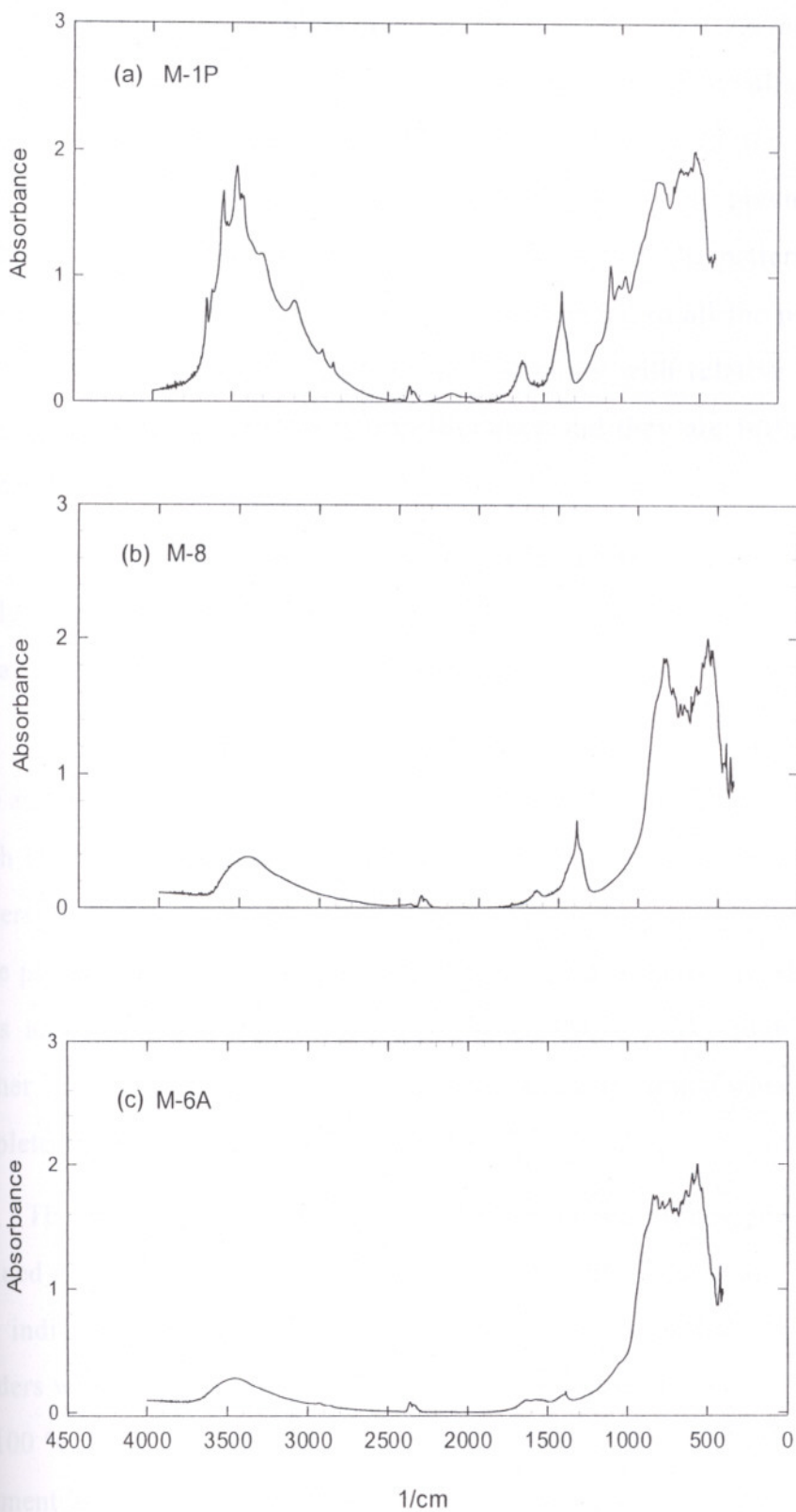


Figure 4.7. FTIR spectra of (a) M-1P, (b) M-8, (c) M-6A

4.1.5 X-ray Powder Diffraction Analysis

XRD analysis was performed in the range 6 to 80° 2 θ range in order to investigate the nature of the alumina phases in the final alumina powders. The XRD patterns of the 10 of the 12 powders along with the pattern of the commercial high purity alpha alumina AKP-53 powder are given in the Figures 4.6 to 4.8. The codes of the powders are indicated on the patterns. XRD peaks of only α and κ phases of the alumina were detected in all the patterns. The 2 θ peak locations and spacings of these phases along with relative line intensities up to about 2 θ = 80° obtained from literature and they are further tabulated in Table 4.3 [57].

The commercial AKP-53 powder XRD pattern shows the presence of mostly sharp 12 alpha (α) peaks. The powder is in pure alpha (α) form with no kappa (κ) or other transition alumina form.

Powders were calcined at three different temperatures in this work (1100, 1200 and 1450 °C). Only powder M-7C was heat treated at 1450 °C for 2 hours, which is a relatively high temperature for the transition alumina to alpha phase conversion. XRD pattern of the powder M-7C is given in Figure 4.10 indicates a phase pure α alumina with relatively sharp α peaks. There are also very weak 5 peaks and three these were assigned as κ . These peaks may also represent another impurity phase containing sodium. The transformation is mostly complete and the powder is high purity α .

The powders M-7B, M-6B and M-1B although processed differently were calcined at 1200 °C for 8 hours. The XRD patterns of these are given in Figure 4.10 indicates that two of these powders are high purity α powders. These powders were heat treated at 900 °C and mechanically treated before calcination at 1100 °C for 1 hour (M-7B ultrasonically treated and M-6B ball milled). Heat treatment at 900 °C seems to favour the phase transformation at 1200°C. The XRD pattern of the third powder (M-1B) showed that the presence of a multiphase structure. This powder was heat treated at 350 °C and subsequently ball milled and calcined at 1200 °C for 8 hours. The heat treatment for a shorter

time (2 hours) at 1200 °C with similar processing (M-1A Figure 4.8) yields a multiphase powder with significantly less sharp α peaks.

The XRD patterns of the powders M-5, M-6A and M-7A (all calcined at 1100 °C) indicated that differences in processing do have some effects on the nucleation of the α phase in the κ phase. Heat treatment of the gibbsite at 900 °C followed by calcination at 1100°C resulted in the formation of almost pure κ phase. Ball milling (M-6A) and ultrasonic treatment (M-7A) prior to calcination at 1100 °C caused partial transformation to the α phase. The XRD patterns of these powders given in Figure 4.9 indicate the presence of multiphase powders.

The processing of the powder M-8 involves all the pre-treatment steps. The XRD pattern indicates an almost single-phase κ powder. This powder also as reported earlier had 69% of the particles finer than 1 μ m. The sintered density was also relatively low (77 % TD). The explanation for the behaviour of this powder is yet unclear.

Table 4.3. Interplanar Spacings and Relative Line Intensities of α and κ [57].

Alpha alumina (a)			Kappa Alumina (b)		
d (spacing)	I (intensity)	2 θ	d (spacing)	I (intensity)	2 θ
3.479	74	25,58	6.2	3	14,27
2.552	92	35,14	4.5	2	19,71
2.379	42	37,78	4,2	1	21,13
2.085	100	43,36	3,04	4	29,35
1.740	43	52,56	2,79	6	32,04
1.601	81	57,52	2,70	2	33,14
1.546	3	59,76	2,57	8	34,88
1.510	7	61,34	2,41	3	37,26
1.404	32	66,54	2,32	4	38,78
1.374	48	68,20	2,26	1	39,84
1,276	2	74,60	2,16	1	41,78
1,289	16	73,40	2,11	8	42,82
1,190	6	80,68	2,06	3	43,90
1,160	1	83,22	1,87	6	48,64
1,147	4	84,38	1,64	6	56,02
1,138	1	85,18	1,49	3	62,24
1,125	5	86,42	1,45	3	64,16
1,099	6	88,98	1,43	8	65,18
1,083	3	90,66	1,39	10	67,30

(a) Prepared for ATM X-ray Powder Data File [57].

(b) Film pattern estimated visually (Stumpf) [57].

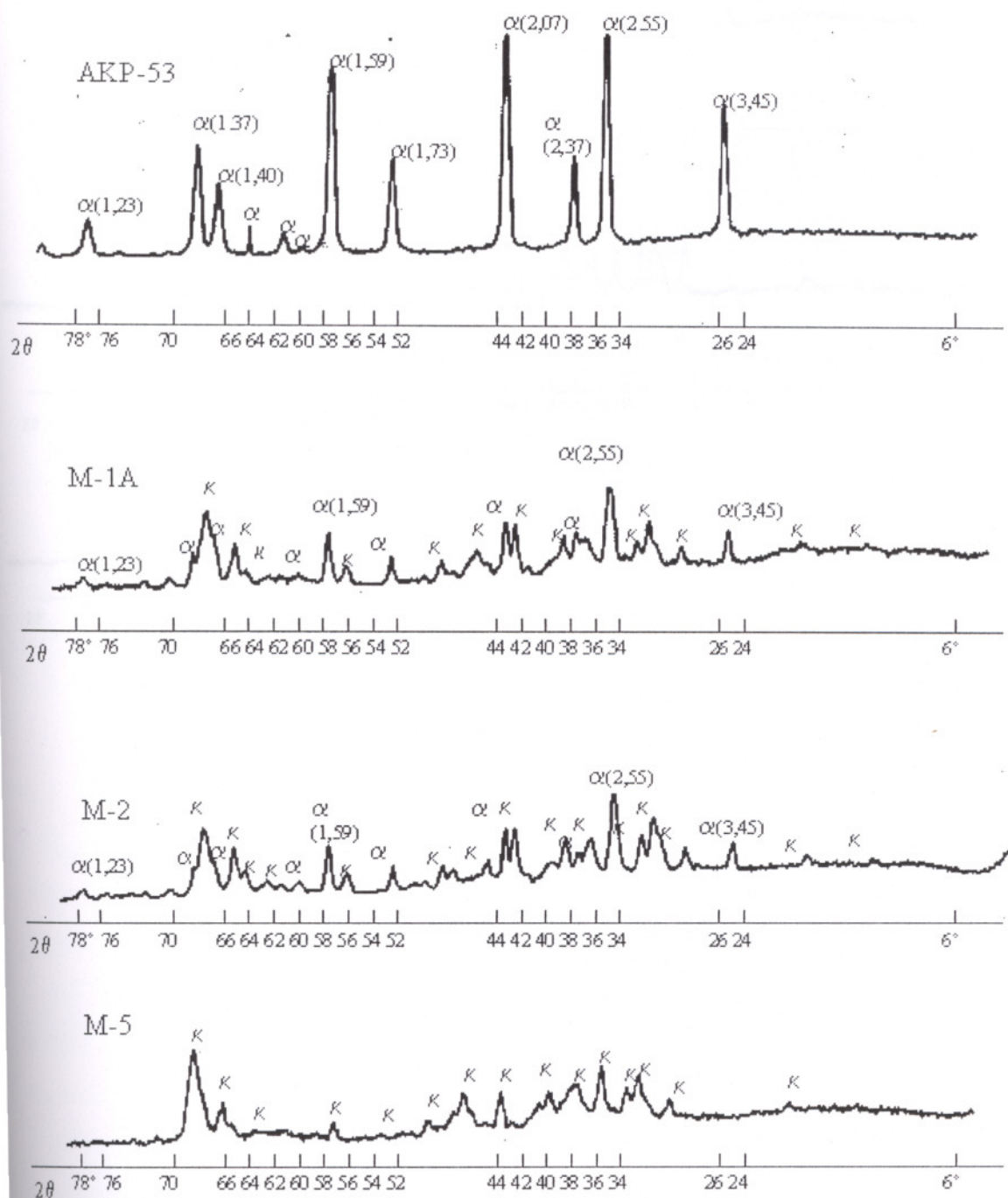


Figure 4.8. XRD diagrams of AKP-53, M-1A, M-2 and M-5.

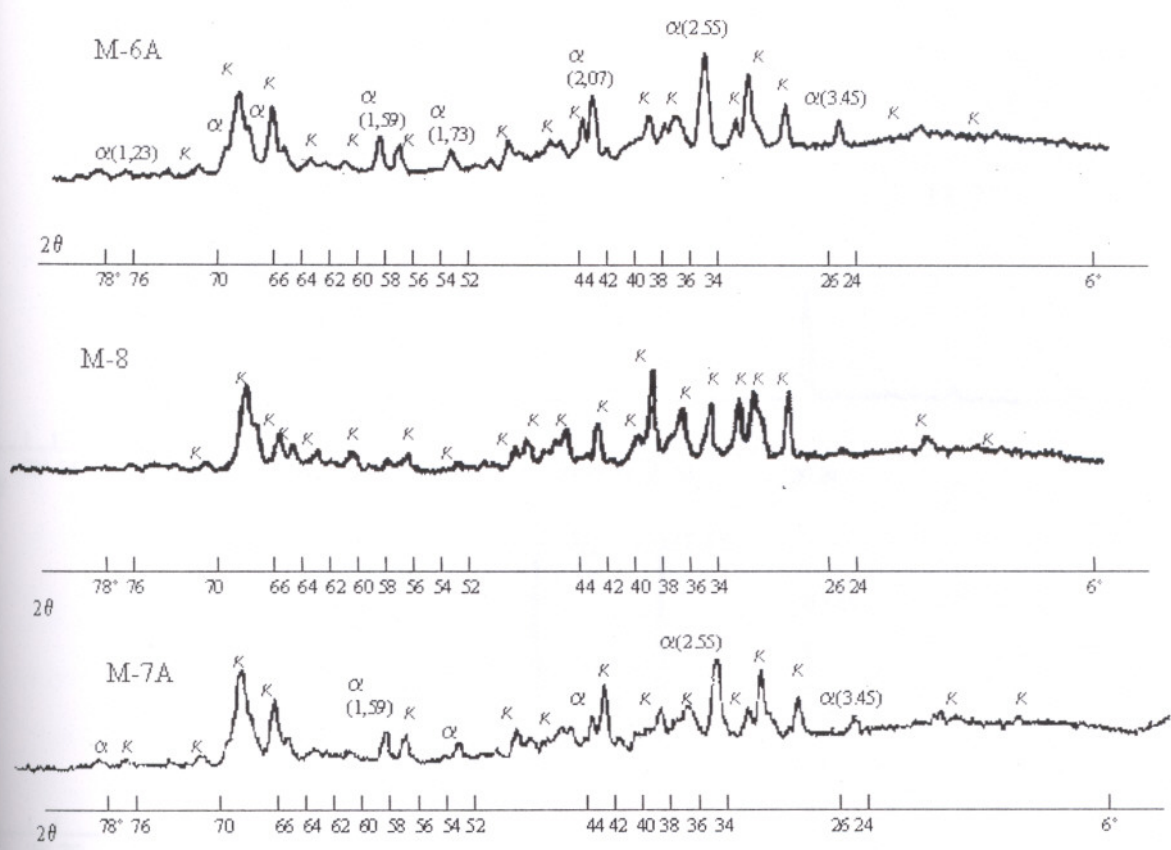


Figure 4.9. XRD diagrams of M-6A, M-7A and M-8.

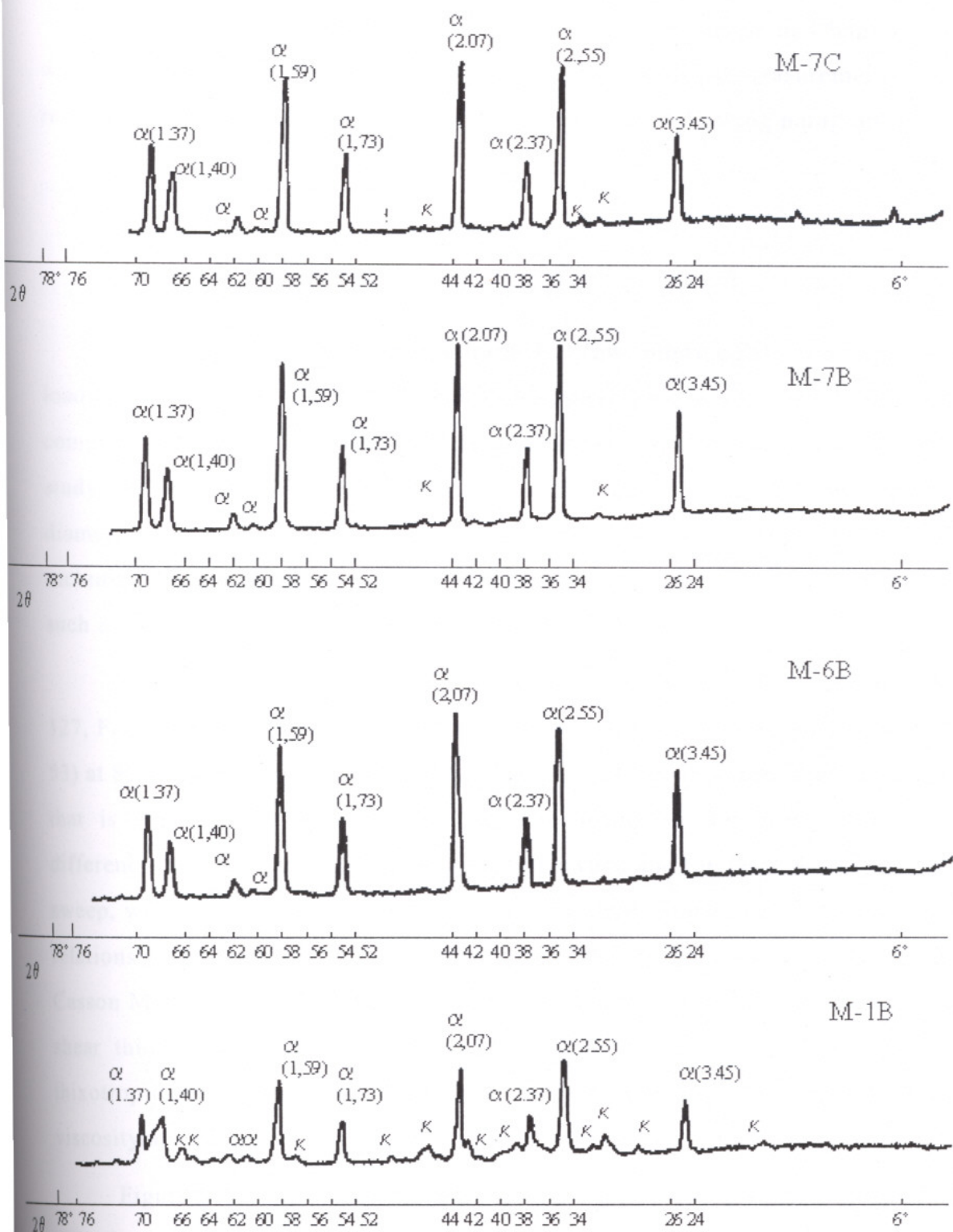


Figure 4.10. XRD Diagrams of M-7B, M-7C, M-6B and M-1B.

4.2 Suspension Preparation and Characterization

Suspensions that were prepared by the methods given in Chapter (III) were characterized by use of the rheological and turbidity measurements. The results of these measurements will be discussed in the following paragraphs.

4.2.1 Rheological Measurements

These measurements were performed at low, intermediate and high solid loadings as 0.125, 1.0, 14, 50 vol%. Measurements were carried out with commercial aluminas AKP-53, Aldrich and the powder that was prepared in this study, M-7A with BET surface area $29.82 \text{ m}^2/\text{g}$ and 62.35 \AA BET average pore diameter. The measured flow curves were fitted to various rheological models, including the Newtonian, Casson, Bingham model and some flow behaviours such as shear thinning (pseudoplastic), shear thickening (dilatant).

Figure 4.12 and 4.13 show the effect of three different surfactants; F-127, F-68, PAA and ultrasonic treatment on alumina powder suspensions (AKP-53) at 80 wt%-(50 vol%) solid loading. Figure 4.12 (a) illustrates the suspension that is prepared by using method (I). According to the graph there is a difference between the initial increasing rate sweep and the later decreasing rate sweep, which was assumed to be due to flocculation. Since there is a non-linear relationship between the shear rate and stress the flow curve was fitted with the Casson Model with 48% confidence of fit. Initial part of the curve has a typical shear thinning character with 1.34 N/m^2 yield stress that may follow by a thixotropic character. In thixotropic materials the apparent shear resistance and viscosity at a particular shear rate may decrease with shearing time.

Figure 4.12 (b) represents the suspension that was prepared by method (II). According to the graph, ultrasonic treatment has a major effect on the dispersion behaviour of the slurry. In that case thixotropic loop diminishes. Here the main function of the ultrasonic treatment was to prevent the

agglomeration of the powder that occurred in the early stages of the suspension. The flow curve shifts from a shear-thinning model to approximately Newtonian model.

In Figure 4.12 group (c) consists of the suspensions that contain PAA at 10^{-6} , 10^{-4} , 10^{-3} M concentrations. These suspensions were prepared by using method (IV). For the concentration of 10^{-6} M PAA, there is a disturbance for the dispersion behaviour. There is also a slight increase in viscosity from 0.5 to 5 mPa.s. As the PAA concentration was increased to 10^{-4} M, the suspension started to give a shear thickening behaviour in the increasing rate sweep. Here the suspension deviated from Newtonian model. Finally at 10^{-3} M there were no measurable data because of strong agglomeration. pH of the suspensions that contain PAA was measured as 5 to 7 at different concentrations. Since around pH 9, alumina surface has a negative charge, the measurements were not conducted at this pH region due to PAA's negative charge. But in case of 10^{-3} M the suspension pH was measured as 3.4. The behaviour of PAA in aqueous solution at different pH values was investigated by Cesarano & Aksay [6].

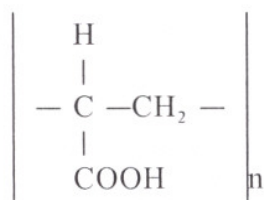


Figure 4.11. Structure of PAA polymer segments [6].

According to their study the carboxylic groups dissociate more with increasing pH, resulting in chain straightening due to repulsion between the monomer units. At pH 9, when almost complete dissociation of the carboxylic groups has taken place, the dispersion property of the polymer is at its greatest. As the pH is decreased, the number of negatively charged sites is continually decreased until the PAA is effectively neutral near pH 3.4 and the fraction dissociated (α) goes to zero. In this condition, the PAA chains approach insolubility and form relatively small coils or clumps. On the other hand, Guo et

al. [12] mentioned that at low pH values such as 4-6, high affinity adsorption occurs, and as the pH increases, the driving force for adsorption due to electrostatic attraction decreases.

Figure 4.13 (d) gives the viscosity results of the suspension in the case of F-68, which shows nearly Newtonian behaviour. Also there is no difference between the initial and the final sweeps.

In Figure 4.12 (e) effects of F-127 were summarized. At concentrations of 10^{-6} M and 10^{-4} M, the initial sweep has a shear thickening behaviour that was followed by final decreasing route. On the other hand at 10^{-3} M surfactant concentrations suspension caught the Newtonian behaviour again. Here as it was shown in Figure 4.13 (e), the viscosity is nearly constant hence the suspension is highly stable in that situation. Similar behaviour was observed in the case of F-68.

In the case of $\Phi = 14$ vol% solid loading, AKP-53 suspensions prepared with method (I), flocculated weakly with a yield value. It had a shear thickening behaviour with yield stress. Also viscosity of the system reaches about 20 mPa.s at 100 (1/s). But the usage of ultrasonic treatment affected the system significantly. Addition of F-68 and F-127 did not bring any majorable change with using ultrasonic treatment. All of the suspensions in the system except PAA, showed a typical shear thickening or Newtonian model and the viscosities were nearly constant (changes between 1.5-3.29 mPa.s) as indicated in Figure 4.14 and Figure 4.15. But PAA at concentrations of 10^{-4} M and 10^{-3} M had a negative effect on the stability. The slurries displaced shear-thinning behaviour with 1.87 (N/m^2) yield value. Here suspensions were in their flocculated form again (Figure 4.15 (e)).

In the case of $\Phi = 1\%$ and 0.125 vol% AKP-53 solid loading, suspensions were approximately Newtonian without any treatment and surfactant addition. These results can be followed from Figures 4.16 to 4.19. Although suspensions are stable in the related figures there is a slight increase in the viscosity values with the shear rate.

For the Aldrich alpha alumina powder at $\Phi=50$ vol%, slurry without any treatment showed an undispersed behaviour. There is a big difference between the initial and the final rate sweeps. The suspension shows a flocculated behaviour as pointed out in Figure 4.20 (a). Also the use of ultrasonic treatment did not bring any sufficient effect on creating a stable dispersion and viscosity of the suspension increased detrimentally. On the other hand F-68 and F-127 improved the dispersion characteristics of the slurry. After the usage of F-68 and F-127 suspensions gained nearly dilatant behaviour. Especially in the case of F-127 at 10^{-3} M minimum viscosity values were obtained ranging between 2.34 to 4.0 mPa.s. At this point the yield value decreased and the loop diminished. The flow curve shifted from a flocculated form to dilatant. But PAA has showed a negative effect at high concentration level, that is 10^{-3} M. At this concentration flow curve was fitted with the shear thinning with >50 mPa.s viscosity and suspension was shifted to strongly flocculated form.

Aldrich alpha alumina with $\Phi=14\%$ and 1 vol% solid loadings had approximately a dispersed nature. So that usage of ultrasonic bath and the surfactants was not shown any major effect. Similar results were obtained with AKP-53 powder at 4% solid loading. All of the suspensions in the case of Aldrich had a shear thickening behaviour as it was denoted in Figures 4.22 and 4.24.

To investigate the effect of ultrasonic bath treatment on the stability of the suspensions, some measurements were performed with AKP-53, Aldrich powder and M-7A alumina at $\Phi= 0.125\%$, 14% and 50 vol%. But in the case of $\Phi= 50$ vol% solid loading for both M-7A and Aldrich powders measurements could not performed because of very high torque values caused by strong flocculation. In this set suspensions were prepared with 10 minutes stirring only without any ultrasonic bath treatment (method III).

For the Aldrich suspensions, addition of PAA at pH=5 and F-127 for all conditions created a flocculated system. As the solid loading was increased, negative effect of these dispersants also increased as indicated in Figures 4.28, 4.29 and 4.30. Especially for the case $\Phi= 40$ wt% Aldrich, viscosities reached to

above 25 mPa.s. Additionally as the surfactant concentration increased the shear thinning behaviour in suspensions became stronger. Hence suspensions became flocculated.

In the case of M-7A suspensions similar results were obtained in Figure 4.31. Here effect of F-127 at 10^{-6} , 10^{-4} and 10^{-3} M surfactant concentrations was studied with method (III) and at 10^{-4} M with method (IV). According to the results M-7A suspensions has a disperse character even at $\Phi = 14$ vol% without any treatment (method I). However usage of surfactant and the ultrasonic treatment created flocculation in the system. So all of the suspensions showed shear thinning behaviour.

For the AKP-53 suspensions effect of F-127 was studied at 10^{-2} M for $\Phi = 0.125\%$, 14% and at 10^{-3} M for $\Phi = 50\%$ respectively. All the suspensions prepared with method (III) showed flocculated character (Figure 4.33). Based on these studies, the following results can be summarized:

- As the solid loadings were increased, the viscosities of the suspensions were also increased.
- For high solid loadings, that is $\Phi = 50\%$, 14% AKP-53 and 50% Aldrich, only stirring of the suspensions (method I) is not sufficient to create dispersion. System gets flocculated in those situations.
- For the AKP-53 suspensions the use of ultrasonic bath (method II) is sufficient to overcome the flocculation and obtaining a dispersed system for all solid loadings. But in the case Aldrich suspension at $\Phi = 50\%$ and M-7A suspensions at $\Phi = 14\%$ usage of ultrasonic bath is not enough to overcome the flocculation.
- The suspensions are exposed to the high frequency vibrations in ultrasonic treatment. Both physical and chemical changes occur as a result of a physical phenomenon, known as cavitation. It is the formation of expansion and implosion of microscopic gas bubbles in liquid absorbs ultrasonic energy. Compression and refraction

waves rapidly move through the liquid media. If the waves are sufficiently intense they will break the attractive forces in the existing molecules and create gas bubbles. This process may create a better dispersion or flocculation.

- When method (IV) was applied, effect of surfactants varied depending on the type and the concentration of the dispersants for all the powders tested. There was no negative effect of F-68 for all suspensions prepared with method (IV). Also for AKP-53 and Aldrich powders best results were obtained in the case of F-127 at 10^{-3} M.
- In the case of Aldrich alumina suspensions at $\Phi = 50\%$ prepared with method (IV), use of F-127 had a positive effect on the dispersion behaviour. On the other hand in that situation PAA created flocculation. Similarly in the case of AKP-53 at $\Phi = 14\%$ and 50% PAA caused flocculation at high dispersant concentrations.
- For all powders, use of F-127 and PAA without any ultrasonic treatment had a negative effect on the dispersion behaviour of the suspensions especially at high solid loadings (method III). Negative effect of these surfactants in that situation increased as the surfactant concentration increased.

The reason for the flocculation of these non-ionic polymeric surfactants such as F-127 in method (III) might be attributed to the depletion flocculation mechanism that occurs at small particle separations. Also bridging effect may cause flocculation. In that mechanism surfactant molecules can cover two or more particles together hence may cause weak flocculation.

It was found in the literature [2, 42] solutions of F-127 in water at very high concentrations (in the gel state) without any powder also have a yield stress value that means they can only flow when the yield stress, which is

applied to them, is larger than a threshold value. Also the yield value increases with increasing F-127 concentrations. The highest yield values are above 1000 Mpa, this is such a high value that in those hard gels large and heavy particles can be suspended without the occurrence of sedimentation [13]. This might be causing some shear thinning behaviour in the presence of very high surfactant concentrations in method (III).

On the other hand dispersion and stabilisation mechanisms of block copolymers will be discussed in Section 4.2.3. This section also gives possible explanation for the stabilisation mechanism of block copolymers such as of F-127 without adsorption to the alumina surface such as depletion stabilization.

AKP-53, 50 vol%

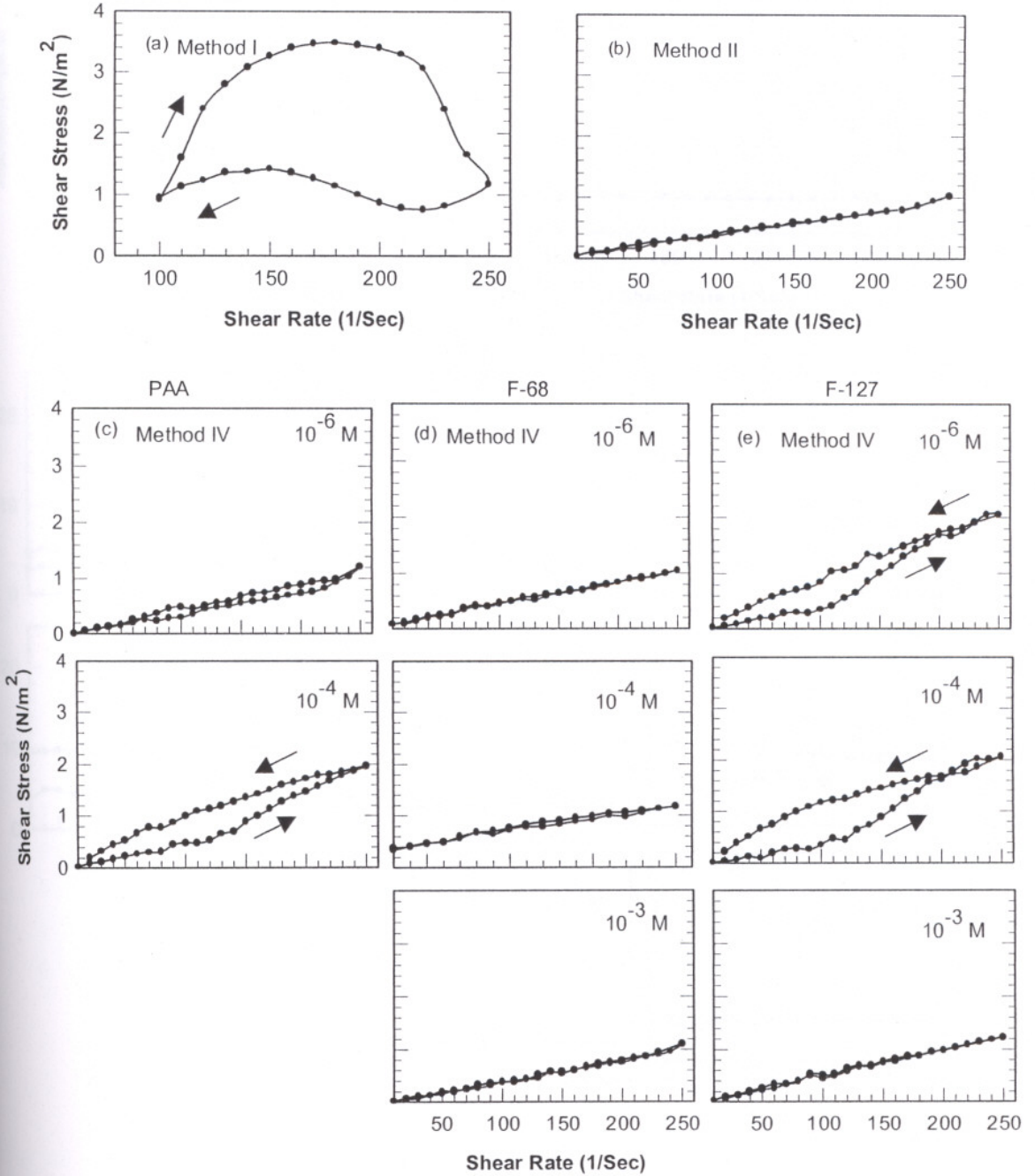


Figure 4.12. Shear rate vs. shear stress graphs of AKP-53 suspensions prepared with Method I, II and IV at 50 vol%-(80 wt%) solid loading

AKP-53 , 50 vol %

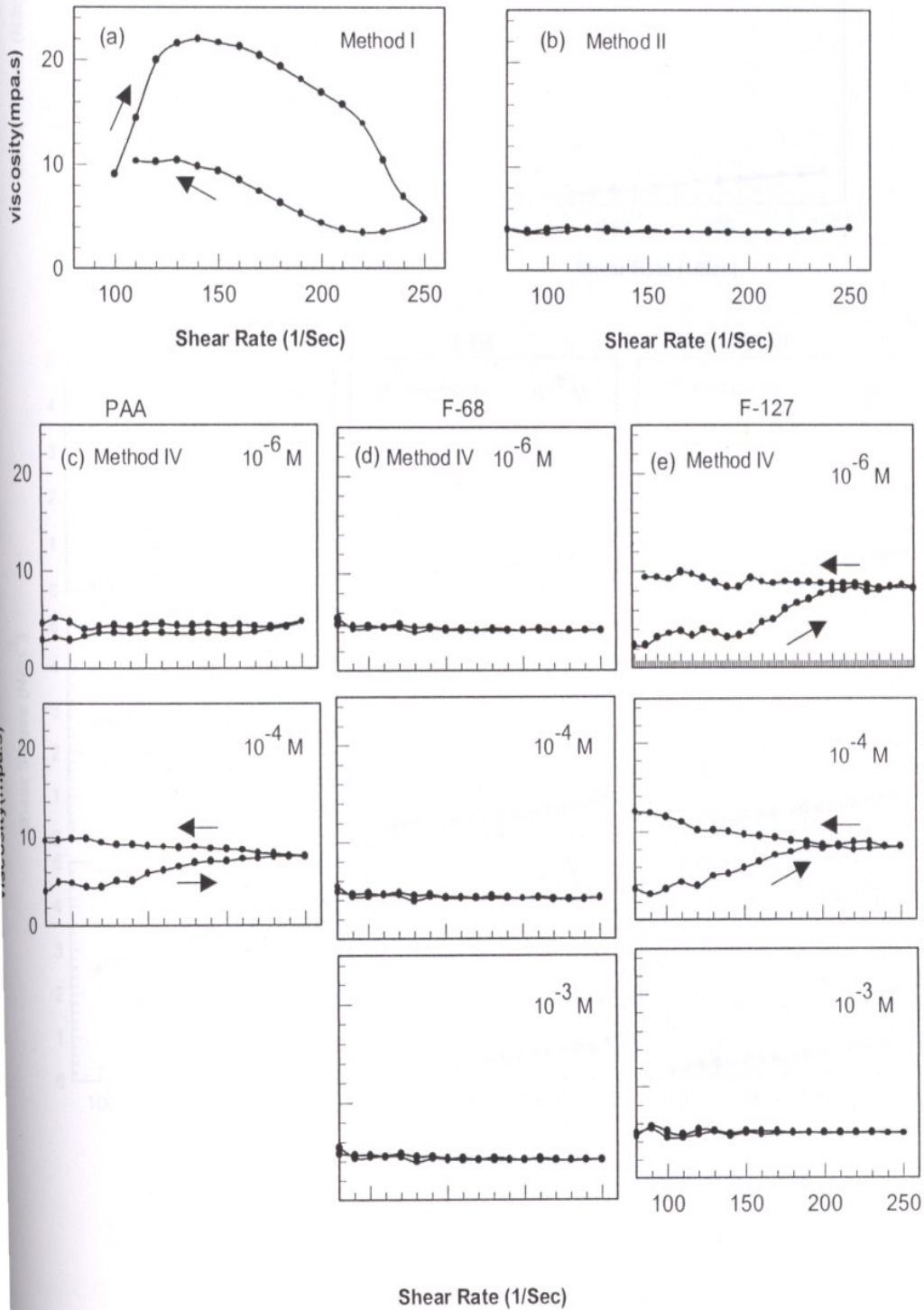


Figure 4.13. Shear rate vs. viscosity graphs of AKP-53 suspensions prepared with Method I, II and IV at 50 vol%-(80 wt%) solid loading.

AKP-53, 14 vol %

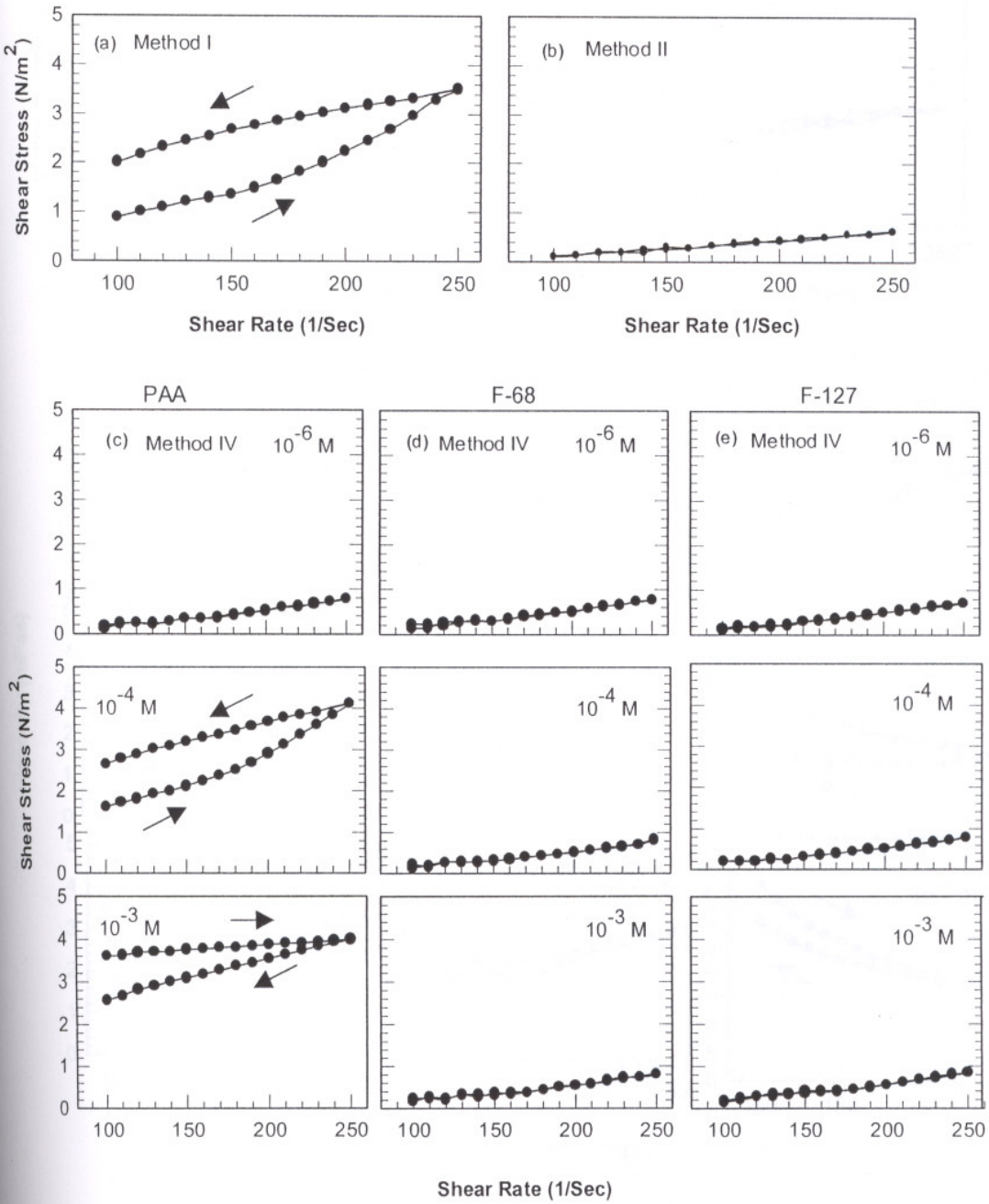


Figure 4.14. Shear rate vs. shear stress graphs of AKP-53 suspensions prepared with Method I, II and IV at 14 vol %-(40 wt%) solid loading

AKP-53, 14 vol%

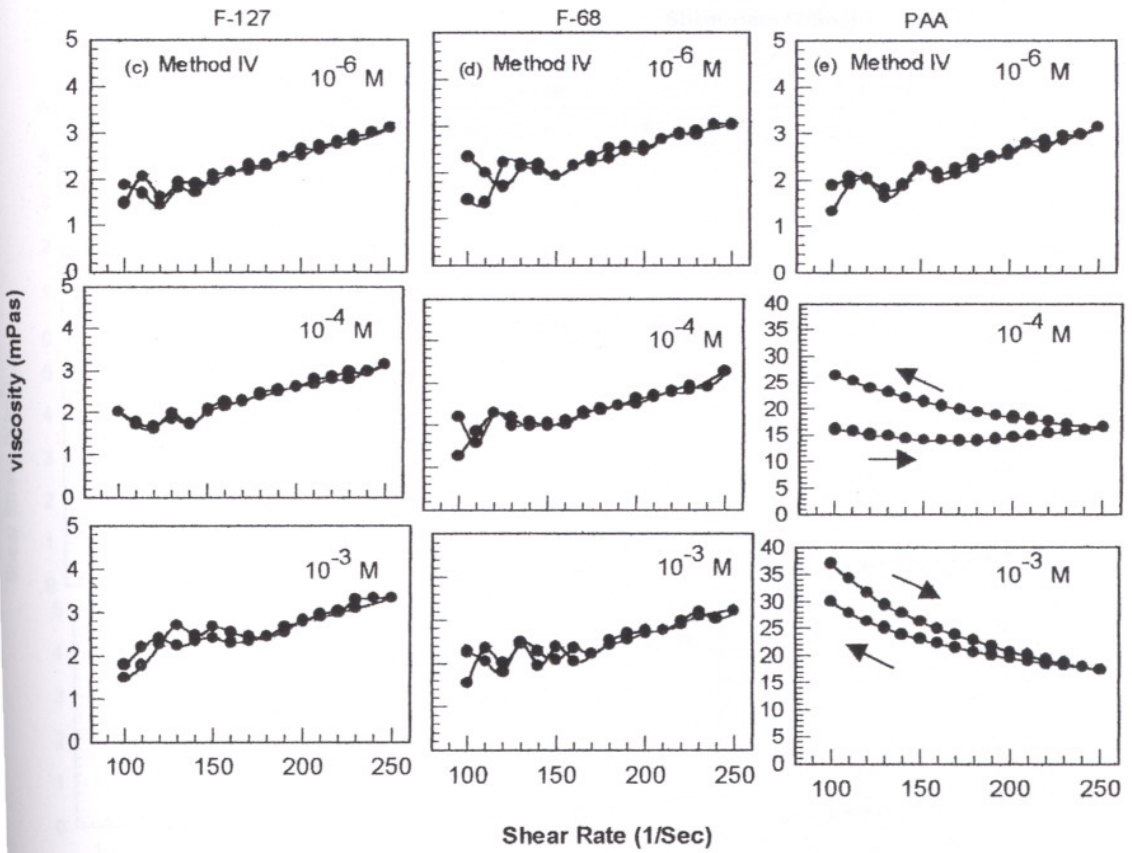
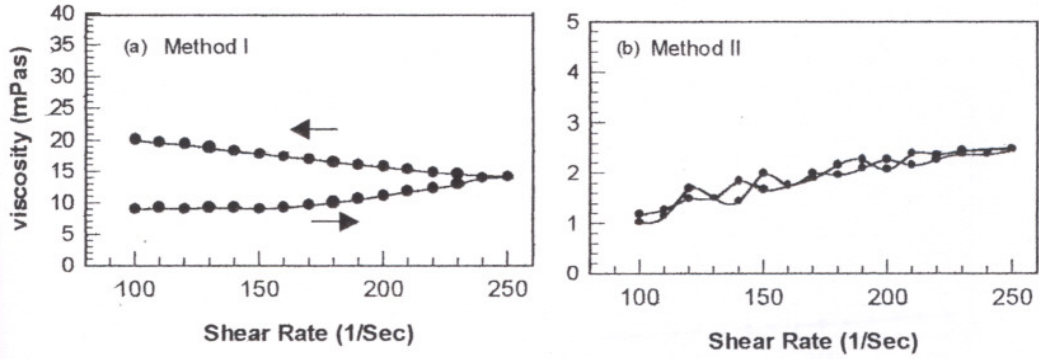


Figure 4.15. Shear rate vs. viscosity graphs of AKP-53 suspensions prepared with Method I, II and IV at 14 vol%-(40wt%) solid loading.

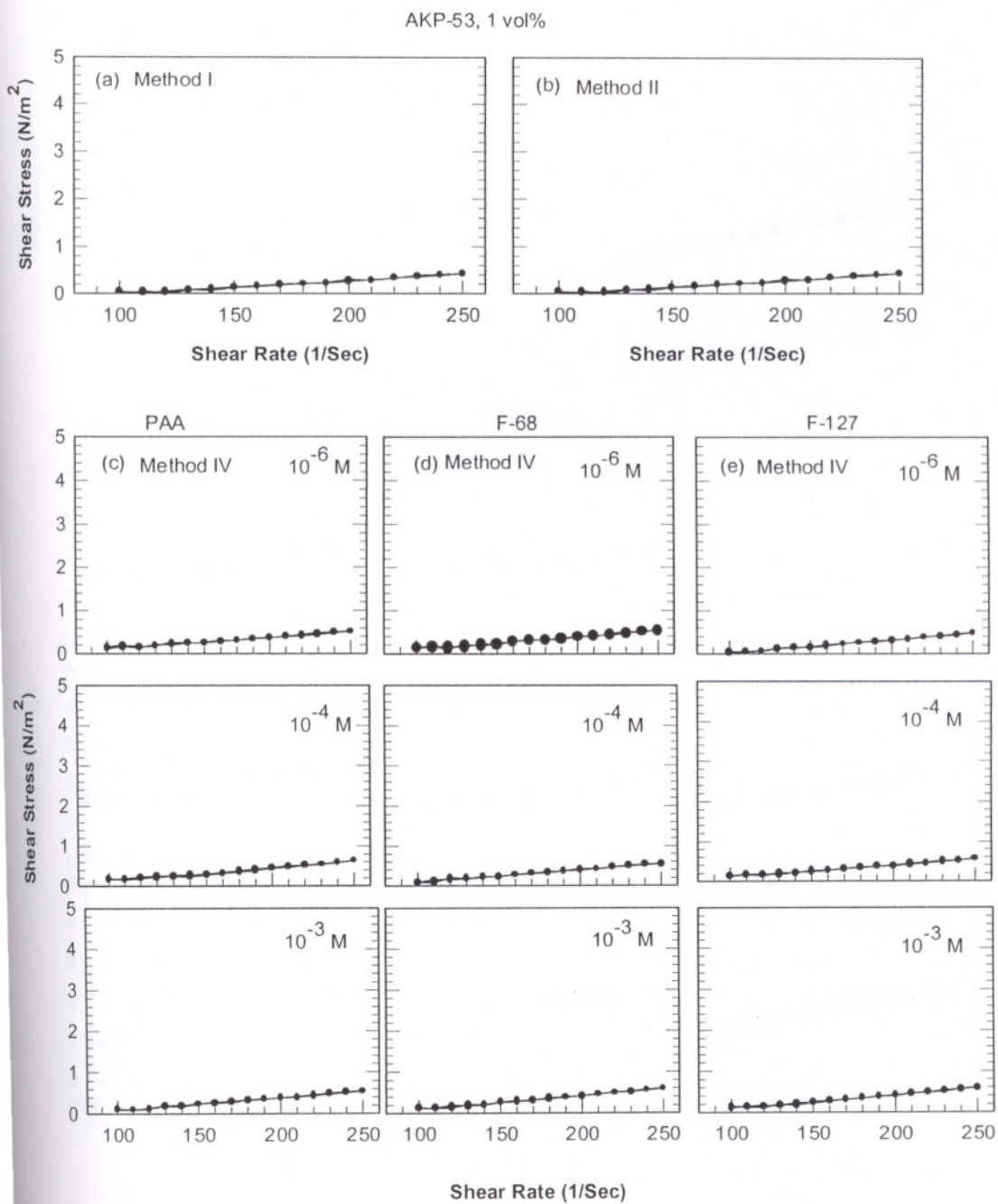


Figure 4.16. Shear rate vs. shear stress graphs of AKP-53 suspensions prepared with Method I, II and IV at 1 vol%-(4 wt%) solid loading.

AKP-53, 1 vol%

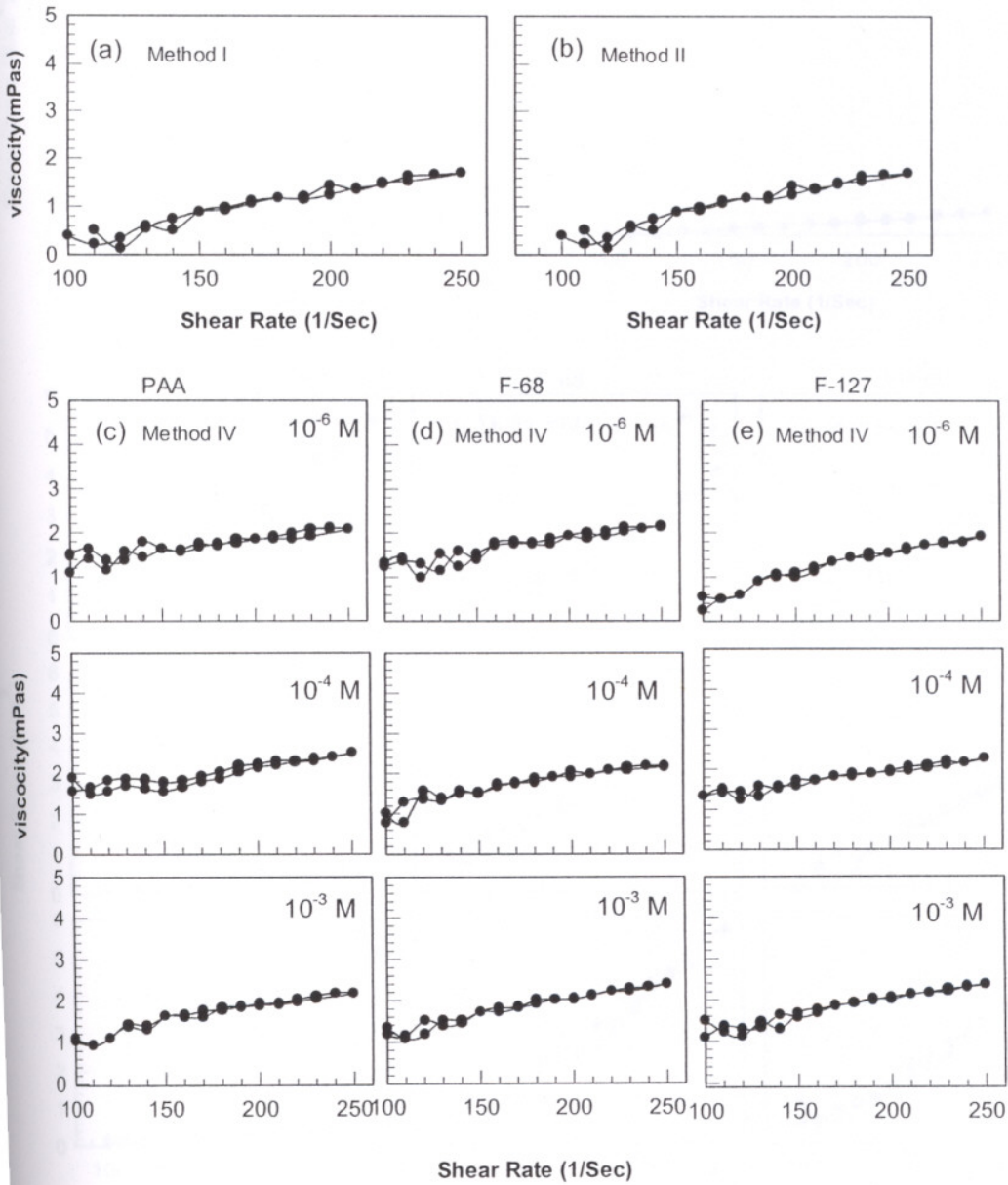


Figure 4.17. Shear rate vs. viscosity graphs of AKP-53 suspensions prepared with Method I, II and IV at 1 vol% -(4 wt%)solid loading.

AKP-53, 0.125 vol%

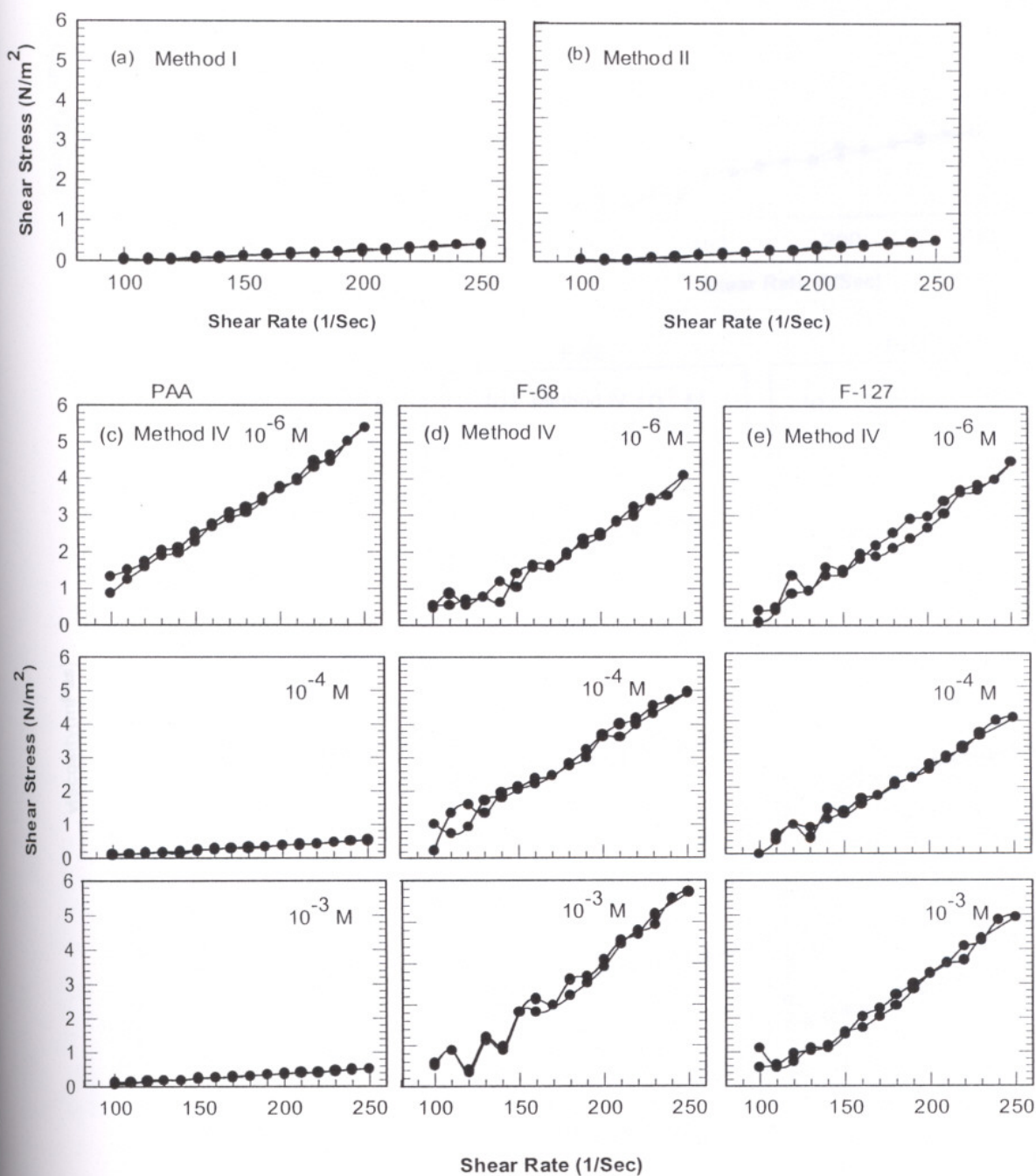


Figure 4.18. Shear rate vs. shear stress graphs of AKP-53 suspensions prepared with Method I, II and IV at 0,125 vol %-(0.5wt%) solid loading.

AKP-53, 0.125 vol%

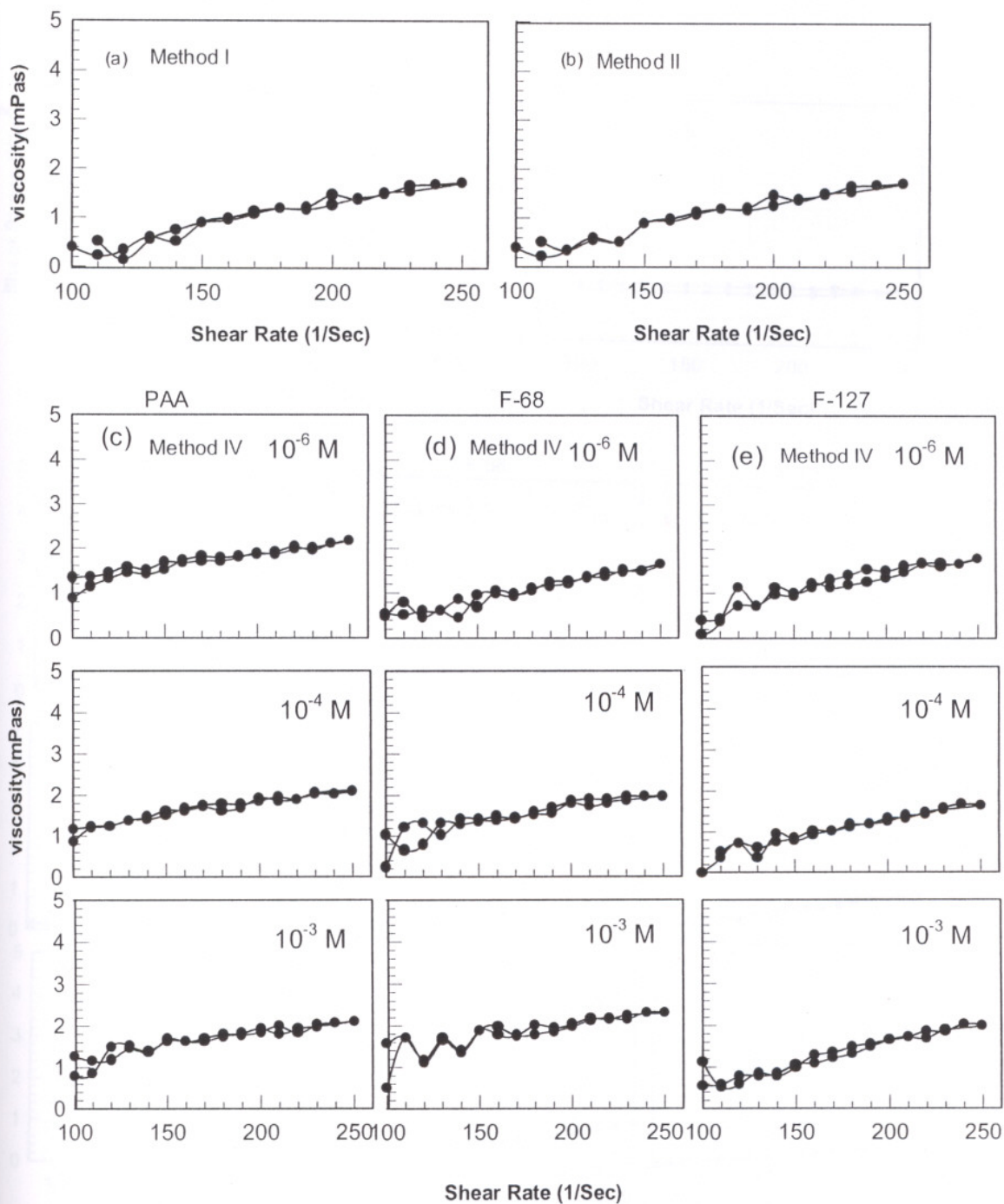


Figure 4.19. Shear rate vs. viscosity graphs of AKP-53 suspensions prepared with Method I, II and IV at 0,125 vol %-(0.5wt%) solid loading.

Aldrich Alumina, 50 vol%

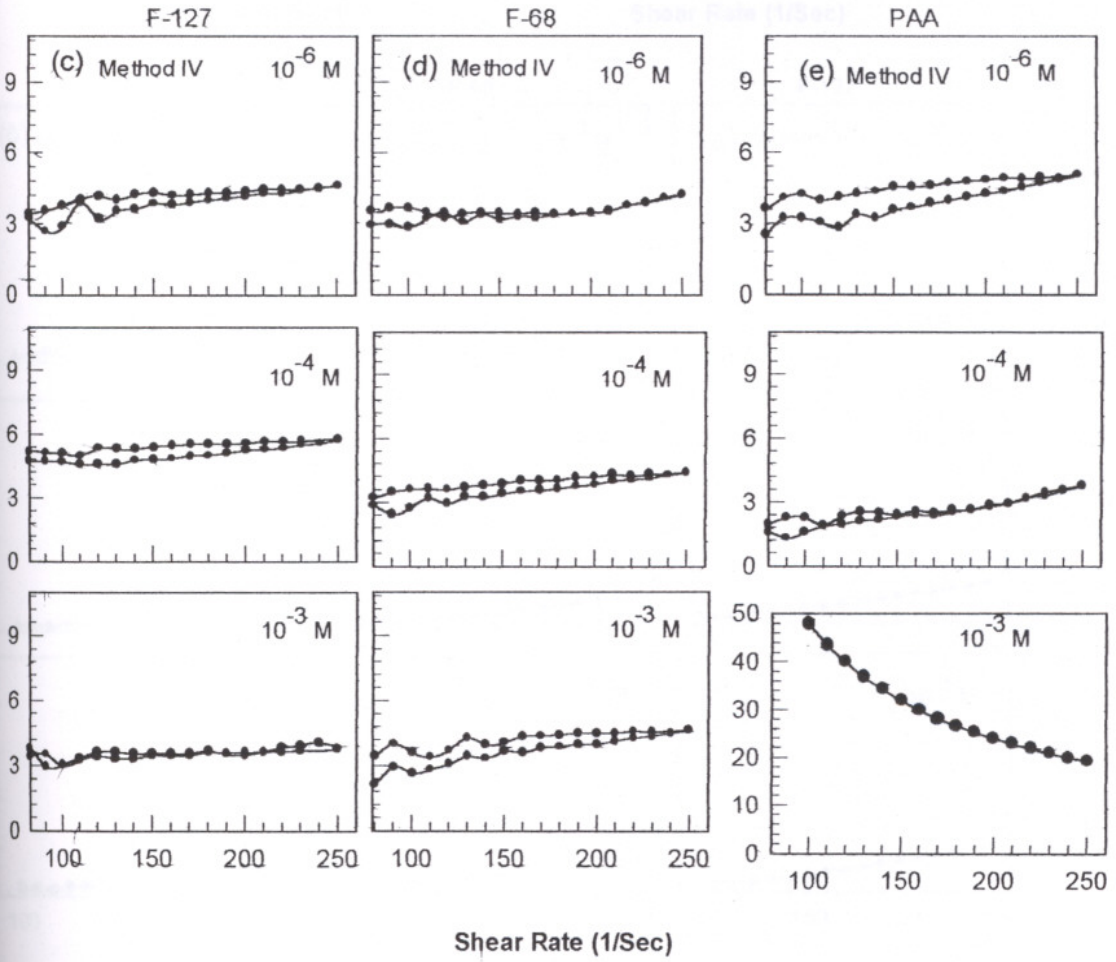
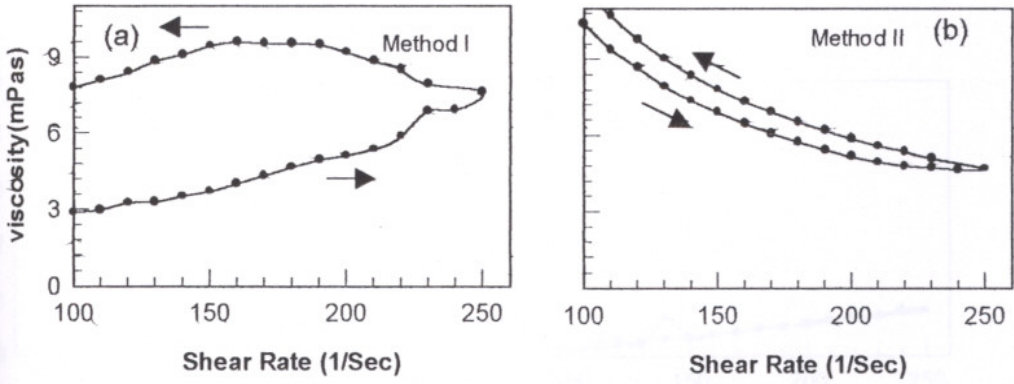


Figure 4.21. Shear rate vs. viscosity graphs of Aldrich suspensions prepared with Method I, II and IV at 50 vol%-(80 wt%) solid loading.

Aldrich Alumina, 14 vol%

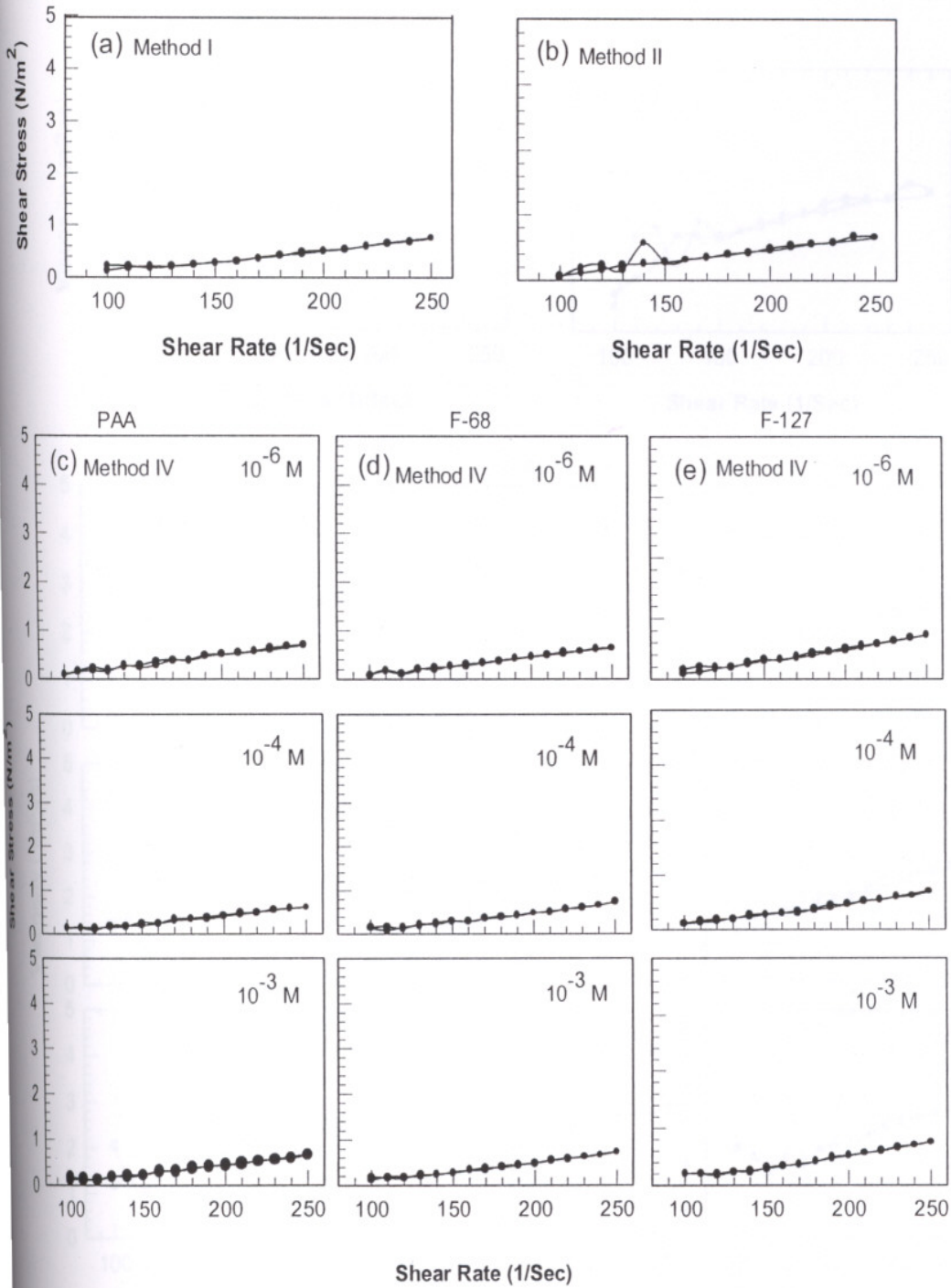


Figure 4.22. Shear rate vs. shear stress graphs of Aldrich alumina suspensions prepared with Method I, II and IV at 14 vol%-(40wt%) solid loading.

Aldrich Alumina, 14 vol%

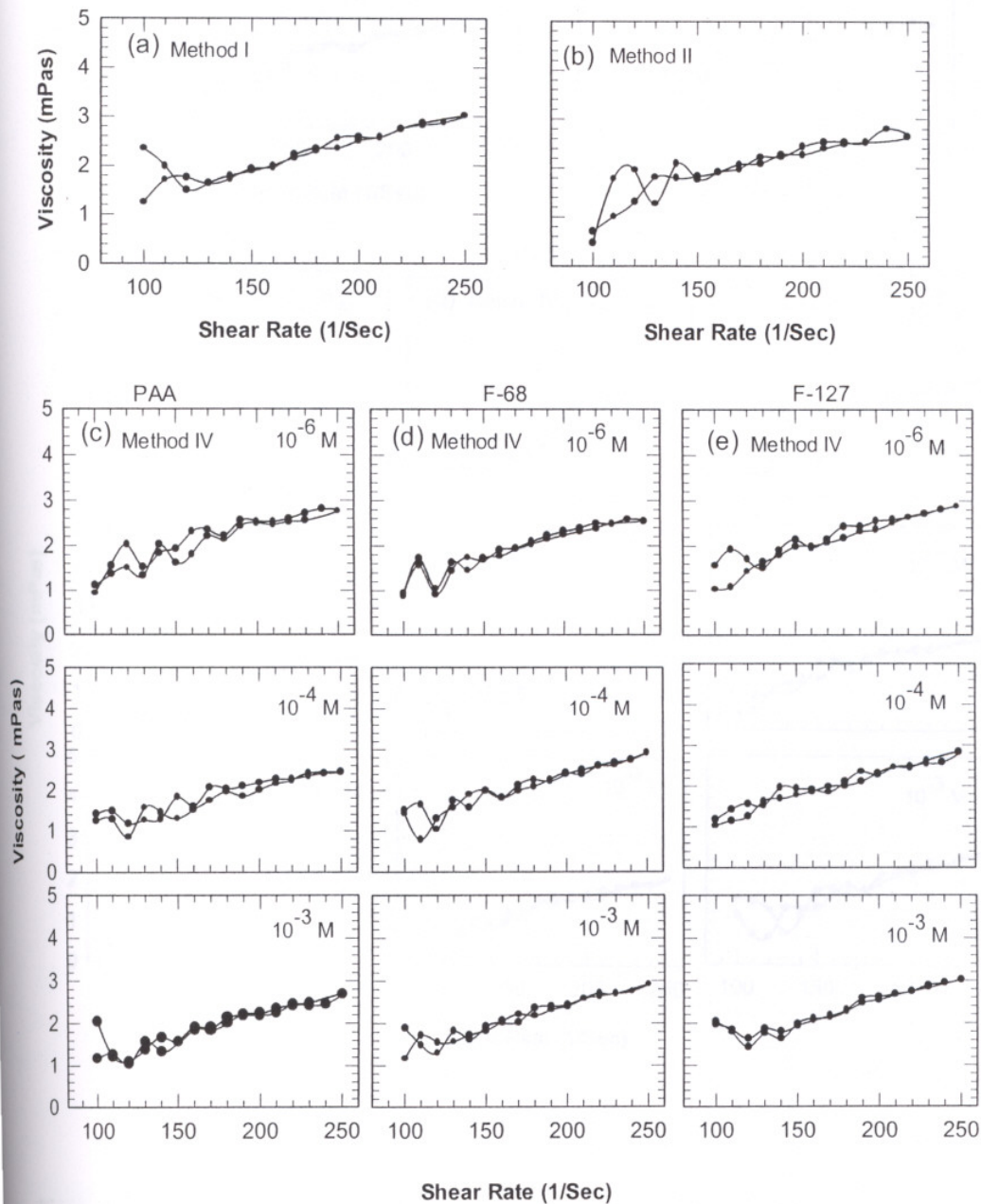


Figure 4.23. Shear rate vs. viscosity graphs of Aldrich suspensions prepared with Method I, II and IV at 14 vol%-(40wt%) solid loading.

Aldrich Alumina, 1 vol%

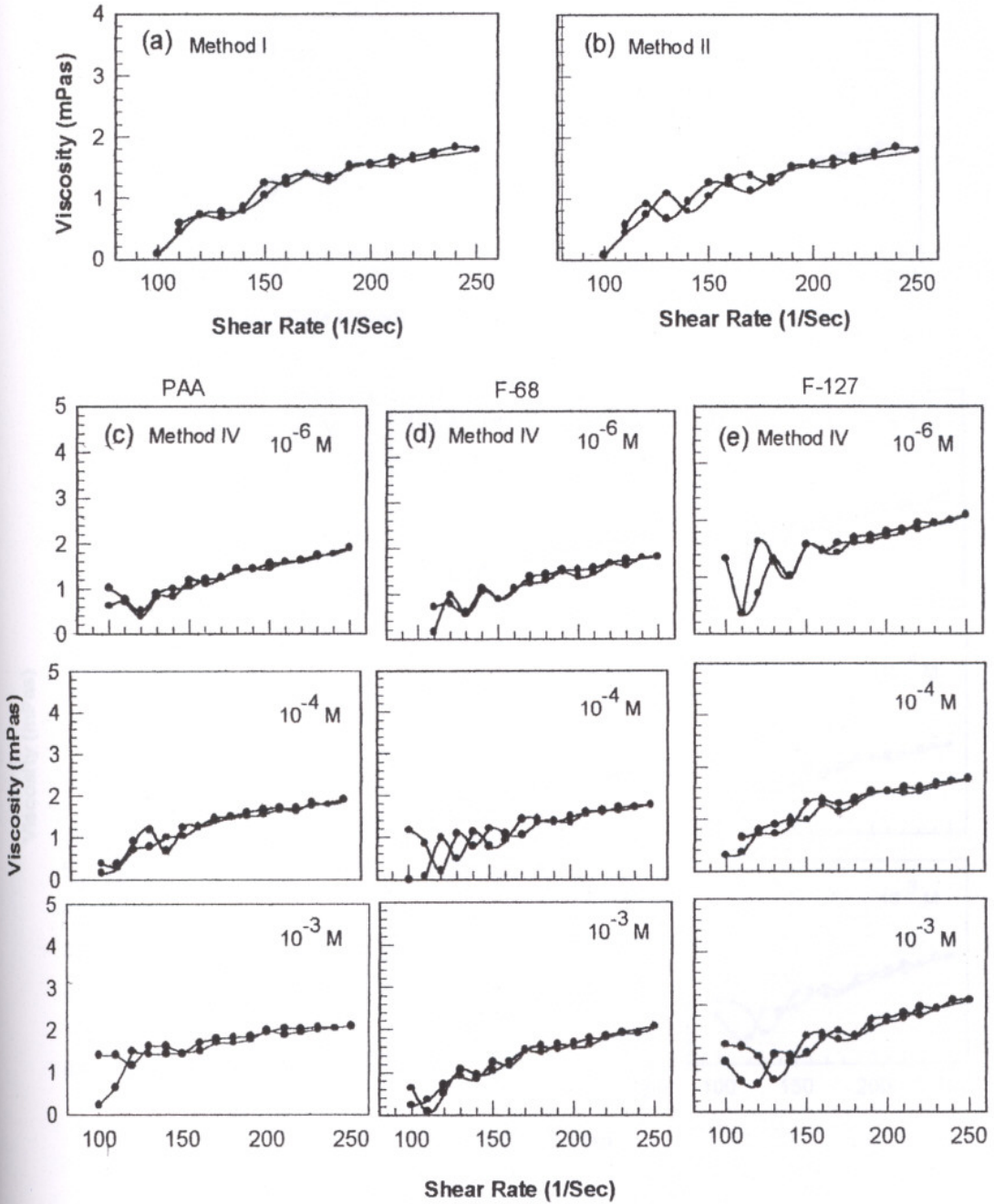


Figure 4.24. Shear rate vs. shear stress graphs of Aldrich alumina suspensions prepared with Method I, II and IV at 1 vol% -(4 wt%) solid loading.

Aldrich Alumina, 1 vol%

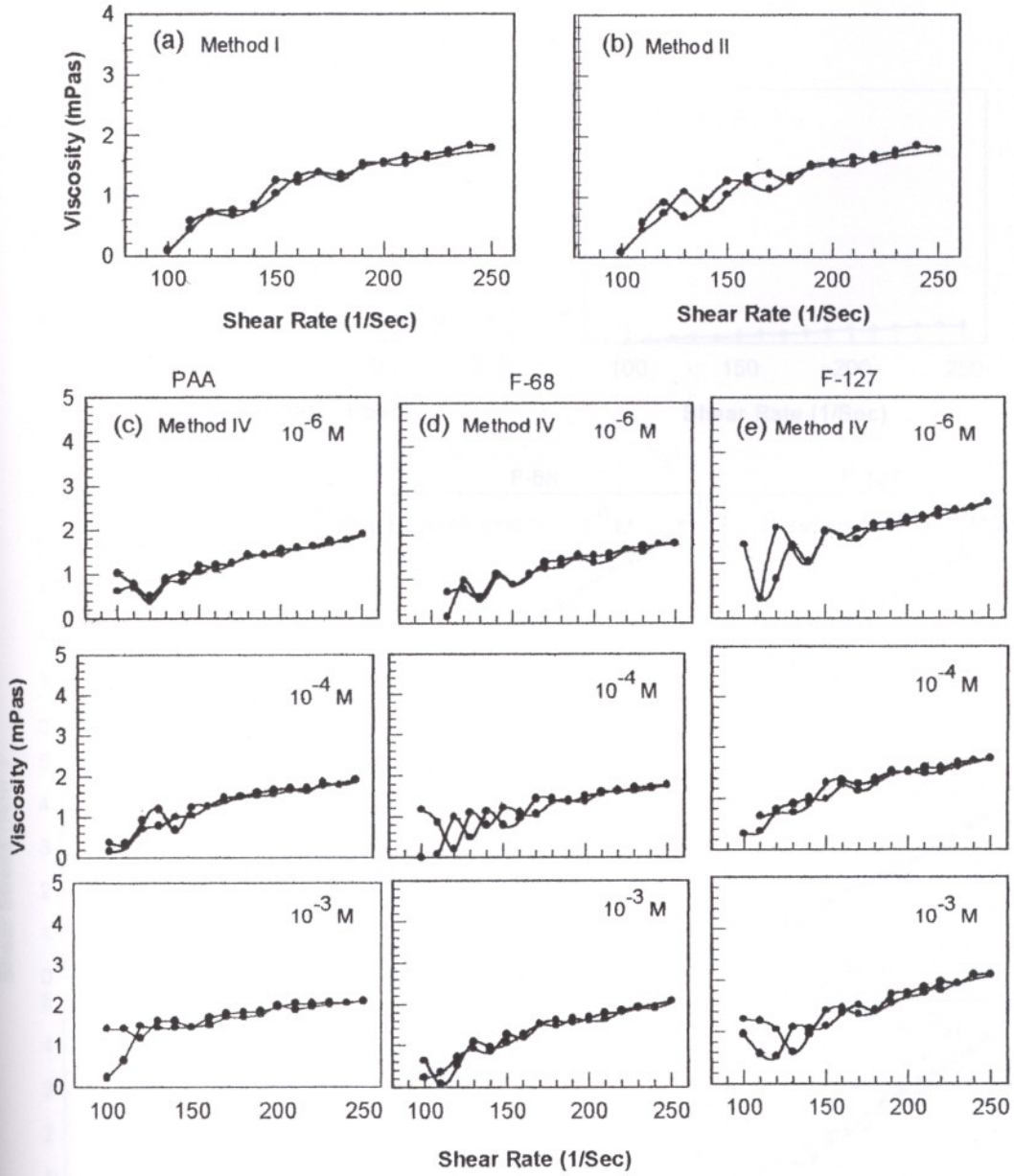


Figure 4.25. Shear rate vs. viscosity graphs of Aldrich alumina suspensions prepared with Method I, II and IV at 1 vol% -(4 wt%) solid loading.

İZMİR YÜKSEK TEKNOLOJİ ENSTİTÜSÜ
REKTÖRLÜĞÜ
Kütüphane ve Dokümantasyon Daire Bşk.

Aldrich Alumina, 0.125 vol%

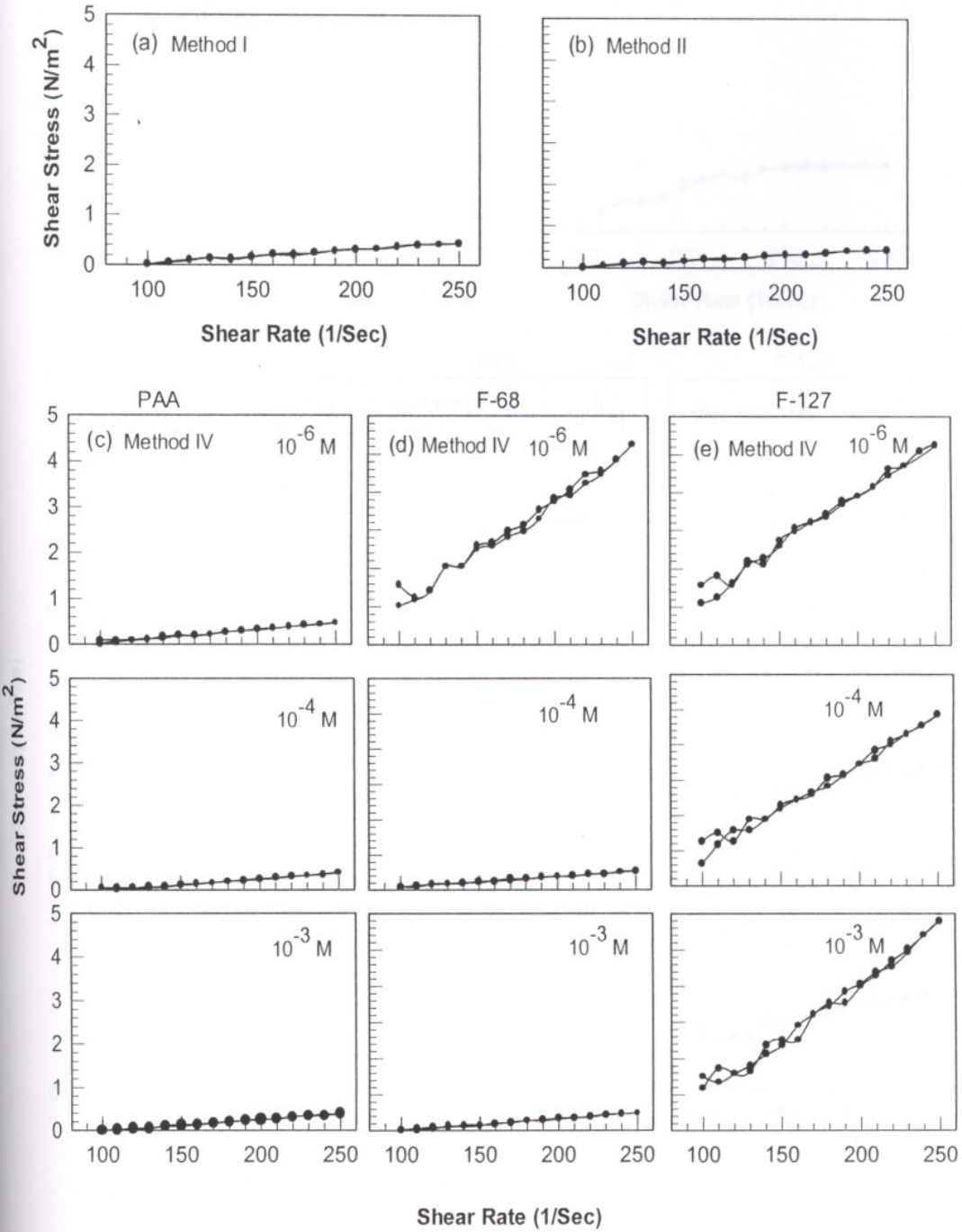


Figure 4.26. Shear rate vs. shear stress graphs of Aldrich alumina suspensions prepared with Method I, II and IV at 0,125 vol %-(0.5wt%) solid loading.

Aldrich Alumina, 0.125 vol%

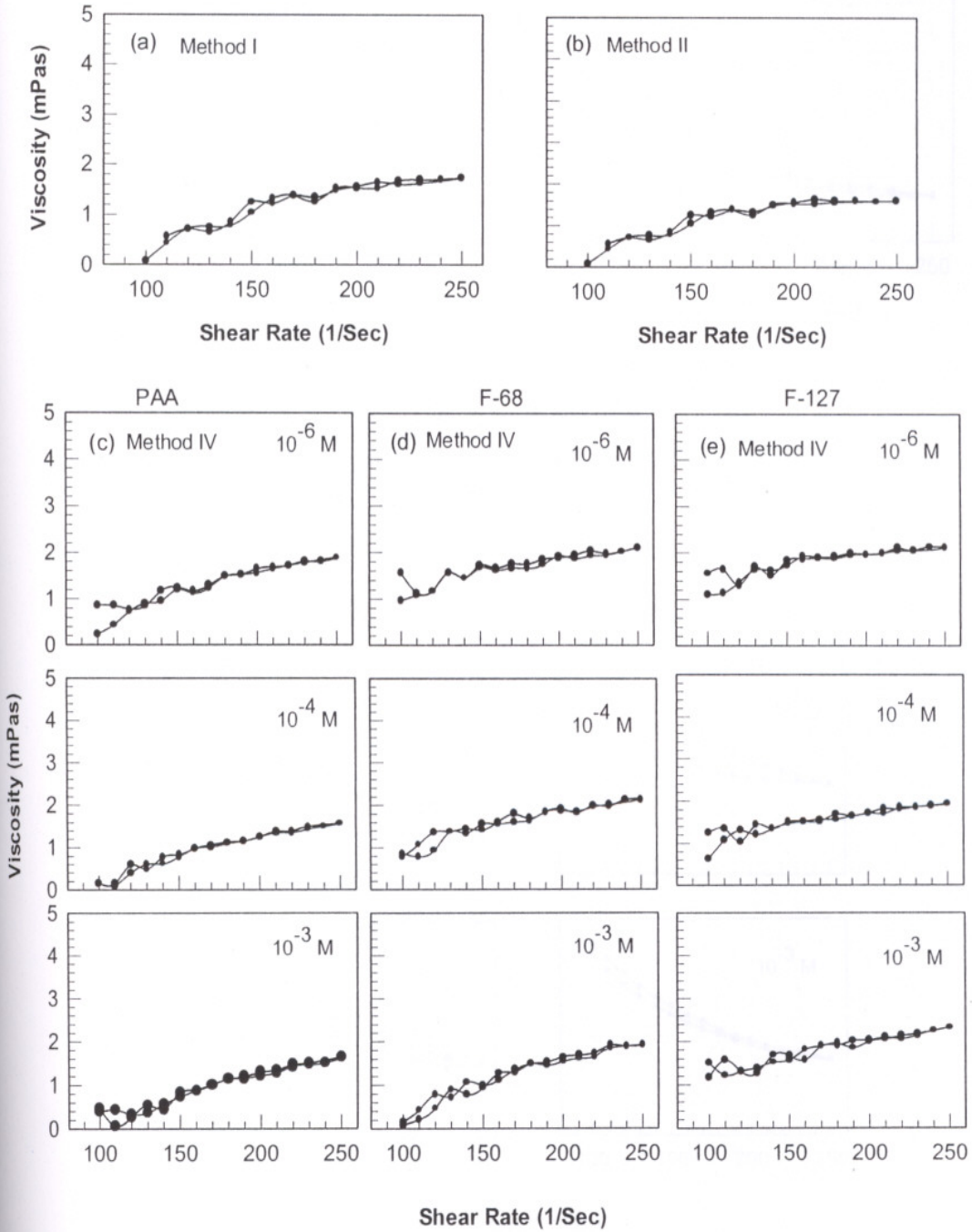


Figure 4.27. Shear rate vs. viscosity graphs of Aldrich alumina suspensions prepared with Method I, II and IV at 0,125 vol %-(0.5wt%) solid loading.

Aldrich Alumina, 50 vol%

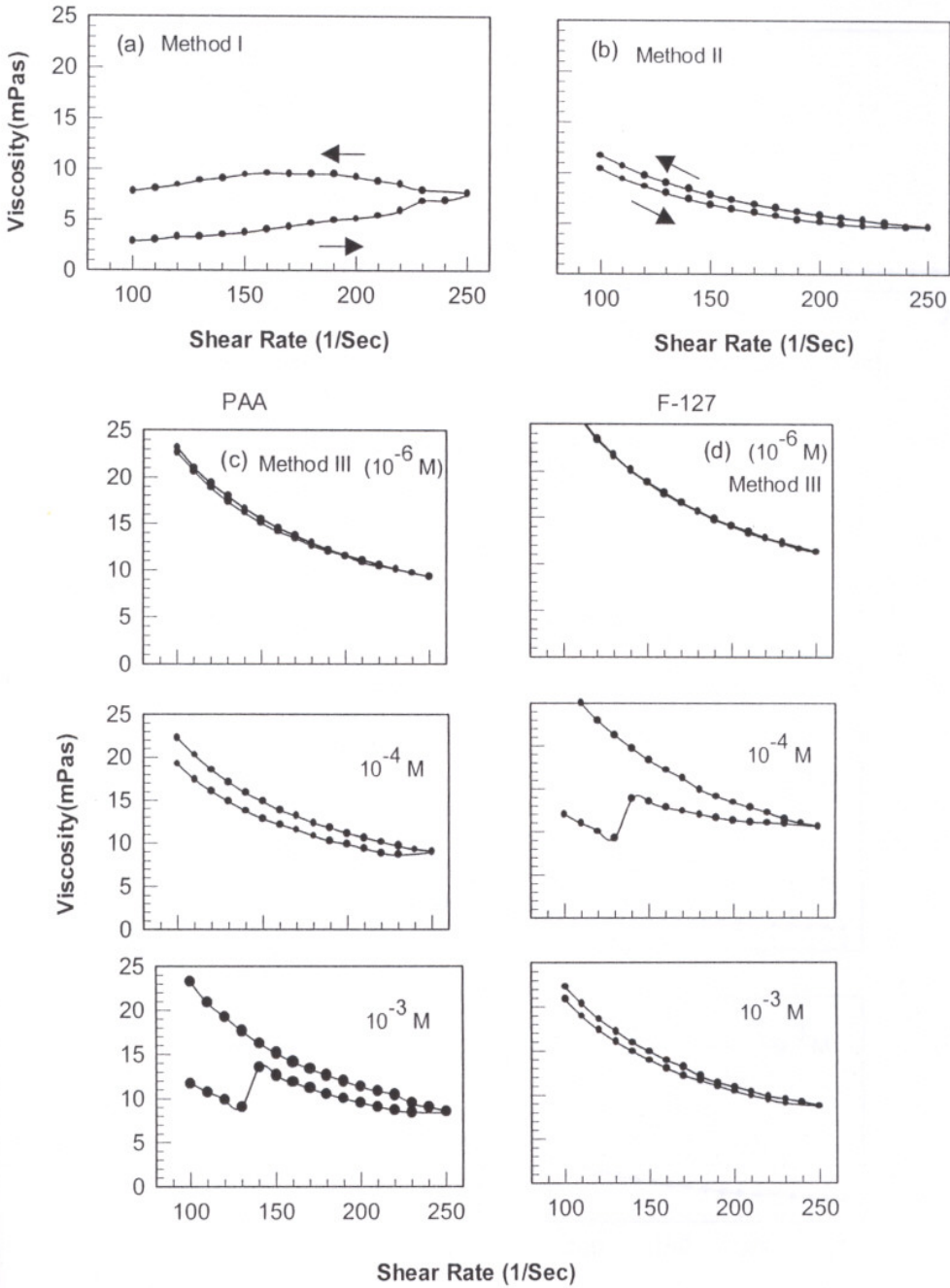


Figure 4.28. Shear rate vs. viscosity graphs of Aldrich alumina suspensions prepared with Method I, II and III at 50 vol%-(80wt%) solid loading.

Aldrich Alumina, 14 vol%

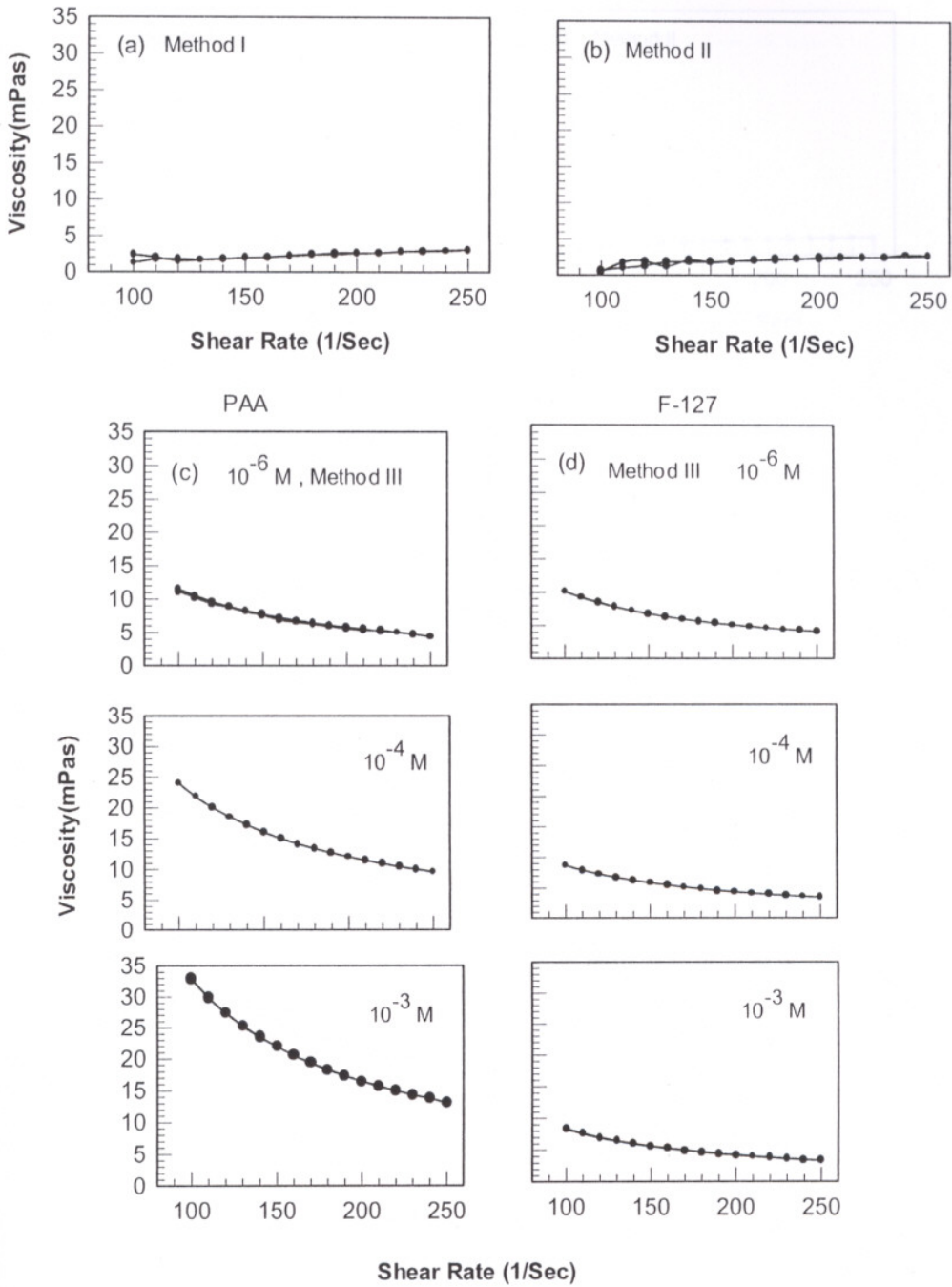


Figure 4.29. Shear rate vs. viscosity graphs of Aldrich alumina suspensions prepared with Method I, II and III at 14 vol%-(40wt%) solid loading.

Aldrich Alumina, 0,125 vol%

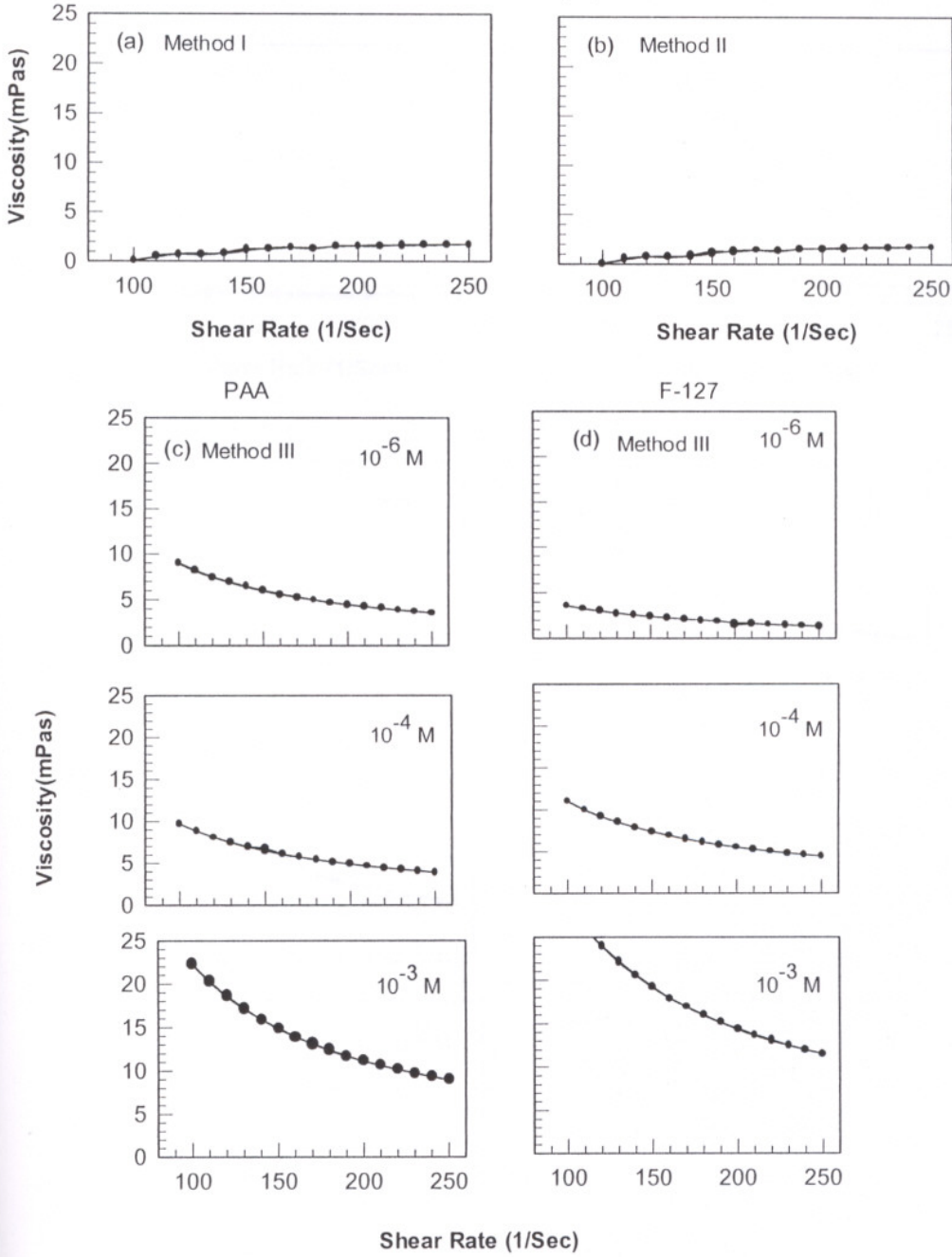


Figure 4.30. Shear rate vs. viscosity graphs of Aldrich alumina suspensions prepared with Method I, II and III at 0,125 vol %-(0.5wt%) solid loading.

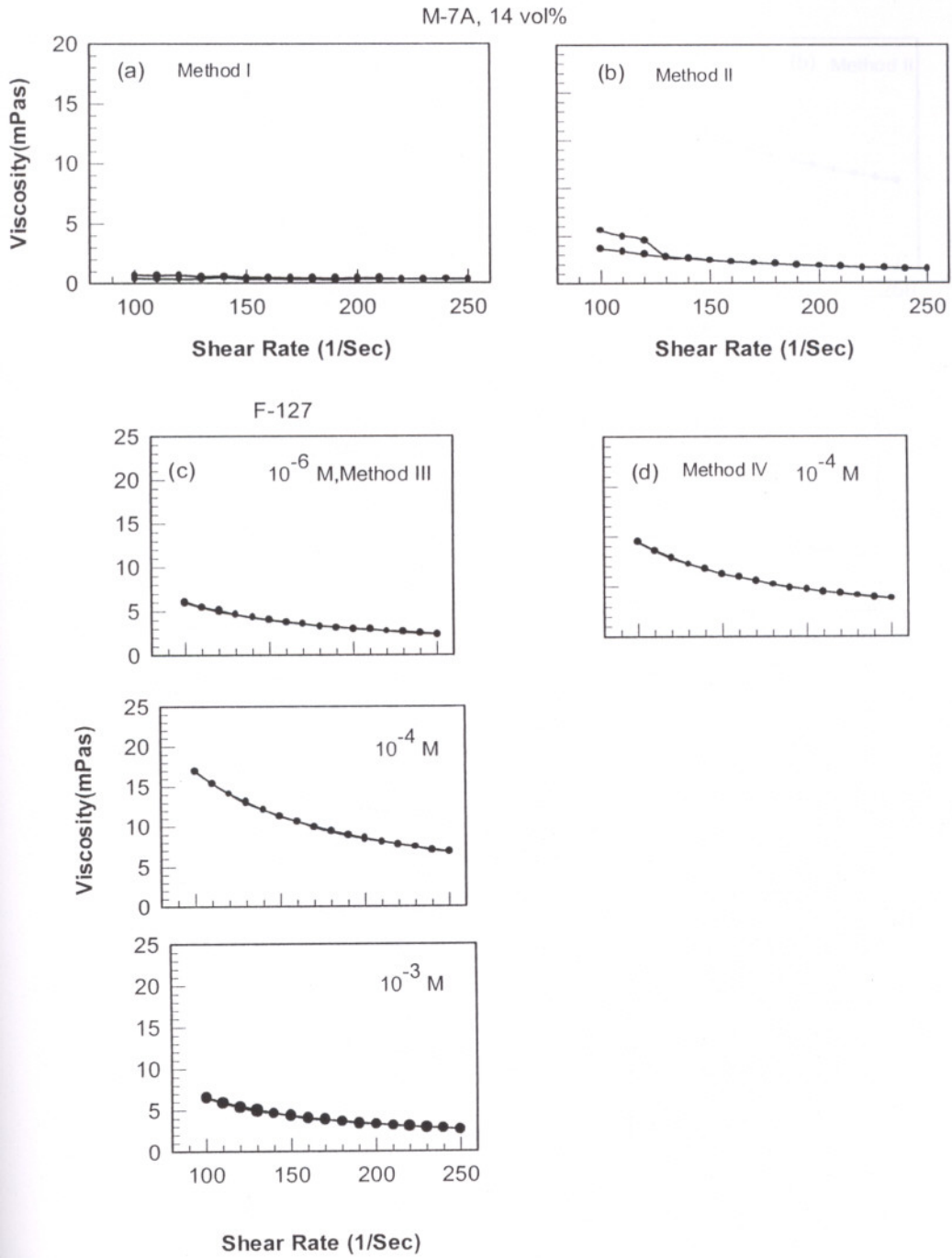


Figure 4.31. Shear rate vs. viscosity graphs of M-7A alumina suspensions prepared with Method I, II, III and IV at 14 vol%-(40wt%) solid loading

M-7A , 0.125 vol%

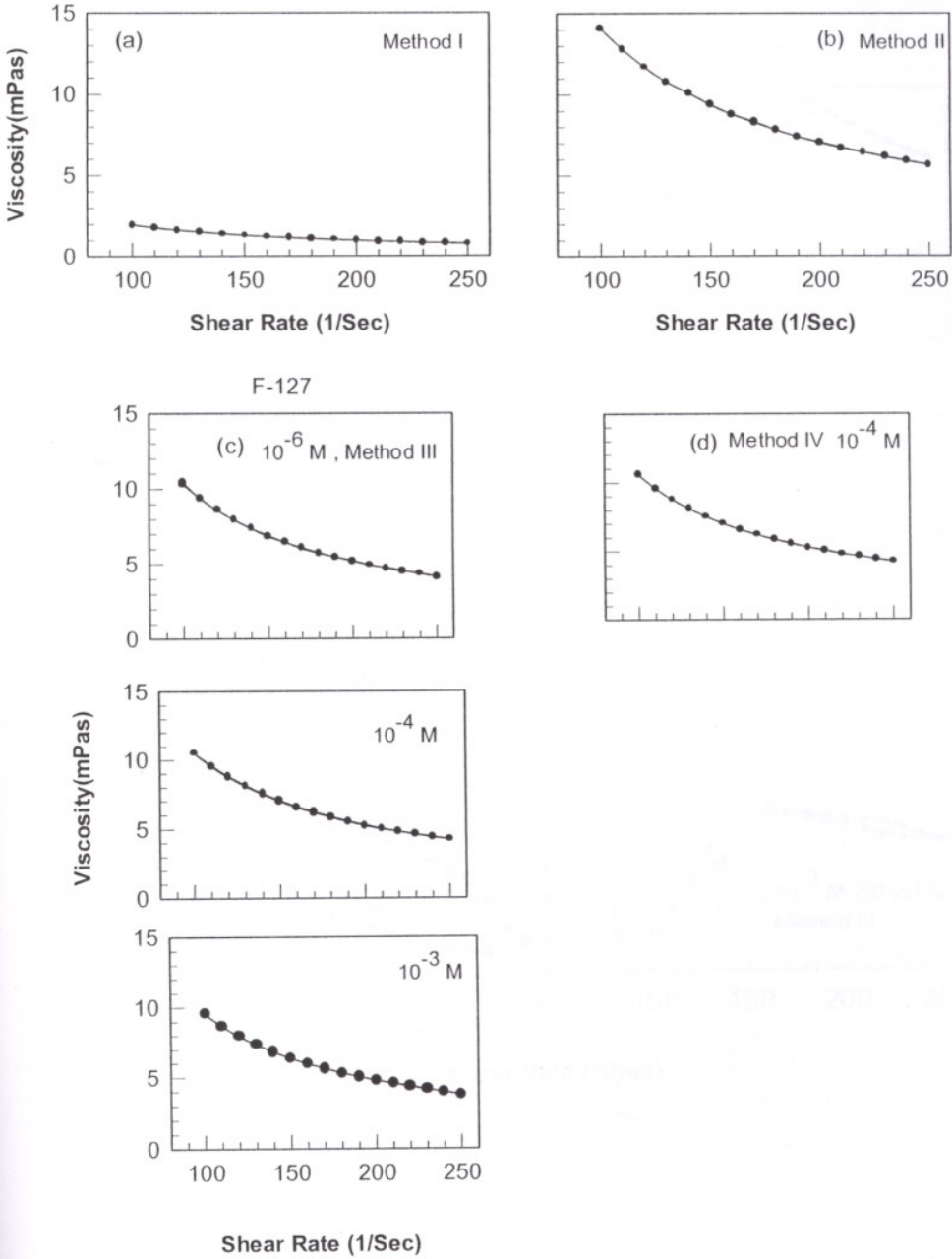


Figure 4.32. Shear rate vs. viscosity graphs of M-7A alumina suspensions prepared with Method I, II, III and IV at 0.125 vol%-(0.5 wt%) solid loading.

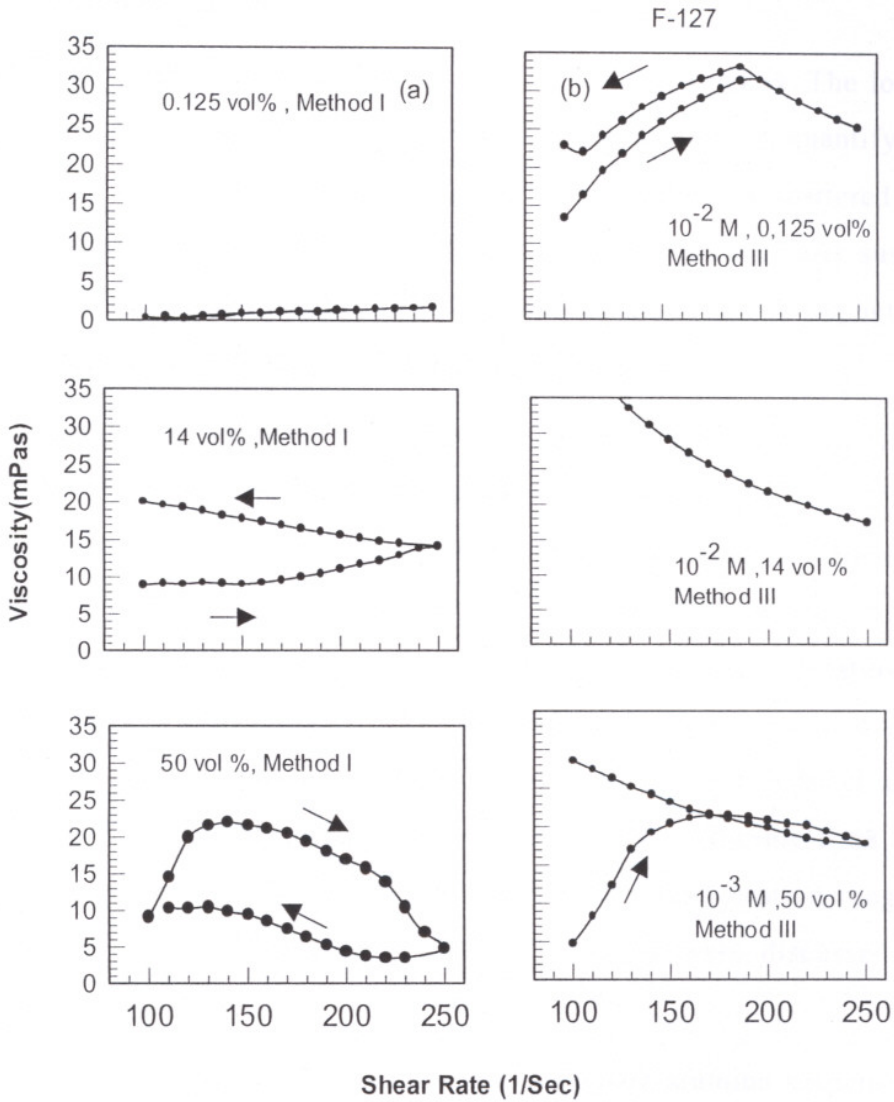


Figure 4.33. Shear rate vs. viscosity graphs of AKP-53 suspensions prepared with Method I and III at 0.125, 14, 50 vol % solid loadings.

4.2.2 Turbidity Measurements

In this part of study, the stability of alumina suspensions was investigated in the absence of stirring.

Turbidity refers to how clear or how cloudy the water is. The lower the turbidity, the clearer the water. It is a unit of measurement quantifying the degree to which light travelling through a water column is scattered by the suspended particles. The scattering of light increases with a greater suspended load. Turbidity in water is generally measured in units called Nephelometric Turbidity Units (NTU) or Jackson Turbidity Units (JTU).

In the study alumina suspensions were prepared by using the four methods described in Chapter III for AKP-53, Aldrich powders. The solid loading was 0.5 wt% and constant through the experiments. Higher solid loadings could not be measured. In addition to the effect of method type on the turbidity of suspensions, the effect of stirring, ultrasonic treating time, surfactant type and concentration was also studied. Various type of dispersing agents such as poly acrylic acid (PAA), citric acid, sodium dodecyl sulphate (SDS), Pluronic F-127, Pluronic P-104, Pluronic 10-R8, Pluronic F-68 and PE 6400 were tested during the experiments within the concentration range from 10^{-7} M to 10^{-2} M. The findings of these experiments were discussed in the following paragraphs.

First of all, the effect of method type to prepare alumina suspensions on their turbidities and therefore on their stabilities were studied. The results are presented in Figure 4.34 for AKP-53. It is seen that there is a considerable difference among the methods in terms of the dispersion and the stability of the system. Method (II) and (IV), which include ultrasonic treatment in the absence and presence of a dispersant respectively, gave very similar results. On the other hand, method (I), just stirring produced more dispersed suspensions. The results that obtained in the presence of polymers, method (III), were much better than the other methods. But to be able to reach the stability some period of time

was required. Therefore some additional tests were conducted to understand the influence of surfactant type and concentration.

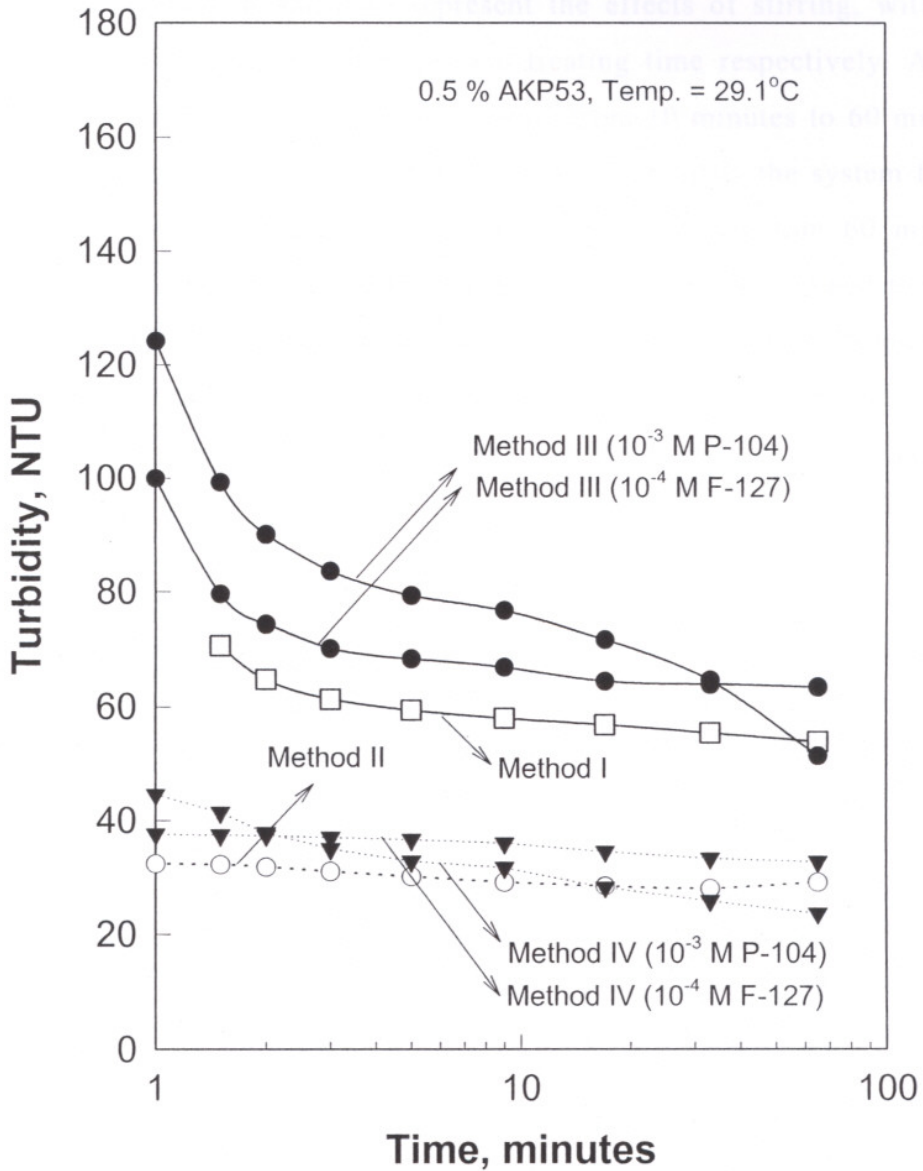


Figure 4.34. Effect of method type on turbidity of the alumina suspensions as a function of time *Solid wt%: 0.5; Alumina type: AKP-53; Temp: 29.1°C; pH: 5.8*

Additional experiments were conducted to understand the effect of the stirring and ultrasonic treating time on the stability of AKP-53 powder. To be able to examine the effect of NaCl on the stability of the system due to its effect on electrical double layer, some tests were also conducted in the presence of 10^{-1} M and 1M NaCl.

Figures 4.35, 4.36 and 4.37 represent the effects of stirring, with and without ultrasonic treatment and ultrasonic treating time respectively. As the stirring time before the measurement increased from 10 minutes to 60 minutes turbidity decrease. When ultrasonic treatment was applied to the system for 10 minutes lower turbidity values were obtained. For the situation 60 minutes stirring and 10 minutes ultrasonic treatment, turbidity values declined to about 30 NTU from 70 NTU starting value. As it is seen from Figures 4.36 and 4.37, the use of ultrasonic treatment destroys the stirring effect on stability. The change in the ultrasonic treating time on the other hand did not make any difference (Figure 4.37).

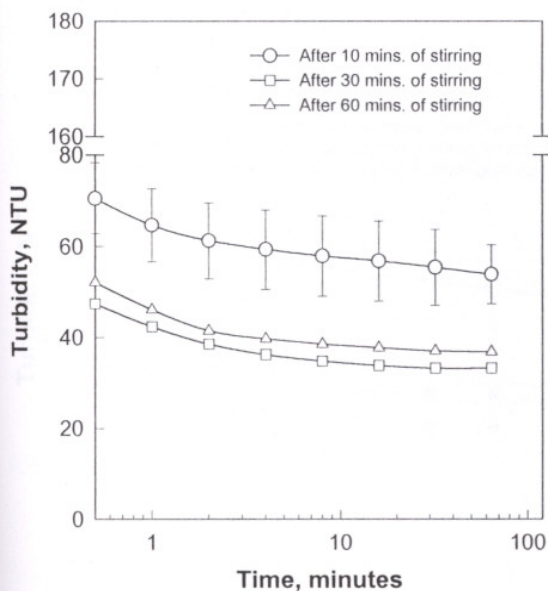


Figure 4.35. Effect of stirring time on turbidity of alumina suspensions prepared by Method I as a function of time. *Solid wt%: 0.5; Alumina type: AKP-53; Temp: 29.1°C; pH: 5.0.*

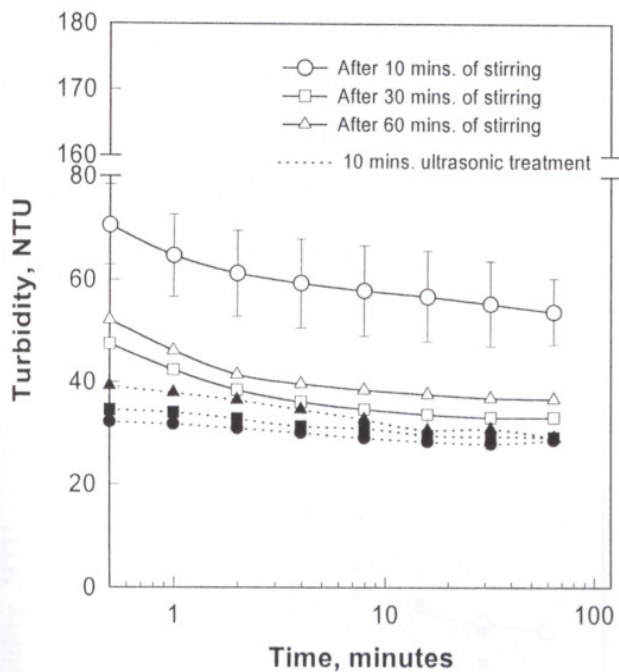


Figure 4.36. Effect of conditioning time on turbidity of the alumina suspensions prepared by Method I and II as a function of time. *Solid wt%: 0.5; Alumina type: AKP-53; Temp: 29 °C; pH: 5.2*

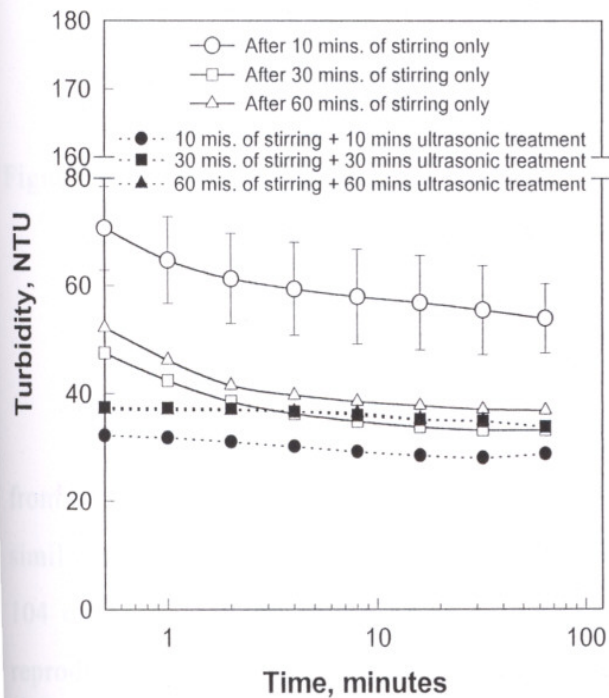


Figure 4.37. Effect of conditioning and ultrasonic treating time on turbidity of the alumina suspensions prepared by Method I and II as a function of time. *Solid wt %: 0.5; Alumina type: AKP-53; Temp: 30°C; pH: 5.3*

As pointed out before some suspensions were prepared with 0.1 M and 1M NaCl solutions and the results were presented in Figure 4.38. It was seen that coagulation starts after a certain time period. That is, according to the Figure 4.38 use of indifferent electrolyte disperses the system up to 10 mins and then coagulates the particles.

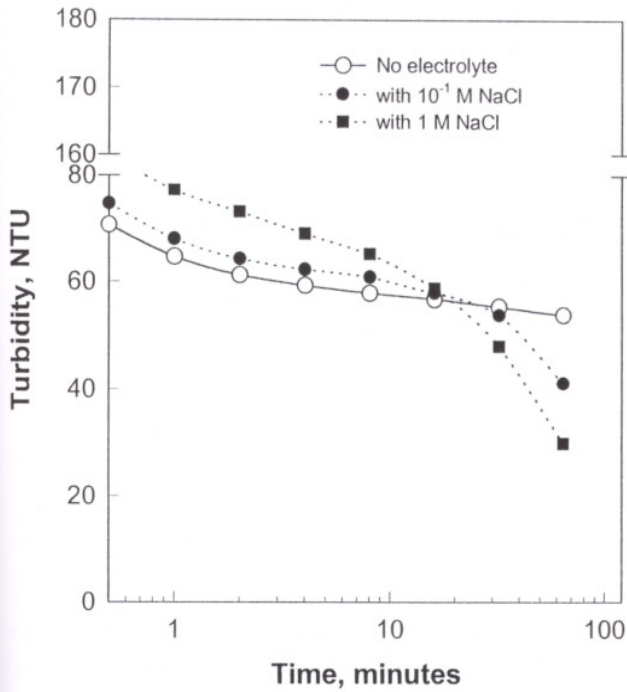


Figure 4.38. Effect of indifferent electrolyte, NaCl, on turbidity of the alumina suspensions prepared by Method I as a function of time. *Solid wt%: 0.5; Alumina type: AKP-53; Temp: 30.2°C; pH: 6.4*

Turbidity results of different dispersing agents were much more different from each other and also different concentrations of the same surfactant had not similar turbidity values. For example Figure 4.39 shows the effect Pluronic P-104 concentration on turbidity as a function of time. Figure 4.40 shows the reproducibility of the results obtained with this polymer. All of the measurements were carried out for 3 times for the accurate data. For this surfactant there was not much difference between the results of different concentrations except the highest concentration of 10⁻³ M. At this concentration coagulation and therefore settling of particles starts after 20 minutes of waiting.

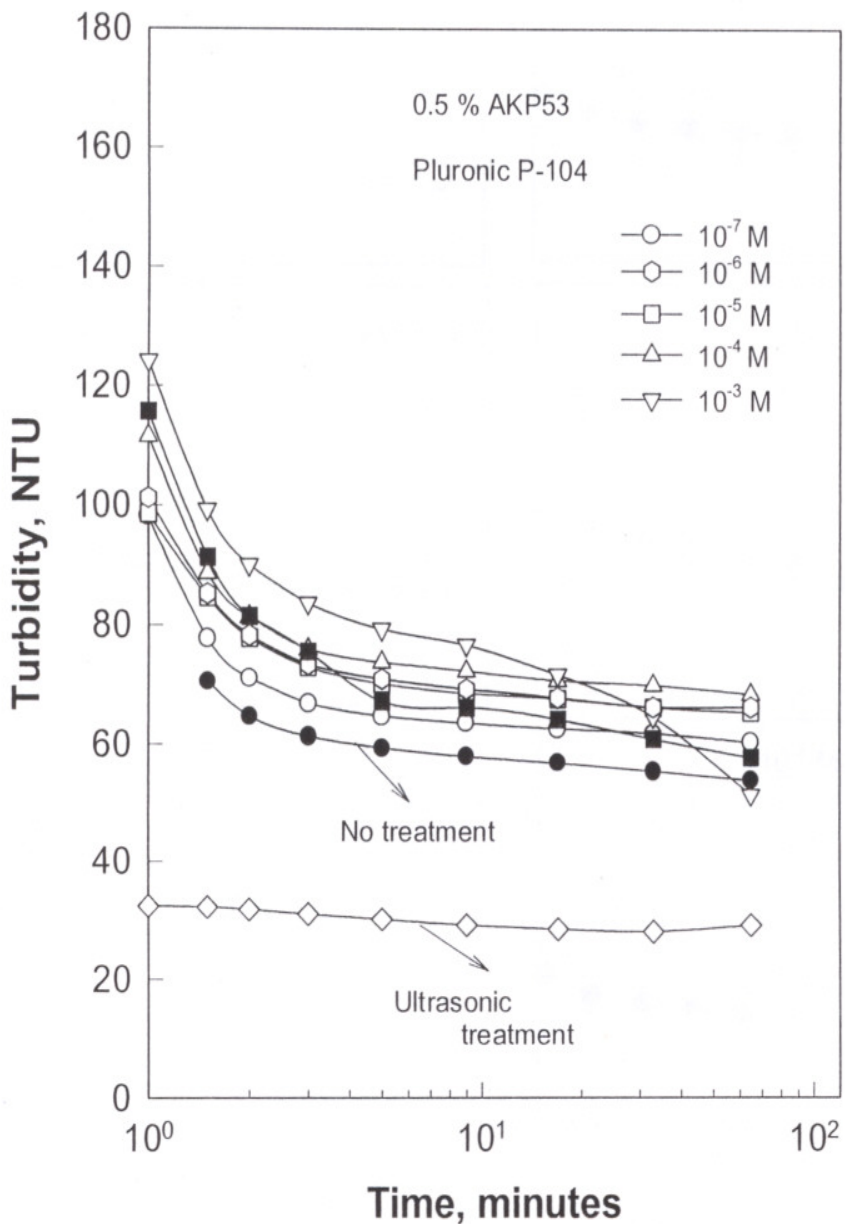


Figure 4.39. Effect of polymeric surfactant, P-104, concentration on turbidity of AKP-53 alumina suspensions prepared by Method I, II and III as a function of time. *Solid wt%: 0.5; Alumina type: AKP-53; Temp: 27.1°C; pH: 5,3-6,3*

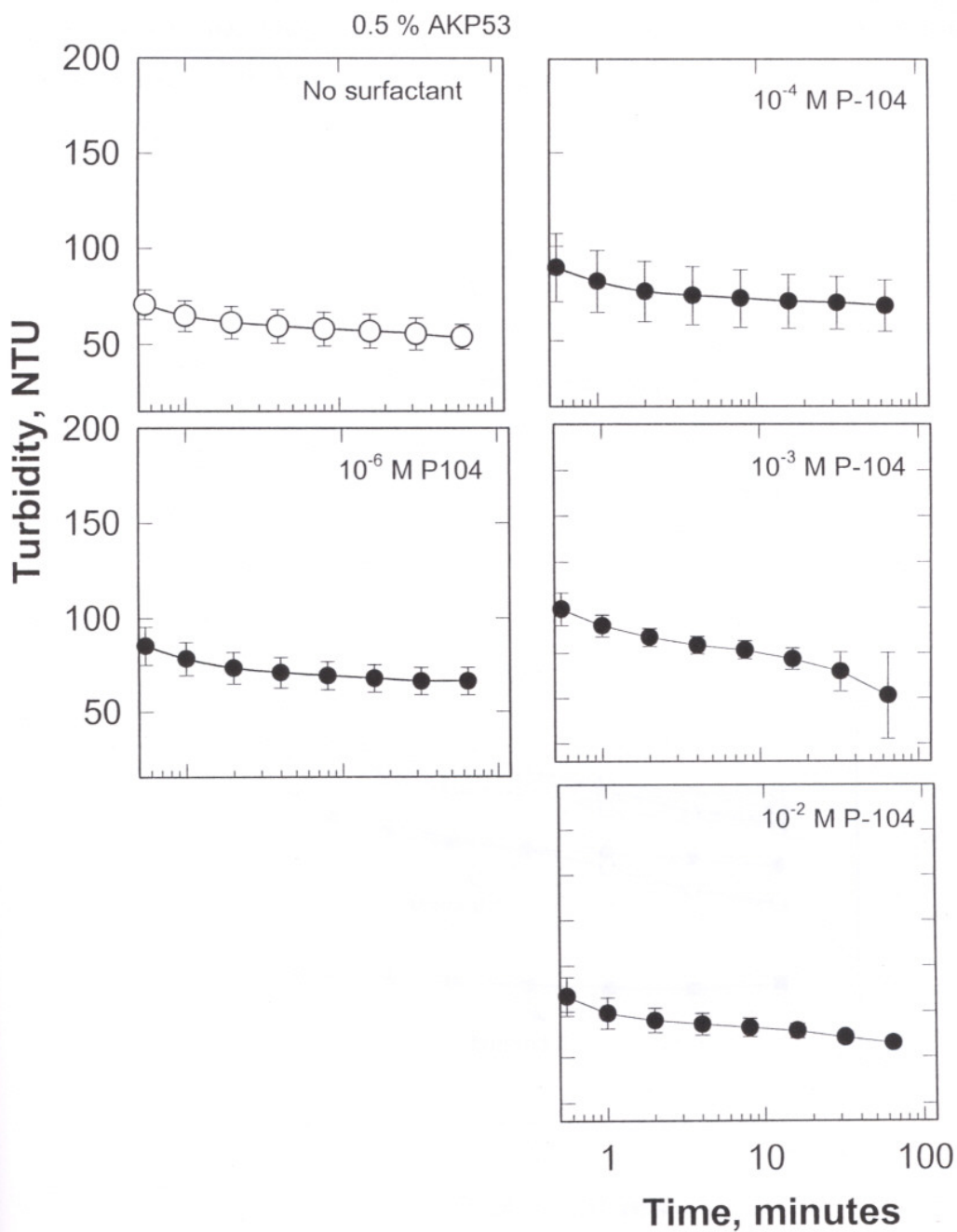


Figure 4.40. The reproducibility of turbidity versus time measurements at different P-104 concentrations (Method II). *Solid wt%: 0.5; Alumina type: AKP-53; Temp: 27 °C; pH: 6,3*

Similarly the Figures 4.41 and 4.42 demonstrate the effect of PAA at different concentrations as a function of time and the reproducibility of these experiments respectively. In general PAA increases the turbidity values of the system except at 10^{-6} M, as denoted in Figure 4.41.

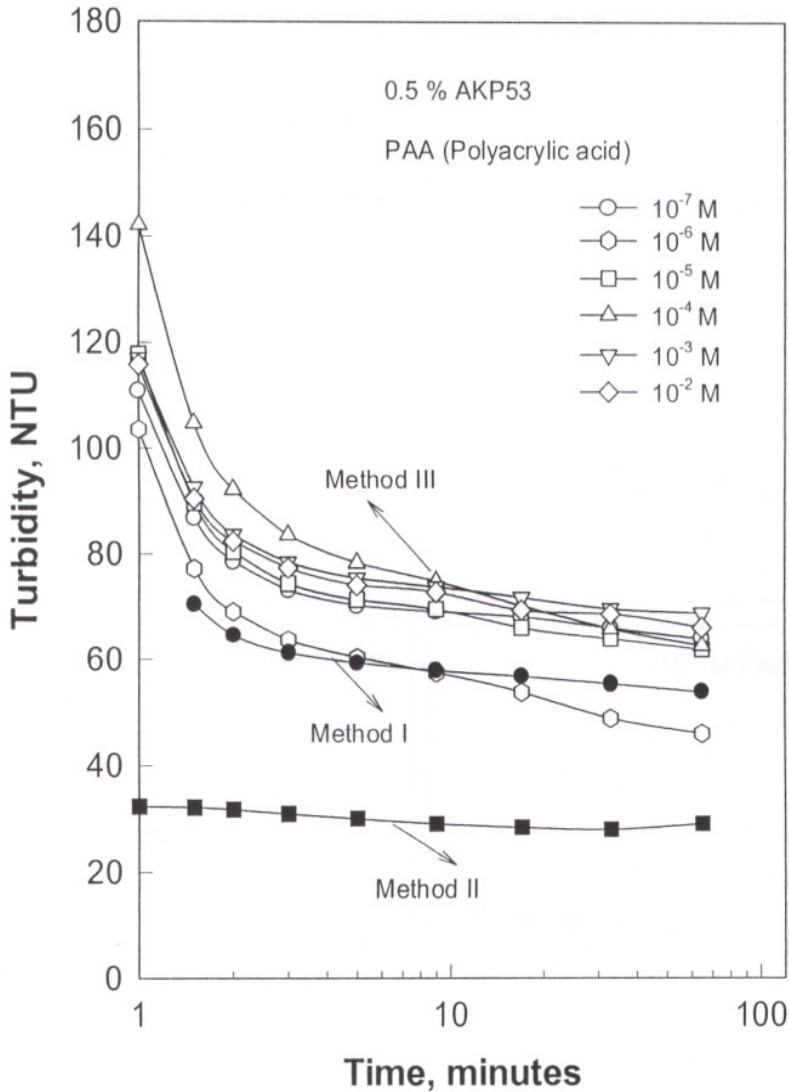


Figure 4.41. Effect of polymer, PAA, concentration on turbidity of AKP-53 alumina suspensions prepared by Method I, II and III as a function of time. *Solid wt%: 0.5; AKP-53; Temp: 25.1°C; pH: 4,5*

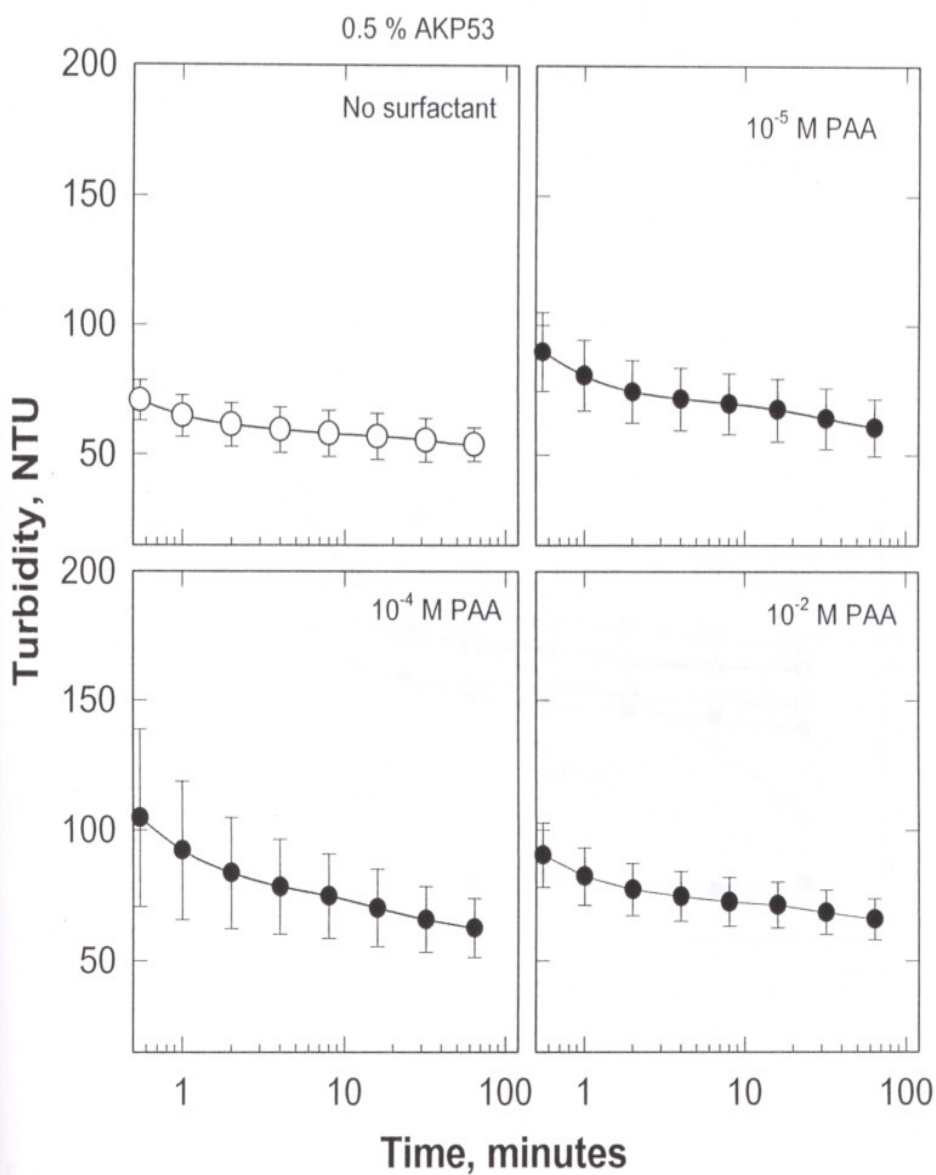


Figure 4.42. The reproducibility of turbidity versus time measurements at different PAA concentrations. *Solid wt%: 0.5; Alumina type: AKP-53; Temp: 25.3°C; pH: 4,5*

In Figure 4.43, turbidity values of suspensions with F-127 at different concentrations were presented. Figure 4.44 shows the reproducibility of the results obtained with F-127. Results rather similar with PAA and P-104 but at 10^{-2} M it behaves very different. At this concentration turbidity of F-127 is very high in the initial stage of the measurement. But the stability changes drastically as a function of time.

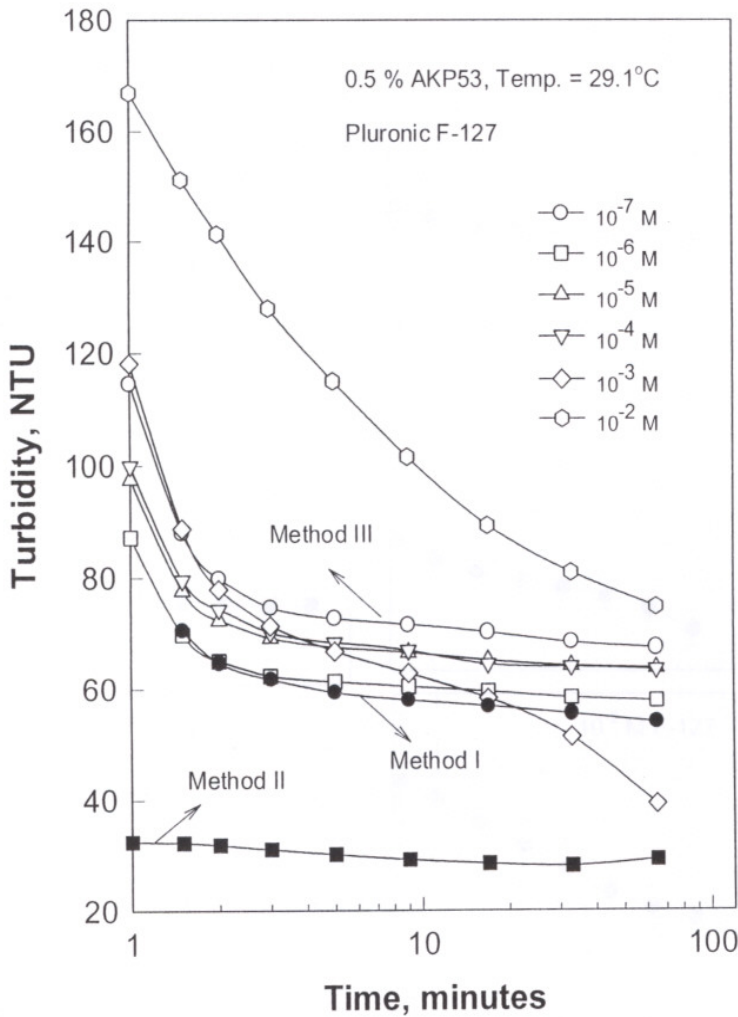


Figure 4.43. Effect of polymer, F-127, concentration on turbidity of AKP-53 alumina suspensions prepared by Method I, II and III as a function of time. Solid wt%: 0.5; Alumina type: AKP-53; Temp: 29.1°C; pH: 5,3

were also tested and the results were similar to those obtained with the simple surfactant SDS, with τ_{50} values of 6-400 respectively.

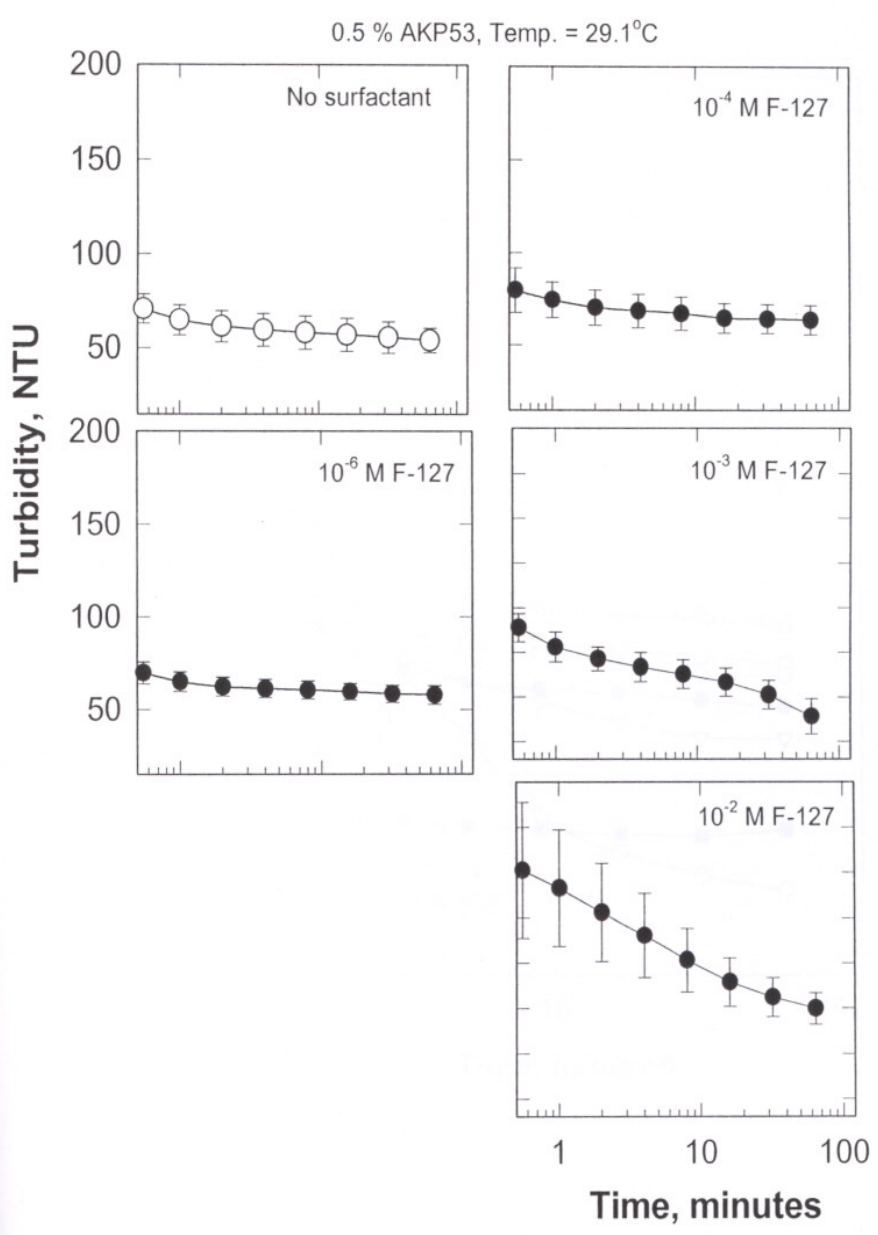


Figure 4.44. The reproducibility of turbidity versus time measurements at different F-127 concentrations. *Solid wt%: 0.5; Alumina type: AKP-53; Temp: 29.1°C; pH: 5.3*

In addition, some other surfactants were also tested and the results are presented in Figures 4.45 to 4.48 for an anionic simple surfactant SDS, citric acid and polymeric surfactants Pluronic 10R-8 and 6400 respectively.

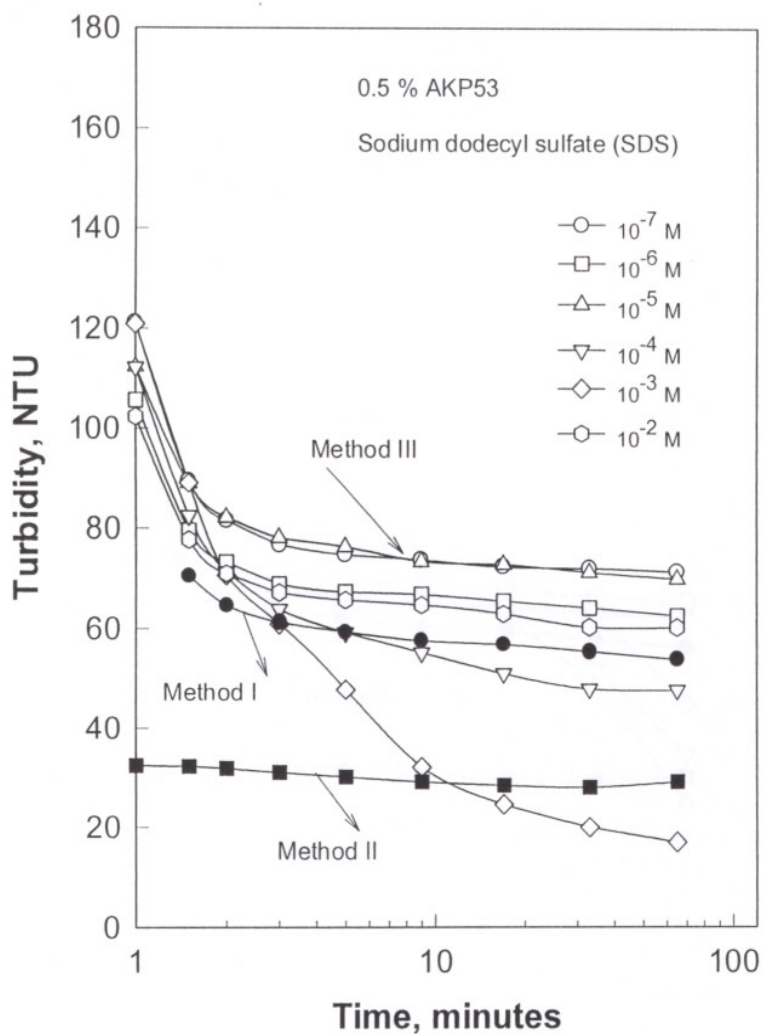


Figure 4.45. Effect of surfactant, SDS, concentration on turbidity of AKP-53 alumina suspensions prepared by Method I, II and III as a function of time. Solid wt%: 0.5; Alumina type: AKP-53; Temp: 24.6°C; pH: 5.2-7.6

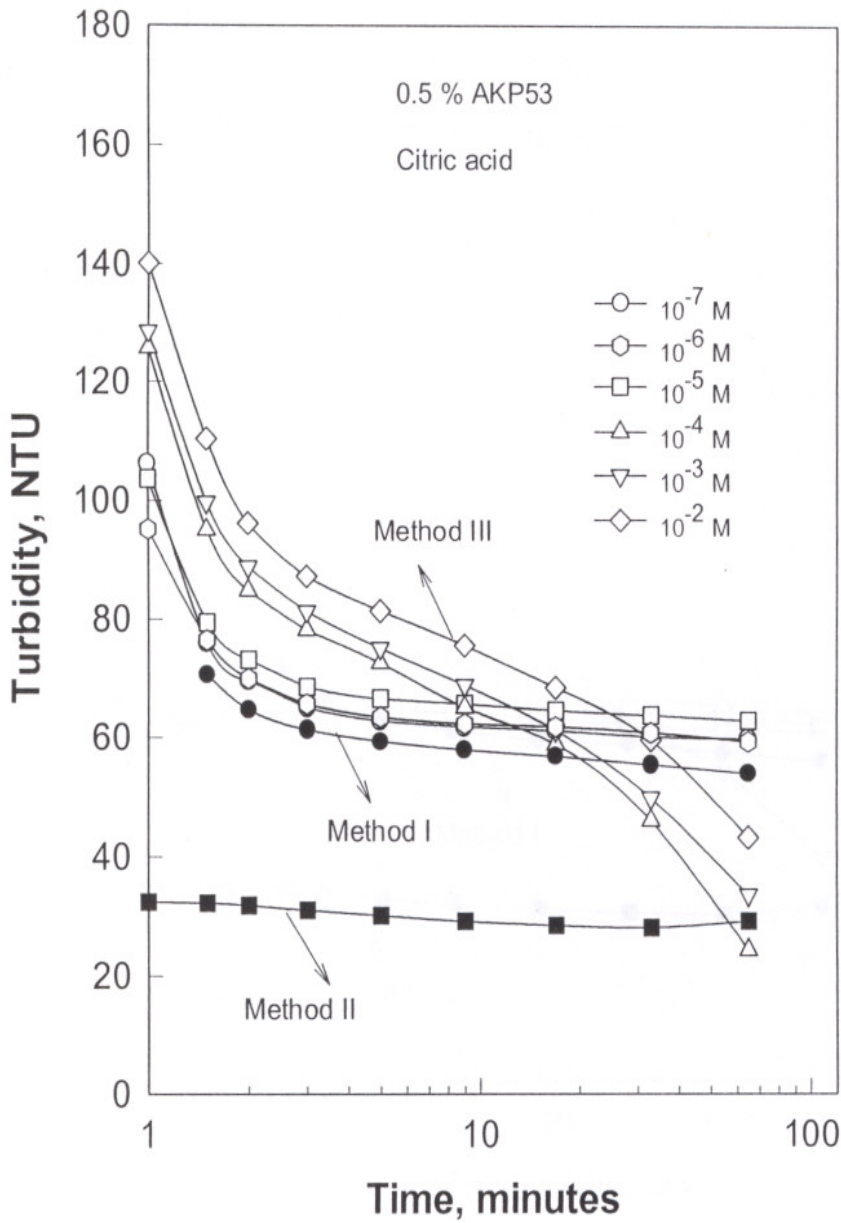


Figure 4.46. Effect of Citric acid concentration on turbidity of AKP-53 alumina suspensions prepared by Method I, II and III as a function of time. Solid wt%: 0.5; Alumina type: AKP-53; Temp: 20.5°C; pH: 6,1-2,77

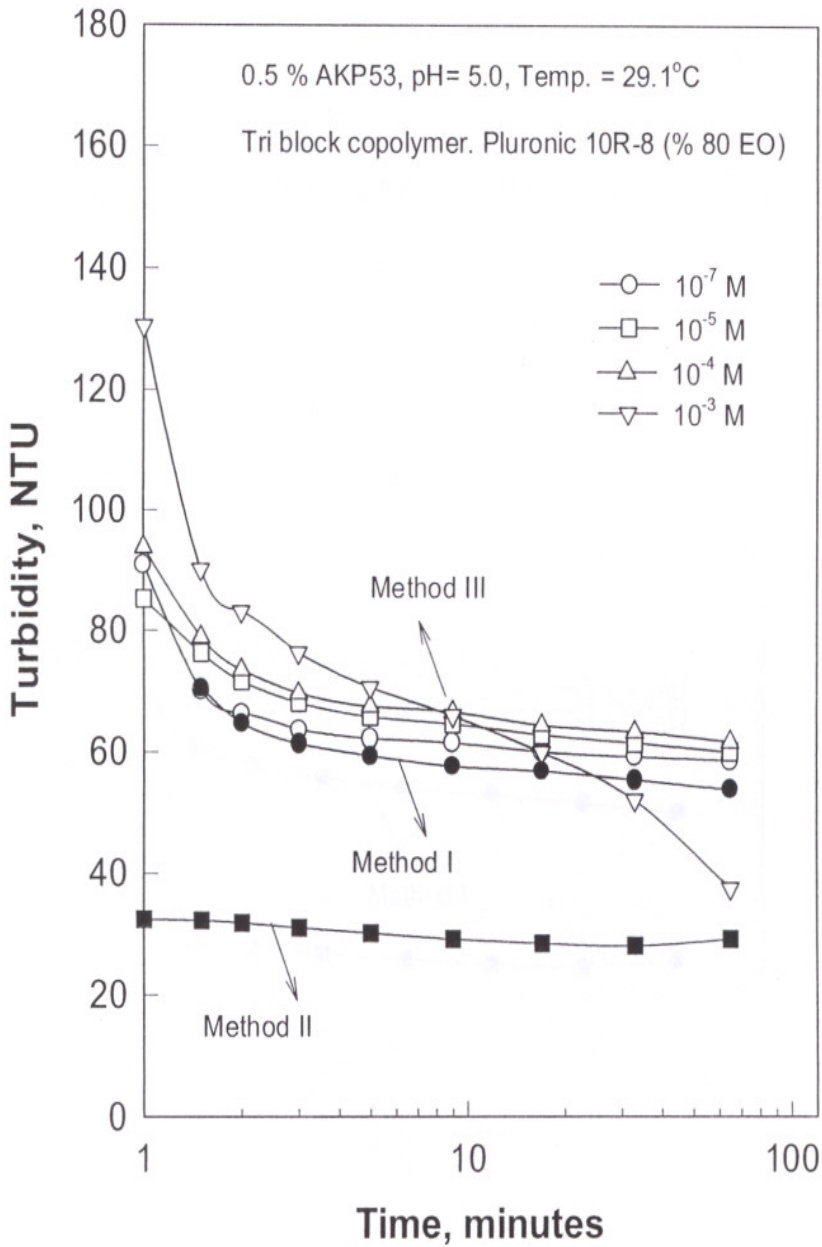


Figure 4.47. Effect of polymer, 10R-8, concentration on turbidity of AKP-53 alumina suspensions prepared by Method I, II and III as a function of time. *Solid wt%: 0.5; Alumina type: AKP-53; Temp: 29.1°C; pH: 5.0.*

For Aldrich alumina powder the effect of the polymeric surfactants were different. These results are given in Figures 4.49 and 4.50 and the comparison of the methods are given in Figures 4.51, 4.52 and 4.53 for F-127, PAA and F-68 respectively. It was seen that 10^{-2} M of F-127 increased the turbidity system considerably. But the system was not stable.

In the case of Aldrich alumina, suspension is unstable and changed with time. The increase in coagulation continued even in the presence of dispersants and the ultrasonic treatment.

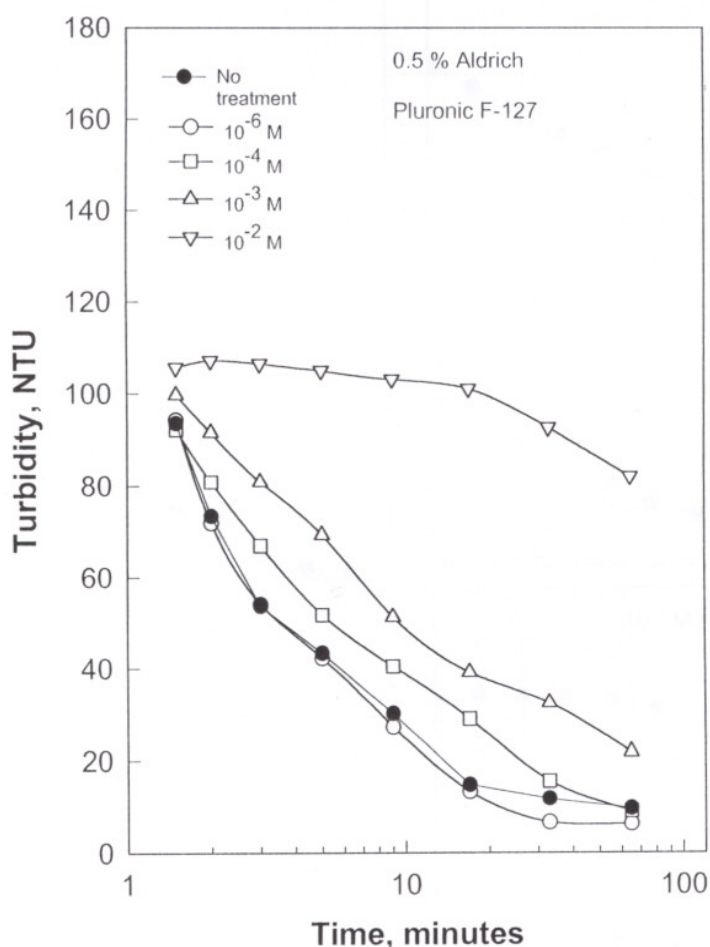


Figure 4.49. Effect of polymer, F-127, concentration on turbidity of Aldrich alumina suspensions prepared by Method I, and III as a function of time. *Solid wt%: 0.5; Alumina type: Aldrich; Temp: 30.1°C; pH: 5.0.*

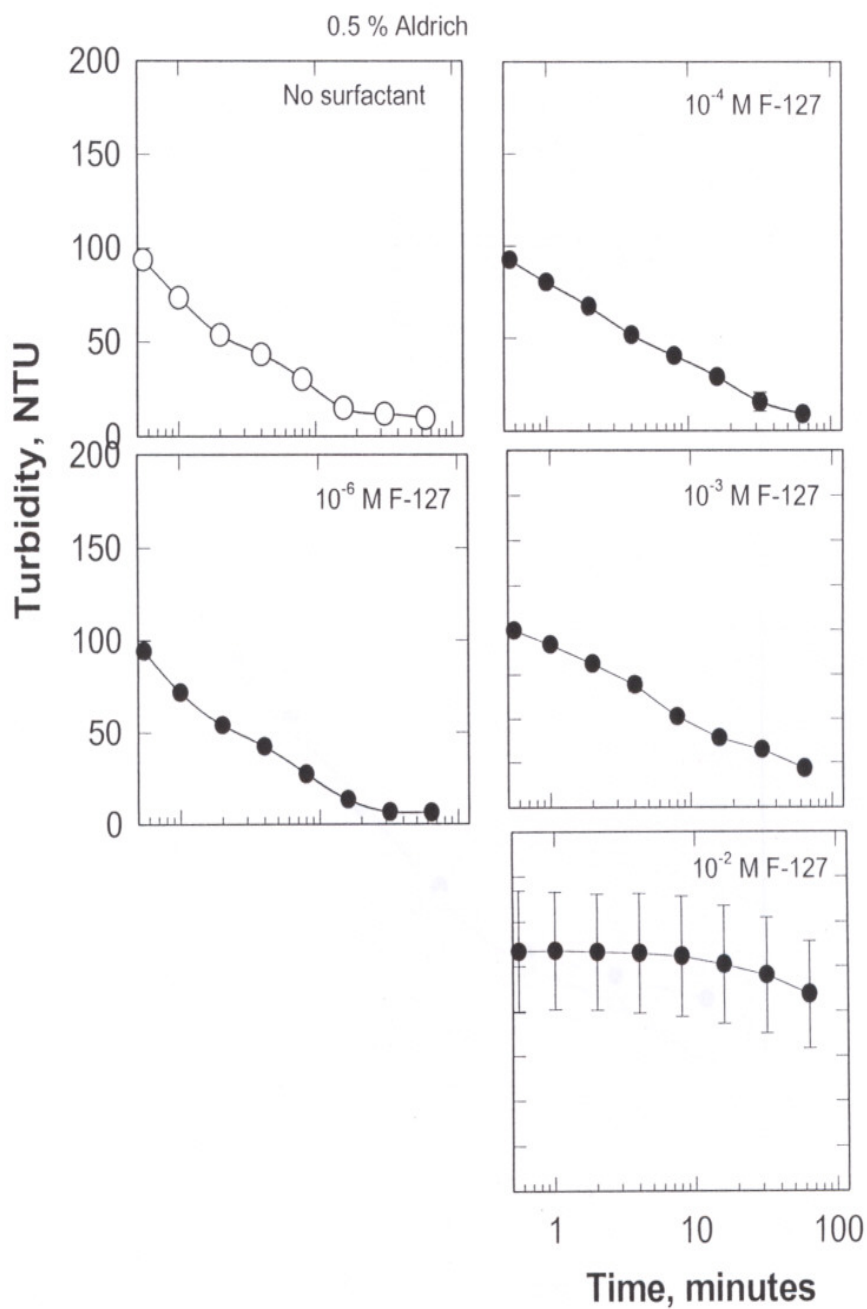


Figure 4.50. The reproducibility of turbidity versus time measurements at different PAA concentrations for Aldrich alumina suspensions. *Solid wt%: 0.5; Alumina type: Aldrich; Temp: 30.1°C; pH: 5.0.*

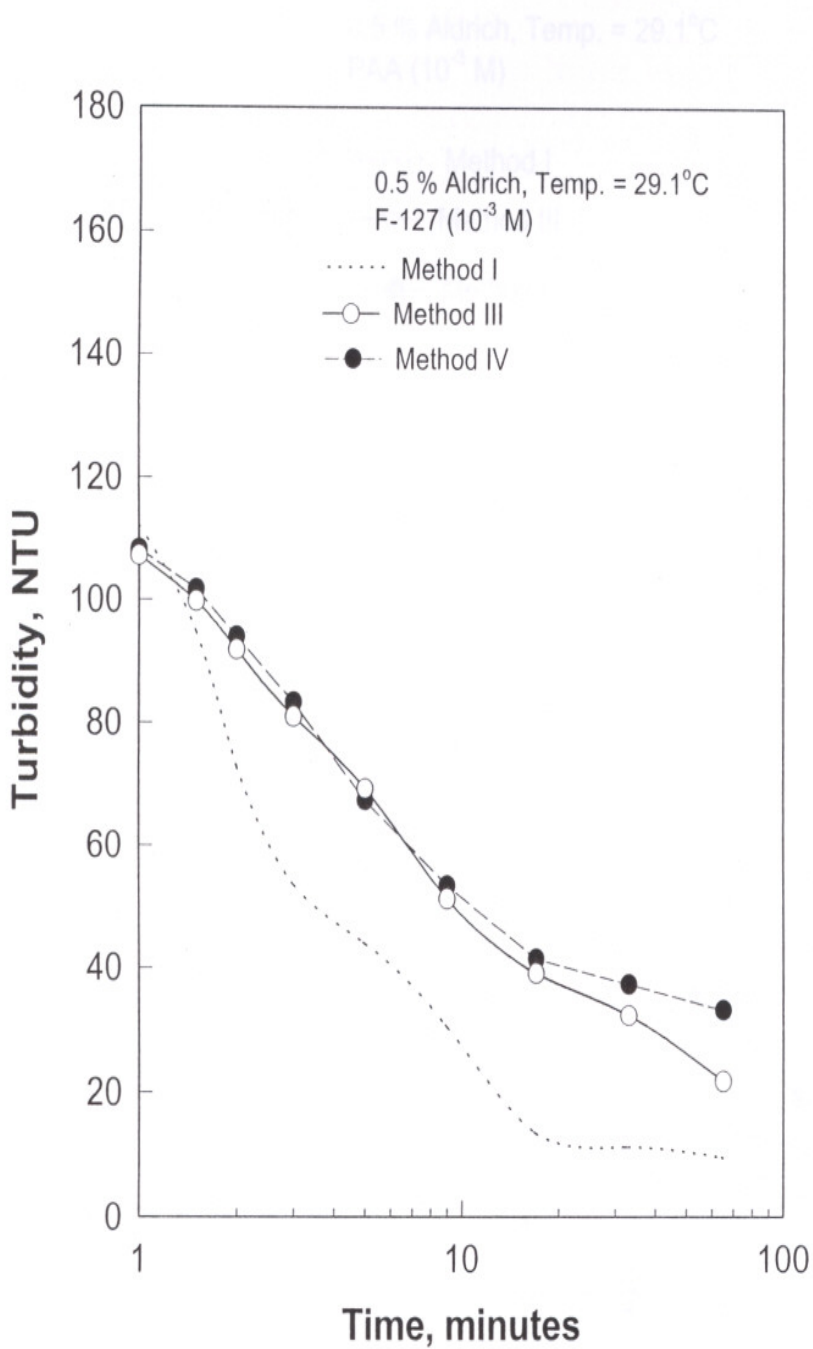


Figure 4.51. Effect of method type on turbidity of the Aldrich alumina suspensions in the presence of Pluronic F-127 (10^{-3} M). *Solid wt%: 0.5; Alumina type: Aldrich; Temp: 29°C; pH: 5.0.*

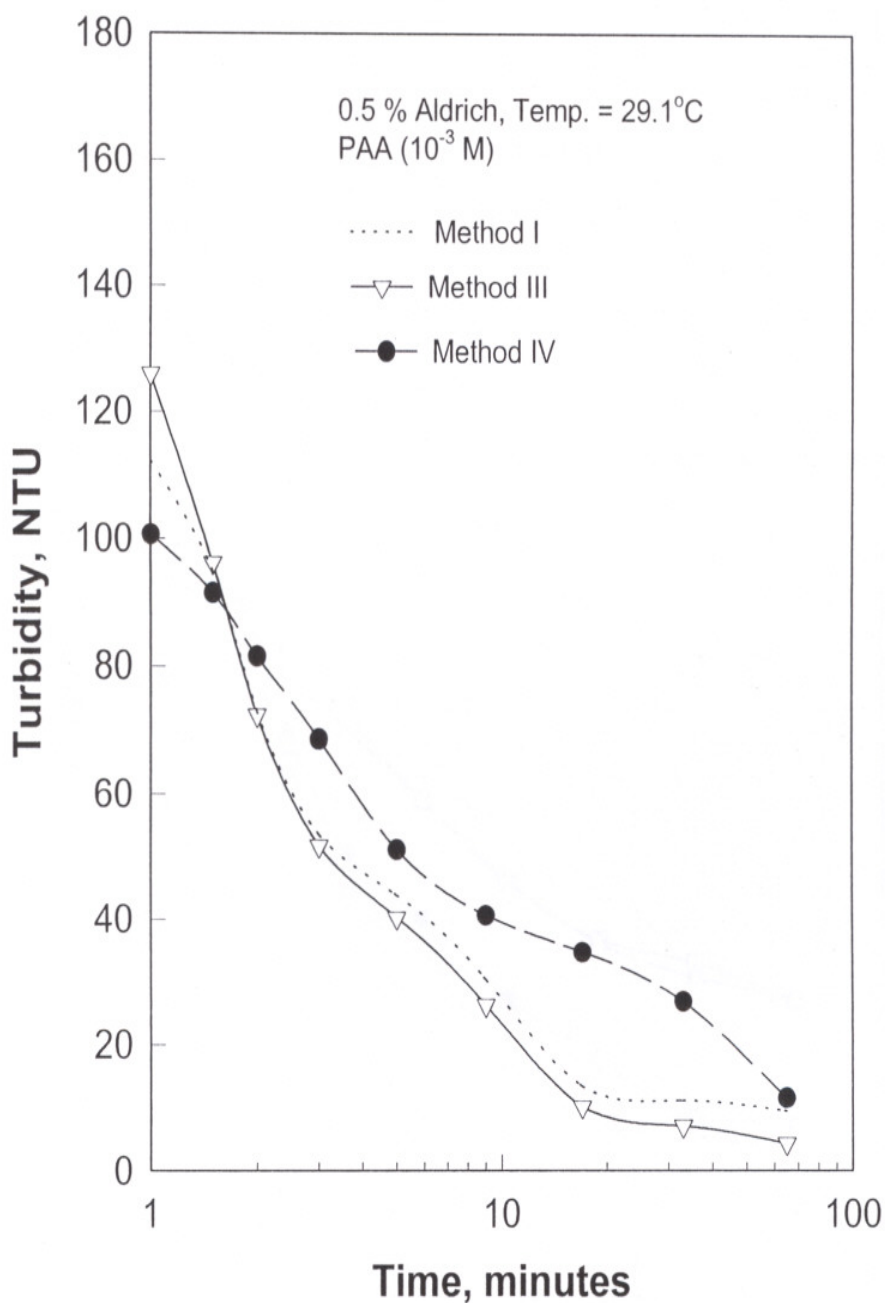


Figure 4.52. Effect of method type on turbidity of the alumina suspensions in the presence of PAA (10^{-3} M). Solid wt%: 0.5; Alumina type: Aldrich; Temp: 29.1°C; pH: 5.0-7.0

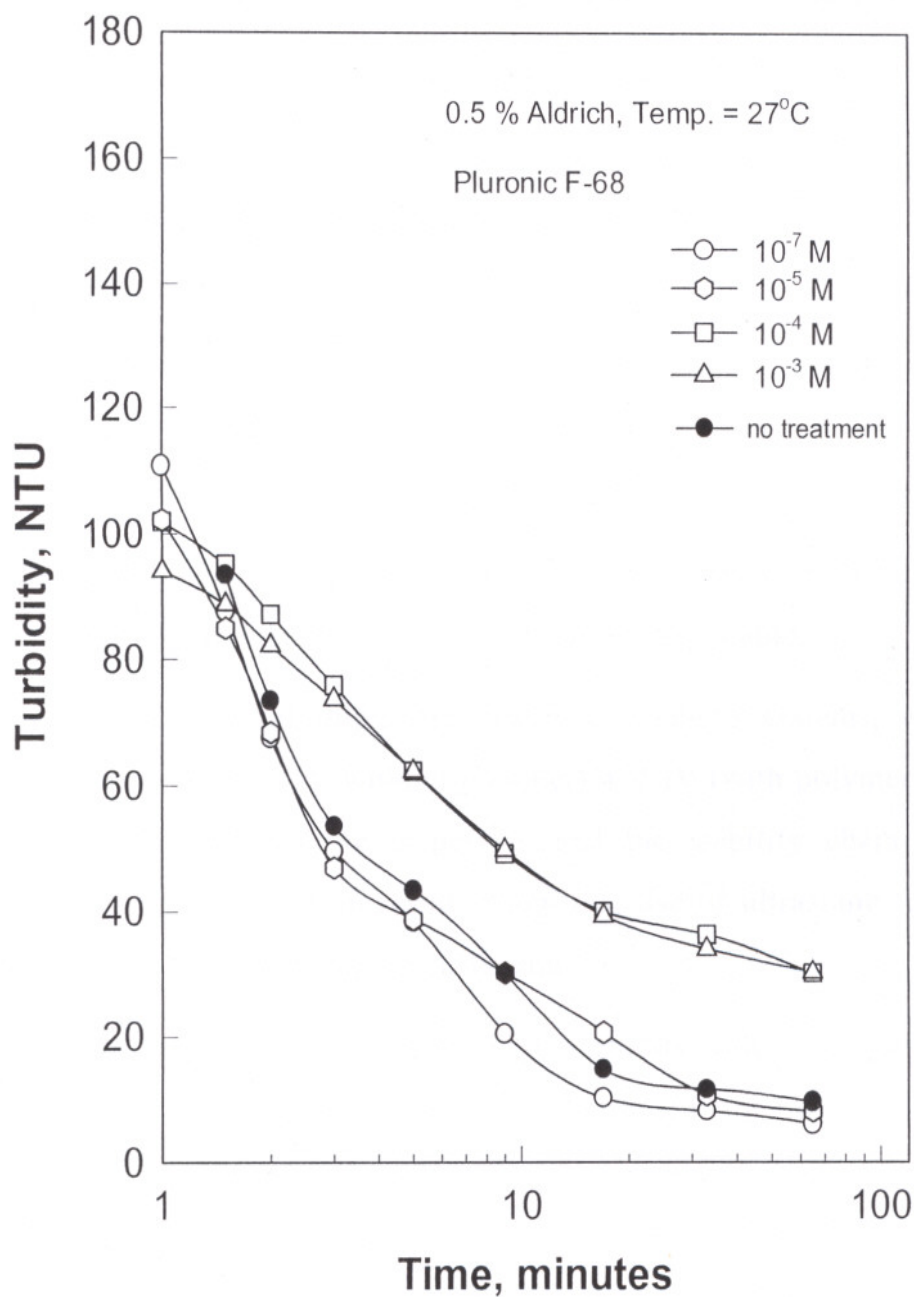


Figure 4.53. Effect of polymer, F-68, concentration on turbidity of Aldrich alumina suspensions prepared by Method I, and IV as a function of time. Solid wt%: 0.5; Alumina type: Aldrich; Temp: 27°C; pH: 4.6

Based on above studies results of the turbidity measurements can be summarized in the followings:

- As the stirring times in method (I) was increased turbidity started to decrease.
- Ultrasonic treatment time did not bring majorable difference in the turbidity values.
- Use of indifferent electrolyte dispersed the system up to 10 mins and then coagulated the particles.
- AKP-53 powder was unstable without any treatments (method I) and but usage of surfactant (in method III) was created a stability after a period time.
- Aldrich powder was also unstable in natural form even in the usage of surfactants. Sedimentation was observed after a short period of time that may be caused by big particle size.
- Ultrasonic treatment in method (IV) decreased the turbidity values for all situations but results of it were rather stable.
- Application of ultrasonic treatment to these systems, which is called method II (without polymer) and IV (with polymer) in this study, changed the dispersion and the stability characteristics (Figure 4.34). Both results show that use of ultrasonic treatment diminishes the effect of surfactant.

The main reason to obtain very high turbidity values in some cases especially at high concentrations may be attributed to the micellization character of the F-127. Also this high surfactant concentration may change the density of the water, so particles will settle down slowly. Wanka et al. [56] studied the aggregation behaviour of F-127 can form micelles in aqueous solutions if the PPO block is large enough and the concentration is high enough. They also measured the critical micelle concentration point of F-127 as nearly 10^{-3} M.

This effect was investigated by measuring turbidity of the system when micelles are present ($>10^{-2}$ M F-127) without particles in the system. But in the case of without powder rather low turbidity values were obtained (5 –15 NTU) for F-127 at 10^{-2} M.

Application of ultrasonic treatment with (method IV) and without (method II) surfactants decreased the turbidity but the stability of the system did not change. This gradual decrease in turbidity may attribute to the network that created by the closer approach of the powders with each other. In that picture, the particles are not agglomerated but come closer with each other and being suspended in the water. In that case turbidimeter will detect the less number particles with a bigger size.

When the two-alumina samples used in this study were compared, the suspension of AKP-53 was more stable with the ultrasonic treatment. On the other hand, in the case of AKP-53 powder, there was a reproducibility problem in the absence of any chemical or mechanical treatment. Hence measurements were repeated more than 10 times and the average values were used. This problem might be due to the very fine particle size distribution of this powder. In general, addition of surfactants disperses the particles, but a certain time is required for the system to become stable.

The reason of the rapid coagulation of Aldrich alumina powder was attributed to its rather coarse particle size. According to the Stoke's law the time required for the settling of the Aldrich particles with $10\ \mu\text{m}$ size is about 4 minutes due to gravitational force. Therefore even in the presence of the surfactants, Aldrich powders are settled down after a short period of time.

Another difference between the stabilization and dispersion behaviors of AKP-53, Aldrich alumina powder might be due to their natural pH values in water. AKP-53 has a rather low pH (5.9) value that is far form the pH_{PZC} of alumina. So it will tend to disperse easily especially at low solid loadings. The natural pH of Aldrich alumina however is around 9.3 that is around pzc value and creates coagulation.

4.2.3 Discussion for Stabilization mechanisms Block copolymers in the Absence of Adsorption on Alumina

The adsorption studies in the literature (Kayes and Rouling, 1979; Tadros and Vincent, 1980; Malmsen et al., 1992; Miano et al., 1992; Faers and Luckham, 1994) elucidate the mechanism of adsorption of block copolymers onto pure hydrophobic (polystyrene latex) and hydrophilic (silica) substrates. For hydrophilic surfaces, adsorption occurs through ethylene oxide groups (PEO) by hydrogen bonding between the oxygen of the EO groups and surface. For hydrophobic surfaces, the adsorption of block copolymer occurs via the hydrophobic portion (PPO) of the molecule through hydrophobic attraction.

Although Fukishama and Kumagai [18] have shown the adsorption of non-ionic surfactants on hydrophilic surfaces, Huang et al. [12,16,18] reported that PEO adsorbs on silica but not alumina. It was proposed that for PEO to adsorb on oxide surfaces, the polymer has to displace enough water molecules bonded to the solid surface and create strong entropic effect. In the case of strongly hydrated alumina surface the polymer cannot displace sufficient water molecules necessary for adsorption. However, there is no explanation for the differences in the adsorption behaviour of the alumina and the silica.

Also, according to the literature, when adsorption capacity and the polymer coverage to the particle surface are high, dispersion and stabilization behaviour of the suspensions is better.

Guo et al. [15] suggested that the presence of the free polymer in the system might cause weak flocculation due to depletion effect. Also effect of free polymer on flocculation becomes stronger as the volume fraction of alumina increases. But the mechanism was unclear and further investigation was suggested.

It is also known that in liquid powder systems, the water film drainage between the particles is necessary for agglomeration and presence of surfactant molecules or micelles in water affect the drainage of this film and prevents agglomeration (Nicolow and Wassan) [45]. Hence this should create dispersion in the system even though there is no adsorption on the surface.

Above explanation was also in good agreement with the depletion stabilization theory. Depletion stabilization is the mechanism that thought to be the effective one in the case of block copolymers in this study.

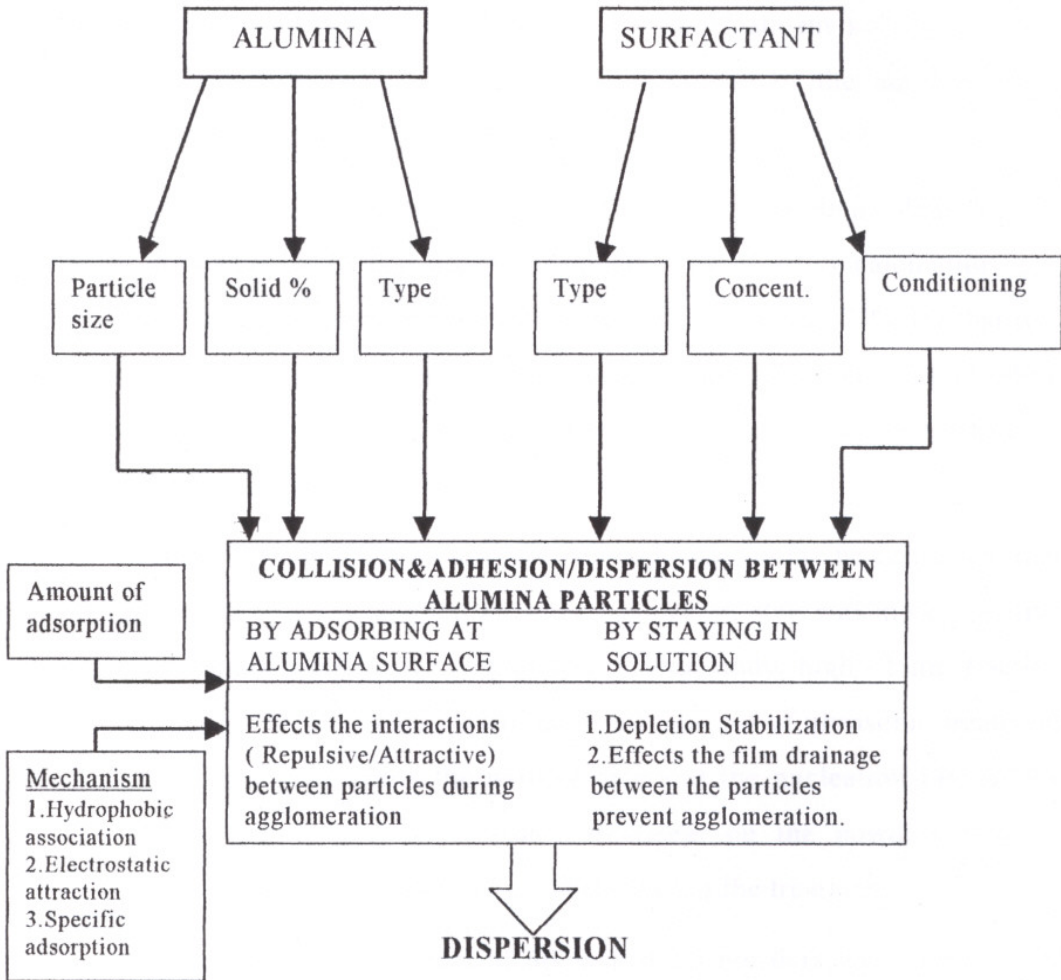


Figure 4.54. A schematic representation of the possible stabilization mechanisms of surfactant in alumina suspensions.

CONCLUSIONS

Preparation of fine alumina powders starting from gibbsite and also dispersion behaviour of alumina suspensions by block copolymers was investigated in this work. Effect of mechanical pre-treatment like ball milling and use of ultrasonic bath on nucleation and growth of the alpha alumina powders in transition form matrix was essayed.

Density measurements exhibited that 91% theoretical density was obtained in powder M-7A that was ultrasonically treated before calcination. The sintered density of the powder pellet M-6A was determined as 73% TD that was ball milled before calcination to improve the transformation. But grinding before calcination to enhance the nucleation and growth rate did not influence the sintered density M-6A powder pellets.

According to the particle size characterizations, it may be concluded that grinding process that was applied after the calcination step was more effective in reduction of the particle size of powders. In this study, high $<1 \mu\text{m}$ fraction of the powder M-7A after calcination indicated that use of ultrasonic treatment before calcination may affect the particle size and the nucleation rate of the transition alumina. Effect of ultrasonic treatment on the powders may be attributed to the formation of the micro cracks during the treatment.

XRD analysis showed that, M-6B and M-7B powders were transformed to complete alpha form at 1200°C calcination temperature in 8 hours. The powder M-1B showed a multiphase structure under the same conditions. So it was concluded that heat treatment at 900°C seems to favour the phase transformation at 1200°C .

On the other hand, rest of the powders, calcined at $1100\text{-}1200^\circ\text{C}$ for 2 hour were not transformed to complete alpha alumina phase but also contain some kappa phase. Powder M-5 that was prepared without mechanical treatment application before the calcination has shown only kappa peaks under the same

conditions. So that, such differences in processing do have some effects on the nucleation of the α phase in the κ phase.

There were no majorable differences in FTIR spectra of the powders. In powders calcined at 1100 °C some OH (stretching and bending) and carbonate peak was detected due to CO₂ adsorption. This indicates that, powders calcined at that temperature has a rather high surface area that means they are still in the transition form.

In characterization of alumina (AKP-53, Aldrich, M-7A) suspensions, rheological measurements were conducted at different solid loadings at 0.125, 1.0, 14 and 50 vol%-(0.5, 4, 40, 80 wt%). Suspensions were prepared by using four different methods. At low solid loadings, the suspension had a Newtonian or dilatant behaviour without any treatment and dispersant. But in the case of higher solid loadings such as 40 and 80 wt% suspensions without any treatment tend to agglomerate. So, as the solid loadings increases, the stabilization of the alumina suspensions becomes more difficult and stronger repulsive forces are required to stabilize the suspensions. At high solid loadings, ultrasonic treatment was found to be effective for all the alumina samples tested in the study. There were differences, however, in terms of the effect of the surfactants on dispersion characteristics. In the case of AKP-53, the influence of surfactant was not significant in the presence of ultrasonic treatment while it was significant and positive for Aldrich alumina sample. This effect was found to be a function of dispersant type and disappeared in the absence of ultrasonic treatment. Positive effect of these surfactants on the dispersion behaviour was attributed to the depletion stabilization mechanism.

The stability of alumina suspensions at 0.5 wt% solid loading when stirring is stopped was also studied by turbidity measurements. Generally, all the surfactants tested gave high turbidity values. For AKP-53 powder these values stayed constant during the time period (64 minutes) In the case of ultrasonic treatment however, somehow turbidity values were much lower. On the other hand, in the case of Aldrich powder, the results were different. The stability of the system was rather poor at all the conditions even in the presence

of surfactants. The amount of the agglomerates was increasing as a function of time. The main reason for rapid sedimentation of Aldrich powders was attributed to its rather big particle size.

As a conclusion, it was observed that the block copolymers of PEO/PPO/PEO, which is F-127 in this study has a dispersing effect when it is combined with ultrasonic treatment on the agglomerated alumina suspensions. Somehow stable dispersions could not be prepared in the absence of ultrasonic bath application.

Although ultrasonic treatment increased the stability of what in rheology and turbidity studies, its mechanism was not completely explained. Further experiments should be carried out to be able to understand this mechanism.

RECOMMENDATIONS

Future work related with this study may include the followings:

To better understanding of kappa to alpha phase transformation some additional kinetic experiments should be performed. XRD analyses should be used as an indirect approach to determining the kinetics.

Mechanism of ultrasonic treatment in phase transformation may be studied as a function of ultrasonic treating time.

Related with alumina suspension preparation part, adsorption experiments of PEO/PPO/PEO block copolymers on alumina should be performed. This may give a clear understanding of the stabilization mechanism of the system in the presence of free polymer molecules. Surface tension measurements may give some information about the adsorption behaviour of these surfactants on the alumina surface.

Adsorption and stabilization mechanism of PEO/PPO/PEO with anionic surfactant mixture on alumina suspensions may be studied.

To investigate the interactions within electrical double layer zeta meter measurements should be done at various conditions.

REFERENCES

1. Alexandridis P., Athanassiou V., Fukuda S., "Surface Activity of Poly (-ethylene oxide)-block-Poly(propylene oxide) block Poly(ethylene oxide) Copolymers", *Journal of The American Chemical Society* ,**10**, (1994), 2604-2612
2. Alexandridis P., Hatton T., "Poly (-ethylene oxide)-block-Poly(propylene oxide) block Poly(ethylene oxide) block copolymer surfactants in aqueous solutions and at interfaces: thermodynamics, structure, dynamics and modelling", *Colloid and Surfaces A. Physicochemical and Engineering Aspects* , **96**, (1995), 1-46
3. Bagwell R., Messing G., "Effect of Seeding and Water Vapor on the Nucleation and Growth of α -Al₂O₃ from γ -Al₂O₃", *Journal of The American Ceramic Society*, **82**, No: 4 (1999), 825-832
4. BASF, Commercial Catalogue for Pluronic Block copolymer Surfactants
5. Callister W., Cutler I., Gordon R., "Thermal Decomposition Kinetics of Boehmite", *Journal of The American Ceramic Society*, **49**, No: 8 (1966), 419-422
6. Cesarano III J., Aksay I., "Processing of Highly Concentrated Aqueous α -Alumina Suspensions Stabilized with Polyelectrolytes." *Journal of The American Ceramic Society*, **71**, No: 12 (1988), 1062-1067
7. Christopher W., Leermakers F., Fleer G., "Multiblock Copolymers and Colloidal Stability", *Journal of Colloid and Interface Science*, **167** (1994), 124-134
8. Colloidal Processing, <http://home.taegau.net/~jisunmi/colloid.htm>
9. Dynys F., Halloran J.W., "Alpha Alumina Formation in Alum Derived Gamma Alumina", *Journal of The American Ceramic Society*, **65**, No: 9 (1982), 442-448

10. Dynys F.W., Halloran J.W., "Influence of Aggregates on Sintering", *Journal of The American Ceramic Society*, **67**, No: 9 (1984)
11. Esumi K., Yamanaka Y., "Interaction Between Sodium Dodecyl Poly(oxyethylene) Sulfate and Alumina Surface in Aqueous Solution", *Journal of Colloid and Interface Science*, **172**, (1995), 116-120
12. Evanko Cynthia, Dzombak D., Novak J., "Influence of Surfactant Addition on the Stability of Concentrated Alumina Dispersions in Water", *Colloid & Surfaces A: Physicochemical & Engineering Aspects* **110**, (1996), 219-223
13. Faers M., Luckham P.F., "Rheology of Polyethylene oxide-Polypropylene oxide Blockcopolymer Stabilized Latices and Emulsions", *Colloid and Surfaces A: Physicochemical and Engineering Aspects*, **86**, (1994), 347-327
14. Grahl Christine- editor, Ceramic Industry, A Publication of Business News Publishing, Materials Handbook section (1999), 70
15. Guo L., Zhang Y., Uchida N., Uematsu K., " Adsorption Effects on the Rheological Properties of Aqueous Alumina Suspensions with Polyelectrolyte", *Journal of The American Ceramic Society*, **81**, No: 3, (1998), 549-556
16. Hecht E., Hoffamn H., "Interaction of ABA Block Copolymers with Ionic Surfactants in Aqueous Solution", *Journal of The American Chemical Society*, **10**, (1994) 86-91
17. Heimenz P.C.; Principles of Colloid & Surface Chemistry, 3rd edition, Marcel Dekker, (1997)
18. Hergeth W.D., Zimmermann R., Schmutzler K., "Adsorption of POE-POP-POE block copolymers onto silica", *Colloids and Surfaces*, **56** (1991), 177-187
19. Hidber P., Graule T., Gauckler L., "Competitive Adsorption of Citric Acid and Poly (vinyl Alcohol) onto Alumina and Its Influence on the

- Binder Migration During Drying”, *Journal of The American Ceramic Society*, **78**, No: 7 (1995), 1755-1780
20. Hinder P., Graule T., Gauckler L., “Influence of the Dispersant Structure on Properties of Electrostatically Stabilized Aqueous Alumina Suspensions”, *Journal of the European Ceramic Society*, **17**, (1997), 239-249
 21. Hinder P., Graule T., Gauckler L., “Citric Acid- A Dispersant for Aqueous Alumina Suspensions”, *Journal of The American Ceramic Society*, **79**, No: 7 (1996), 1857-1867
 22. Hough D., Thompson L., “Effects of Nonionic surfactants on the Stability of Dispersions” Nonionic Surfactants, Chapter 11, (602-667)
 23. Iler R.,” Fibrillar Colloidal Boehmite; Progressive Conversion to Gamma, Theta and Alpha Aluminas”, *Journal of The American Ceramic Society*, **44**, No: 12 (1961), 618-624
 24. Incorvati C.M., Lee D.H., Reed J., “Obtaining Dispersible Bayer Process Aluminas In Water”, *Journal of The American Ceramic Society Bulletin*, **76**, No: 9 (1997)
 25. Ipekçioğlu N., Production of Ceramic Grade Alumina by Bayer Process, diploma project (1992)
 26. Israelachvili J., Intermolecular and Surface Forces, Academic Press, Harcourt Brace and Company publishers, (1992)
 27. Jang M. Hyun,” Colloid Interface Science for Ceramic powder Processing”, Chemical Processing of Ceramics, edited by Burtrand Lee, Edward Pope, by Marcel Dekker, (1994)
 28. Kasiner J., Carbone T., SparrP.” Aluminas For Tomorrow’s Ceramics”, Aluminum Company of America, Ceramic Engineering and Science Proceedings, **6**, No: 9-12 (1985)
 29. Kingery, Bowen H., Uhlmann D.R., Introduction to Ceramics, John Wiley&Sons Inc. (1976)

30. Kumagai M., Messing G., "Controlled Transformation of a Boehmite Sol-Gel By α -Alumina Seeding", *Journal of The American Ceramic Society*, **65**, No: 9 (1985), 500-505
31. Lee D.H., Condrate R.A., "A FTIR Spectral Investigation of the Structural Species Found on Alumina Surfaces" [http:// students.Alfred.edu/youj/ Ceramics.18.htm](http://students.Alfred.edu/youj/Ceramics.18.htm)
32. Levin I., Brandon D., "Metastable Alumina Polymorphs: Crystal Structures and Transition Sequences", *Journal of The American Ceramic Society*, **81**, No: 8 (1998), 1995-2012
33. Maczura G., Francis T.L., Roesel R.E., "Special Aluminas for Ceramics and Other Industrial Applications", Reprint from Interceram. No.3/1976 Alcoa International Inc.
34. *Material Science and Technology*, edited by R.W.Cahn, P Haasen, E.J. Kramer, **11**, "Structure and Properties of Ceramics", (1994), 84-87
35. *Material Science and Technology*, edited by R.W.Cahn, P Haasen, E.J. Kramer, **17 A**, "Processing of Ceramics" – Part I, (1996)
36. Mauro John, "Alumina Suspension Preparation and Rheology", <http://www.cs.alfred.edu/~maurojc/papers/alumina.html>
37. Messing G., Kumagai M., "Low Temperature Sintering of α -Alumina Seeded Boehmite Gel", *American Ceramic Society Bulletin*, **73**, No: 10, (1994), 88-91
38. Miano F., Bailey A., Luckham P.F., Tadros F., "Adsorption of Poly (ethylene oxide)- poly (propylene oxide) ABA block copolymers on carbon black and the rheology of the resulting dispersions", *Colloids and Surfaces*, **68**, (1992), 9-16
39. Morrissey K., Czanderna K., Carter C.B., "Growth of alpha alumina Within a Transition Alumina Matrix", *Communications of the American Ceramic Society*, C-88 ; C-90, (1984)

40. Mutsuddy B.C., "Rheology and Mixing of Ceramic Mixtures Used in Plastic Molding" Chemical Processing of Ceramics, edited by Burtrand Lee, Edward Pope, by Marcel Dekker, (1994)
41. Myers D., Surfaces Interfaces and Colloids Principles and Applications, VCH Publishers (1991)
42. Nagarajan R., Ganesh K., "Block copolymer self-assembly in selective solvents: Spherical micelles with segregated cores", *J. Chem. Phys.* **90** No: 10 ,(1989), 5843-5855
43. Orth J., Meyer H., Bellman C., Wegner G., "Stabilization of Aqueous α -Al₂O₃ Suspensions with Block Copolymers", *Acta Polymer*, **48**, (1997), 490-501
44. Pconnell, Howard J., "Adsorption of Polymers at the Solution –Solid Interface II. Polyethers on Carbon" *The Journal Physical Chemistry*, **71** No: 98, (1997), 2981-2989
45. Polat H., Chander S., "Adsorption of PEO/PPO Triblock Copolymers At Air/Water and Coal/Water Interfaces", (1995)
46. Reed J.S., Principles of Ceramic Processing, John Wiley & Sons, Second Edition, Canada (1995)
47. Richardson W.D., Modern Ceramic Engineering, Properties, Processing and Use in Design, 2nd edition, Marcel Dekker (1992)
48. Rosen M., Surfactants and Interfacial Phenomena; 2nd edition, Wiley & Sons (1989)
49. Saito Y., Takei T., Hayashi S., Yasumori A., "Effects of Amorphous and Crystalline SiO₂ Additives on α -Al₂O₃ to γ - Al₂O₃ Phase Transitions", *Journal of The American Ceramic Society*, **81**, No: 8, (1998), 2197-2200
50. Schwartz Mel, Handbook of Structural ceramics, McGraw –Hill, Inc., 1992

51. Sharma P., Jilavi M., Burgard D., Nass R., "Hydrothermal Synthesis of Nanosize α -Alumina from Seeded Aluminum Hydroxide", *Journal of The American Ceramic Society*, **81**, No: 10, (1998), 2732-2734
52. Studart A.R., Zhong W., Pandolfelli V.C., "Rheological Design of Zero-Cement Self Flow Castables", *American Ceramic Society Bulletin*, (May 1999), 65-72
53. Sumita S., Rhine W., Bowen H., "Effects of Organic Dispersants on the Dispersion, Packing and Sintering of Alumina", *Journal of The American Ceramic Society*, **74**, No: 9, (1991), 2189-21996
54. Valera A.E., Bailey A., Doroszkowski A., "Graft copolymers as stabilizers for oil in water emulsions Part1. Synthesis of the copolymers and their behaviour as monolayers spread at the air-water and oil -water interfaces", *Colloid and Surfaces A. Physicochemical and Engineering Aspects*, **96**, (1995) 53-67
55. Wang G., Sarkar P., Nicholson S., "Surface Chemistry and Rheology of Electrostatically Stabilized Alumina Suspensions in Polar Organic Media", *Journal of The American Ceramic Society*, **82**, No: 4, (1999), 849-856
56. Wanka G., Hoffmann H., Ulbricht, " The aggregation behaviour of poly-(oxyethylene)-poly-(oxypropylene)-poly-(oxyethylene)-block copolymers in aqueous solution", *Colloid&Polymer Science*, 268, (1990) ,101-117
57. Wefers K., Bell G., "Oxides and Hydroxides of Aluminium", Technical Paper No: 19 Aluminium Company of America, Pittsburgh 1972
58. Williams R.A., "Applications in the Process Industries", Colloid and Surface Engineering, Butterworth –Heinemann Ltd (1992)
59. Wilson S., Stacey M., "The Porosity of Aluminum Oxide Derived from Well-Crystallized Boehmite: Correlated Electron Microscope, Adsorption and Porosimetry Studies", *Journal of Colloid and Interface Science*, **82** No: 2 (1981)